STUDY OF NUCLEAR STRUCTURE OF SOME NUCLEI IN MEDIUM MASS REGION

A Thesis
Submitted
In Partial Fulfillment of the Requirements
for the Degree of

DOCTOR OF PHILOSOPHY

Dr. Kamlesh Kumar Sharma
Co- Supervisor

Dr. Satendra Sharma
Supervisor

Research Scholar

REETU KAUSHIK
(Enrollment No.MUR1001393)

DEPARTMENT OF PHYSICS
FACULTY OF SCIENCE & TECHNOLOGY
MEWAR UNIVERSITY, CHITTORGARH
(RAJASTHAN)

FEBRUARY, 2016

UNDERTAKING FROM THE CANDIDATE

This is to certify that I Reetu Kaushik have completed the Ph.D. thesis work on the topic "Study of Nuclear Structure of Some Nuclei in Medium Mass Region" under the guidance of Dr. Satendra Sharma l (Supervisor) & Dr. K.K.Sharma (Co-Supervisor) for the partial fulfillment of the requirement for the degree of Doctor of Philosophy, Mewar University. This is an original piece of work and I have not submitted it earlier elsewhere.

Date: (Research Scholar)

Place: Chittorgarh

DECLARATION

I, Reetu Kaushik, certify that the work embodied in this Ph.D. thesis is my own bonafide work carried out by me under the supervision of Dr. Satendra Sharma (Supervisor) and Dr. Kamlesh Kumar Sharma (Co-Supervisor) for a period of 5.2 years from December, 2010 to February, 2016 at Mewar University. The matter embodied in this Ph.D. thesis has not been submitted elsewhere for the award of any other degree/diploma.

I declare that I have faithfully acknowledged, given credit to and referred to the research workers wherever their works have been cited in the text and the body of the thesis. I further certify that I have not willfully lifted up some other's work, para, text, data, results, and so on reported in the journals , books, magazines, reports, dissertations, thesis, and so on, or available at web-sites and have included them in this Ph.D. thesis and cited as my own work.

Date: (Signature of the Research Scholar)

Place: (Name of the Research Scholar)

Certificate from the Supervisors

This is to certify that the above statement made by the candidate is correct to the best of our knowledge.

Supervisors:

Dr. Kamlesh Kumar Sharma
(Co- Supervisor)

Dr. Satendra Sharma
(Supervisor)

COURSE WORK COMPLETION CERTIFICATE

This is to certify that Mrs. Reetu Kaushik, a bonafide research scholar of this department, has satisfactorily completed the course work requirements which are a part of her Ph.D. programme.

Date: Director (Research)

Place:

PRE- SUBMISSION SEMINAR COMPLETION CERTIFICATE

This is to certify that Mrs. Reetu Kaushik, is a bonafide research scholar of this Department and, has satisfactorily completed the pre- submission seminar requirements which are a part of her Ph.D. programme.

Date: Director (Research)

Place:

COPYRIGHT TRANSFER CERTIFICATE

Title of the Thesis: Study of Nuclear Structure of Some Nuclei in Medium Mass Region.
Research Scholar Name: Mrs. Reetu Kaushik

Copyright Transfer

The undersigned hereby assigns to the Mewar University all rights under copyright that may exist in and for the above thesis submitted for the award of the Ph.D. degree.

Signature of Research Scholar

Note: However, the author may reproduce or authorize others to reproduce material extracted verbatim from the thesis or derivative of the thesis for author's personal use provided that the source and the University's copyright notice are indicated.

ACKNOWLEDGEMENT

I am thankful to God who provided me the strength to complete the work. The co-operation of numerous people is involved in the research work. Firstly, I take the opportunity to thank my Supervisor Dr. Satendra Sharma, Professor, and Co-Supervisor Dr. Kamlesh Kumar Sharma Professor, for their valuable guidance throughout the thesis work, which enabled me to complete the thesis smoothly. They have always answered all my queries and e-mails in time. Their kindness and enthusiasm helped me to keep abreast of the latest developments in Physics and showing me that research in Physics can lead to a better life.

Secondly, I am very thankful to Prof. J. B. Gupta, Department of Physics, Ramjas College, University of Delhi, Delhi- 110007, for his precious guidance and support throughout the work.

I want to say thank to the Registrar, Mewar University, Chittorgarh, Rajasthan, for providing research facilities. I am also grateful to Department of Physics, Mewar University, Chittorgarh, Rajasthan, for providing research environment and facilities.

I am also thankful to Mr. Pankaj Goel, Chairman, Mr. Jagdish Kumar, Treasurer, Mr. Navneet Mittal, Joint Secretary of Panchwati Institute of Engineering & Technology, Meerut, for providing research facilities in the Institute.

I am thankful to Dr. Rajesh Kumar, Professor and Head, Department of Applied Physics, Noida Institute of Engineering & Technology, Gr. Noida and Dr. Vikas Katoch, Assistant Professor, Department of Physics, Raj Kumar Goel Institute of Technology, Ghaziabad for his valuable help and co- operation.

I wish to express my deep and sincere gratitude to Dr. Y. P. Garg Professor and Principal, Panchwati Institute of Polytechnic Meerut, and my friend Mrs. Shruti Agarwal, Assistant Professor PIET, Meerut, for their support and co- operation. I pay my special thanks to Mr. Atul Shukla, Assistant Professor and System Administrator, PIET, Meerut, for providing adequate computer and internet facilities.

The library facilities at Banaras Hindu University, Varanasi, Panchwati Institute of Engineering & Technology, Meerut Central Science Library, University of Delhi and Inter University Accelerator Centre (IUAC), New Delhi, are also acknowledged.

Last but not the least I am highly obliged to my parents and my family members for their encouragement and valuable support for completing the research work.

(Reetu Kaushik)

STUDY OF NUCLEAR STRUCTURE OF SOME NUCLEI IN MEDIUM MASS REGION

REETU KAUSHIK

ABSTRACT

This research work is limited to the medium mass region (A=150-200). In this work, the collective nuclear structures of some medium mass nuclei have been analyzed, using empirical studies, phenomenological, geometrical, group theoretical models. The research work is divided into five Chapters. The Introduction is given in the Chapter I and Nuclear Models are discussed in Chapter II. In Chapter III, the values of asymmetry parameter (γ_0) of Davydov and Filippov model are calculated using the experimental energies of $E2_2^+$ and $E2_1^+$ states for $50 \leq Z \leq 82$ and $82 \leq N \leq 126$ region. The whole calculated data is divided into four quadrants. The Quadrant I (Q-I) is for $50 \leq Z \leq 66$ and $82 \leq N \leq 104$ shell space with particle like proton-bosons and neutron-bosons and it is forming the p-p space. The Quadrant II (Q-II) is for $66 \leq Z \leq 82$ and $82 \leq N \leq 104$ shell space, with hole like proton-bosons space and particle like neutron-bosons space and it is forming the h-p space. The Quadrant III (Q-III) is for $66 \leq Z \leq 82$ and $104 \leq N \leq 126$ region shell space, with hole like proton-bosons and neutron-bosons and it is forming h-h space. The quadrant IV (Q-IV) is for $50 \leq Z \leq 66$ and $104 \leq N \leq 126$ shell space with particle like proton-bosons and hole like neutron-bosons and it is forming the p-h space. The study of systematic dependence of γ_0 on N, N_B and NpNn has been carried out on *quadrant wise basis* to find out the role of valence nucleons and holes on the nuclear structure. The role of Z=64 subshell effect for $N \leq 90$ region is also discussed. The NpNn product is a good measure of its effect in producing the deformation in atomic nuclei. This product is also an indicator of the n-p interaction among the valance proton and/or neutron nucleons causing the deformation of nuclear core. In quadrant-I and quadrant-II, the asymmetry parameter decreases; from 30^0 in Q-I and from 22^0 in Q-II to 9^0- 10^0; with increasing N from 82 to 104 (i.e. the mid of N=82 to 126 neutron shell), signifying that the nuclear deformation (β) is increasing, while the energy ratio R_4 increases from 2 (for harmonic vibrators or SU(5) type nuclei) to 10/3 (for good rotors or SU(3) type nuclei). This indicates that in this region the nuclear structure depends

much more on Z. In quadrant-I, the asymmetry parameter is having more correlated dependence on N, rather than on NpNn. Also in quadrant- I, the Z=64 sub-shell effect for N≤90 nuclei affect the variation of asymmetry parameter with N and NpNn product. The existence of X(5) symmetry in N=90 isotones established in recent works supports the formation of isotonic multiplets in this work. The systematic dependence of asymmetric parameter on NpNn has strong dependence in quadrant-II. In Q-II, the line of β- stability runs nearly diagonally, i.e. parallel to N_B and leading to the formation of F-spin multiplets. The same feature had been observed earlier for the energy of first excited state i.e. E2g. In quadrant-III, the variation of asymmetry parameter is different from quadrant I and II because the asymmetry parameter increases sharply from 9^0 - 10^0 to 30^0 with increasing N from 104 to 126. This is signifying that the nuclear deformation (β) is decreasing and the nuclear structure changes from pure rotor SU(3) type to vibrational SU(5) or γ-unstable O(6) type. Further, the asymmetry parameter for different elements has smooth curve with NpNn with almost same slopes except for Hg isotopes. In Chapter IV, the predictions of asymmetric rotor model of Davydov and Filippov for B(E2;4g→2g)/B(E2;2g→0g) branching ratio are compared with the experimental data in medium mass region. It is found that the observed data point of this ratio for N=88 isotones (Nd, Sm, Gd, Er) are indicating the shape phase transition from an ideal spherical harmonic vibrator or SU(5) to an axially symmetric deformed rotor or SU(3). It is also noted that this B(E2) ratio is anomalously small in case of two non- magic nuclei i.e., $^{198}_{80}Hg_{118}$ [=0.375(18)] and $^{144}_{60}Nd_{84}$ [=0.73(9)] with only two vacancy of protons for Z =82 and two valence neutrons outside N=82, respectively. The data points for other nuclei are lying between SU(5) and SU(3) limits. The calculated B(E2) ratios of ARM are very close to the SU(3) limit of IBM indicating that it can explain the structure of only well deformed nuclei. Therefore the ARM is partially successful in explaining this branching ratio. The variation of experimental B(E2; 4g→2g)/ B(E2;2g→0g) branching ratio with N and Z is carried out for Nd–Hg nuclei. It is found that the there is shape phase transition for N=88 and 90 isotones (Nd, Sm, Gd, Er) from an ideal spherical harmonic vibrator or SU(5) to an axially symmetric deformed rotor or SU(3). The present study supports the sub shell closer effect around Z=64, for N≤ 90 and the constant nuclear structure of N=90 isotones. Finally, in

Chapter V, the interacting Boson Model-1is used to study the nuclear structure of ^{152,154}Sm nuclei. The ^{152}Sm is chosen for study, because it is a best example of recently discovered X(5) symmetry of IBM and ^{154}Sm is a rotor type i.e. SU(3) symmetry. The bunching of various levels in ^{152,154}Sm is reproduced well in present calculation and is in agreement with the observed energy level diagram of experimental data. In ^{152,154}Sm, the B(E2) branching values and B(E2) branching ratios are calculated for inter-band and intra-band transitions for g-, β-, γ- and β_2- bands and the calculated results are in good agreement with experimental data. In ^{152,154}Sm nuclei, the IBM-1 Hamiltonian reproduce the energy spectrum, B(E2) values and B(E2) ratios for g-, β- and γ– bands. Present calculation supports that ^{152}Sm is as a best example of X(5) symmetry and ^{154}Sm is a SU(3) type in nature.

TABLE OF CONTENTS

LIST OF THE TABLES

LIST OF THE FIGURE

LIST OF SYMBOLS, ABBREVIATIONS AND NOMENCLATURE

A	Atomic mass
Z	Proton number
N	Neutron number
N_B	Total nucleon pair number
N_P	Valence proton pair number
N_n	Valence neutron pair number
$N_P N_n$	Valence nucleons pair product
B(E2)	Transition probability
$E(2_1^+)$	Energy of first excited 2_1^+ level of ground state band
γ	γ -band
K^π	0_1^+ for g -band and 2_1^+ for γ -band
Eγ	γ-ray energy
Gsb	Ground state band energy
I_γ	γ-ray intensity
J	Moment of inertia (MoI)
L	Angular momentum
Q	Quadrupole moment
R_4	Energy ratio
γ_0	Asymmetry parameter
R_0	Average nuclear radius
RMSD	Root mean square deviation

CHAPTER-I

1.1 PREHISTORY OF NUCLEAR PHYSICS

Nuclear physics is a stimulating subject, in an attempt to explain the structure of atom, J. J. Thomson suggested that the atom consisted of an equal number of positive and negative charges (proton and electron) distributed uniformly within its spherical volume. The radius of the atom was estimated to be the order of 10^{-10} meters. Since the famous α- ray scattering developed by Rutherford (1911), established that the mass of an atom is concentrated within a small, positive charge region at the centre of the atom. This central core is surrounded by electron cloud, is called nucleus. Since Rutherford's times many scattering experiments, using highly energetic electron and neutrons as the scattering particles, have been performed to determine the size of nucleus. Later, Chadwick (1932) discovered the neutron as the constituent of nucleus. Heisenberg (1932) introduced the concept of isospin, viz. that proton and neutron merely two different states of the same elementary particle known as nucleon. From the phenomena of nuclear fission of heavy nuclei, Neils Bohr developed the liquid drop model based on strong interaction of the nucleons. However, Mayer (1949, 1950) proposed the nuclear shell model based on the average field produced by all the nucleons moving independently in the potential well. The regular rotation like spectra in medium mass nuclei led Bohr and Mottelson (1953) to develop the collective model, a combination of the liquid drop model and shell model.

It is well known that the nuclear model is applicable in explaining the different nuclear properties such as prediction of energies of g-band, β-band, γ-band and other higher multi phonon bands or B(E2) values and B(E2) ratios for inter and intra band transitions of nuclei for light and medium mass region with varying degrees of success. In this chapter we give the basic definition, useful concept and facts relating to the consequent chapters. This chapter also sketches the brief summary of theoretical models which have been used in the present thesis work for understanding of experimental data and the collective nuclear structure.

In this chapter we give the brief summary of the different types of models.

1.1.1 Angular Momentum of Nuclei

The angular momentum **L** of a particle about a given origin is defined as:

$$\mathbf{L} = \mathbf{r} \times \mathbf{p} \tag{1.1}$$

where, **r** is the position vector of the particle relative to the origin, **p** is the linear momentum of the particle and × denotes the cross product. The derived SI units of angular momentum is Newton meter second (N·m·s or kg·m^2/s) or Joule- second (J·s). Because of the cross product, **L** is a pseudo vector perpendicular to both the radial vector **r** and the momentum vector **p.** For an object with a fixed mass that is rotating about a fixed symmetry axis, the angular momentum is expressed as the product of the moment of inertia (I) of the object and its angular velocity (**ω**) vector:

$$\mathbf{L} = I\boldsymbol{\omega} \ . \tag{1.2}$$

The angular momentum of a particle or rigid body in rectilinear motion (pure translation) is a vector with constant magnitude and direction. If the path of the particle or centre of mass of the rigid body passes through the given origin, its angular momentum is zero. Angular momentum is also known as moment of momentum.

1.1.2 Electric Quadrupole Moment of Nuclei

The nuclear electric quadrupole moment is a parameter which describes the effective shape of the ellipsoid of nuclear charge distribution. A non-zero quadrupole moment Q indicates that the charge distribution is not spherically symmetric. By convention, the value of Q is taken to be positive if the ellipsoid is prolate and negative if it is oblate.

1.1.3 Nuclear Forces

Every nucleus consists of protons and neutrons (known as nucleons). The nuclear forces acting between these nucleons, called nuclear force. These forces have been discovered by James Chadwick studied in terms of models, and since models do not involve the detailed behavior of these forces, we have learned only about certain of their general features. To a large extent, this force can be understood in terms of

exchange of virtual light meson, such as the pions. Sometimes the nuclear force is called the residual strong force. Further, characteristics of the nuclear force are the following.

(i) The nuclear force is short range and central, with small non-central part.

(ii) The nuclear force is repulsive at very short range to prevent the collapse of the nucleus.

(iii) The constants density and binding energy per nucleon (B/A) indicates the saturation property of the nuclear force.

(iv) As nucleons are Fermi-Dirac particles (spin) the nuclear force exhibits the saturation property of the nuclear force.

(v) The nuclear force is charge independent i.e. neutron-neutron (n-n), proton-proton (p-p), neutron-proton (n-p) interactions are equal.

(vi) The main knowledge about the nucleon interaction came from the p-p, n-p scattering experiments and study of deuteron.

1.1.4 Magic Number and Stability of Nucleus

It has been observed that nuclei have protons and neutrons. If numbers of any of these nucleons Z or N is equal to 2, 8, 20, 28, 50, 82 and 126 then the nucleus becomes more stable. These numbers are called *magic numbers*. If both N and Z are magic numbers, then nucleus becomes very stable. The existence of magic number is explained using shell model and it also describes spin and parities of low lying state of closed major shell nuclei. At this number of nucleon a shell becomes complete.

1.2 LIQUID DROP MODEL

The liquid drop model in nuclear physics treats the nucleus as a drop of incompressible nuclear fluid. It was first proposed by George Gamow and then developed by Niels Bohr and John Archibald Wheeler. The fluid is made of nucleons (protons and neutrons), which are held together by the strong nuclear force. This is a basic model that does not explain all the properties of the nucleus, but does explain the spherical shape of most nuclei. It also helps to predict the binding energy of the nucleus.

Mathematical analysis of the theory delivers an equation which attempts to predict the binding energy of a nucleus in terms of the numbers of protons and neutrons it contains. This equation has five terms on its right hand side. These correspond to the cohesive binding of all the nucleons by the strong nuclear force, the electrostatic mutual repulsion of the protons, a surface energy term, an asymmetry term (derivable from the protons and neutrons occupying independent quantum momentum states) and a pairing term (partly derivable from the protons and neutrons occupying independent quantum spin states).

If we consider the sum of the following five types of energies, then the picture of a nucleus as a drop of incompressible liquid roughly accounts for the observed variation of binding energy of the nucleus.

1.3 NUCLEAR SHELL MODEL

In nuclear physics, the nuclear shell model is a model of the atomic nucleus which uses the Pauli exclusion principle to describe the structure of the nucleus in terms of energy levels. The shell model is partly analogous to the atomic shell model which describes the arrangement of electrons in an atom, in that a filled shell results in greater stability. When adding nucleons (protons or neutrons) to a nucleus, there are certain points where the binding energy of the next nucleon is significantly less than the last one. This observation, that there are certain magic numbers of nucleons: 2, 8, 20, 28, 50, 82, 126 which are more tightly bound than the next higher number, is the origin of the shell model.

1.3.1 Successes and the Limitations of the Shell model

Shell model explains correct magic number, spin, parity, binding energy of nuclei, cross section of neutron captured by nuclei, magnetic dipole moment with some deviation from experimental observation and transition probabilities of emission of gamma rays from the nuclei.

Whereas, it gives zero quadrupole moment of the nuclei and does not give information about nuclei having more valence nucleons. This model is best for lighter nuclei.

1.4 BOHR-MOTTELSON COLLECTIVE MODEL

Unified collective model of nucleus was proposed by Bohr and Mottelson (1953). Collective model is the combination of liquid drop model. It views the nucleus as vibrating –rotating core capable of being deformed to various shapes i.e. prolate, oblate or tri-axial. This is called the geometric view of the collective motion of the nucleus. The law energy levels of the nucleus are grouped in three collective bands, called $K^{\pi}=0_1^+$ g- band; $K^{\pi}=0_2^+$ β- band; $K^{\pi}=2_1^+$ γ- band and higher energy levels are called multi-phonon bands.

The Bohr-Mottelson (1975) series expression for level energies in a band is given as:

$$E_I=AI(I+1)+B\{I(I+1)\}^2+C\{I(I+1)\}^3+..... \quad (1.3)$$

In the shell model, core is made of paired nucleons and the core may be spherically symmetric or may be axially deformed. The non spherical potential arises due the valence nucleons which polarise the nuclear core. Thus the single particle energies are calculated in a non spherical potential. In this model the nucleus consists of an even-even core plus one or more nucleons moving in the shell model orbits. The coupling of core and nucleons may be weak (or strong) which corresponds to the vibrational, rotational model.

1.4.1 Successes and the Limitations of the Collective model

In the Bohr-Mottelson model the even Z and even N nucleus has vibration and rotational motion. The vibrational model predicts the following properties:
(i) The vibrational nuclei have low lying collective excited states.
(ii) The E2 transition from two phonon triplets to one phonon 2_1^+ level is strong.
(iii) The cross over E2 transition from second 2_1^+ state to the ground state should vanish.
(iv) The Quadrupole moment of the first 2_1^+ excited states is zero.

The rotational model (RM) can explain the following properties:

(i) The energy spectrum of rotational nuclei has the ground state rotational band, β band and γ-vibration band.

(ii) The transition for ($0^{+}\rightarrow 2_{+}$) has the large absolute B(E2) value and Quadrupole moment.

(iii) The deformed nuclei have the magnetic moment with sign and finite magnitude.

(iv) The nuclear deformation is given by the expression:

$$\beta = B(E2; 0_1^+ \longrightarrow 2_1^+)^{\frac{1}{2}} \times \frac{4\pi}{3Z_e R_0^2} \qquad (1.4)$$

(v) The K selection rule for electromagnetic transition is $\Delta K = |K_f - K_i| \leq \boldsymbol{\lambda}$, where K_i and K_f are the values of K for initial and final bands for a particular transition, and λ is mode of transition.

The limiting collective model approach could not explain the observed properties of those nuclei which posses both the rotational and vibrational model feature. In the limiting model the rotational-vibration interaction was not taken into account.

1.5 ROTATIONAL-VIBRATIONAL MODEL

The complete rotational –vibrational interaction model (RVM) was developed by Fasessler et al. (1965), which allow the diagonalization of the Bohr-Mottelson collective Hamiltonian. In this model the nucleus is assumed to be axially symmetric deformed i.e. $\beta_0>0$ and $\gamma_0=0$. The RVM succeeds in the reproduction of the low lying energy spectra of the g-, β- and γ-bands and the B(E2) ratios for transition from γ- and β-bands.

1.6 ASYMMETRICAL ROTOR MODEL

Davydov and Filippov (1958) proposed asymmetric rotor model (ARM) to investigate the energy levels corresponding to rotation of nucleus which does not change its internal state. According to which nucleus is triaxially deformed with $\gamma_0 \neq 0$ and the ground band, β-band and γ-bands are due to rotation of triaxial ellipsoid

nucleus about different axis. One can derive the value of angle of triaxiality or asymmetry parameter γ_0 from ratio R_γ as given below:

$$\gamma_0 = \frac{1}{3}\sin^{-1}\{\frac{9}{8}[1-\left(\frac{R_\gamma - 1}{R\gamma + 1}\right)^2\}^{1/2}, \text{ where } R_\gamma = \frac{E_{22}}{E_{21}}. \quad (1.5)$$

1.7 DYNAMIC PAIRING PLUS QUADRUPOLE MODEL

The dynamic pairing-plus-quadrupole (DPPQ) model was proposed by Kumar and Baranger (1967, 1968). They predicted successfully the prolate to oblate shape transition in Os - Pt region. The DPPQ model can treat spherical, deformed and transition nuclei within a single frame work. Kumar and Baranger also developed the dynamic deformation model (DDM), in which there was no inert core assumed. In DPPQ model and DDM, instead of assuming a fixed shape (axially symmetric deformed or axially deformed) the nucleus is allowed to take its own shape in the (β, γ) plane. The Bohr collective Hamiltonian is given by

$H_C = V(\beta, \gamma) + T_{rot} + T_{vib}$ with (1.6)

$T_{rot} = \frac{1}{2}\sum_{k=1}^{3} \theta_k(\beta,\gamma)\, \omega_k^2$ and

$$T_{vib} = \frac{1}{2}\{B_{\beta\beta}(\beta,\gamma)\dot{\beta}^2 + 2B_{\beta\gamma}(\beta,\gamma)\dot{\beta}\beta\dot{\gamma} + B_{\gamma\gamma}(\beta,\gamma)\beta^2\dot{\gamma}^2\}$$

where θ_k (k=1, 2, 3) are the nuclear moment of inertia, ω_k is the angular velocities, $B_{\beta\beta}$, $B_{\beta\gamma}$, $B_{\gamma\gamma}$ are the three mass parameters for β-vibrations, β-γ coupled motions, γ-vibrations. All the coefficients of H_c are determined from the solution of H_{PPQ}.

1.8 INTERACTING BOSON MODEL

The interacting boson model (IBM) is a model in nuclear physics in which nucleons pair up, basically acting as a single particle with boson properties, with integral spin of 0, 2 or 4.

The IBM-I treats both types of nucleons the same and considers only pairs of nucleons together to total angular momentum 0 and 2, called respectively, s- and d-bosons. The IBM-II treats protons and neutrons separately. The IBM is suitable for

describing intermediate and heavy atomic nuclei. Adjusting a small number of parameters, it reproduces the majority of the low-lying states of such nuclei. This model of the atomic nucleus has to be able to describe nuclear properties such as spins and energies of the lowest levels, decay probabilities for the emission of gamma quantas, probabilities (spectroscopic factors) of transfer reactions, multiple moments and so into the world. Outlined from which the IBM comes. This theoretical result is not far from the real situation of even-even nuclei, from which it is known that their total spin mainly is even. These and other arguments lead to the basic statement of the IBM which Postulates that the nucleon pairs are represented by bosons with angular momentum L = 0 or 2. The multitude of shells which appears in the shell model is reduced to the simple s-shell (L= 0) and the d-shell (L = 2) which is composed vectorially by d-bosons analogously to the shell model technique. The IBM builds on a closed shell i.e. the number of bosons depends on the number of active nucleon (or hole) pairs outside a closed shell. Each type of bosons, the s- and the d-boson, has its own binding energy with regard to the closed shell. Analogously to the standard shell model, the interacting potential of the bosons acts only in pairs.

Moreover, the number of bosons is unlimited and is not a good quantum number in compare to the situation in the IBM. The simplest versions of the IBM describe the even-even nucleus as an inert core combined with bosons which represent pairs of identical nucleons. The analogy between nucleon pairs and bosons does not go so far that in the IBM the wave functions of the corresponding nucleons would appear. However, in the interacting boson-fermions model which deals with odd numbers of identical nucleons, bosons are coupled to nucleons.

The models IBM1 and IBM2 are restricted to nuclei with even numbers of protons and neutrons. In order to fix the number of bosons one takes into account that both types of nucleons constitute closed shells with particle numbers: 2, 8, 50, 82 and 126 (magic numbers). Three-boson interactions are excluded in analogy with the assumptions of the standard shell model. In contrast to the collective model, in the IBM one does not obtain a semi classical, vivid picture of the nucleus but one describes the algebraic structure of the Hamiltonian operator and of the states, for which reason it is named an algebraic model.

1.9 SUBJECT OF STUDY IN THIS THESIS

1.9.1 Chapter 1

The current work is based on the study of nuclear structure for A=150-200 for medium mass region. The study is carried out by in-between this A=150-200 region in four quadrants. We studied all the models, viz, the geometrical, empirical and group theoretical models. The predictions of these models have been compared with available experimental data.

1.9.2 Chapter 2

In Chapter II, the theory of nuclear models such as liquid drop model, nuclear shell model, collective model, dynamic- pairing –plus quadrupole model, interacting boson model etc. are discussed.

1.9.3 Chapter 3

In Chapter III, the values of asymmetry parameter (γ_0) of Davydov and Filippov model (1958) are calculated using the experimental energies of $E2_2^+$ and $E2_1^+$ states. Its variation with N, Z, NpNn, N_B is studied qudrant wise.

1.9.4 Chapter 4

In Chapter IV, the predictions of asymmetric rotor model of Davydov and Filippov (1958) for B(E2;4g→2g)/B(E2;2g→0g) branching ratio are compared with the recent experimental data in medium mass region.

1.9.5 Chapter 5

In Chapter V, the interacting boson model-1 of Arima and Iachello (1976) is applied to study the nuclear structure of $^{152, 154}$Sm isotopes. The predictions of IBM are compared with the experimental data and the data of other nuclear models.

CHAPTER- II

NUCLEAR MODELS

2.1 INTRODUCTION

Different models for nucleus have been proposed each of which explains the behavior of nucleus in some specific situation. But at the same time each of these models is in noticeable contradiction with other models or with known facts about nuclear forces. We will limit ourselves only to some basic models for the nucleus that can be explaining the general characteristics.

2.2 BOHR-MOTTELSON UNIFIED COLLECTIVE MODEL

It is also called unified model, description of atomic nuclei that incorporates aspects of both the shell nuclear model and the liquid-drop model to explain certain magnetic and electric properties that neither of the two separately can explain. It views the nucleus as vibrating –rotating core capable of being deformed to various shapes i.e. prolate, oblate or tri-axial.

In the shell model, nuclear energy levels are calculated on the basis of a single nucleon (proton or neutron) moving in a potential field produced by all the other nucleons. Nuclear structure and behaviour are then explained by considering single nucleons beyond a passive nuclear core composed of paired protons and paired neutrons that fill groups of energy levels, or shells. In the liquid-drop model, nuclear structure and behaviour are explained on the basis of statistical contributions of all the nucleons (much as the molecules of a spherical drop of water contribute to the overall energy and surface tension). In the collective model, high-energy states of the nucleus and certain magnetic and electric properties are explained by the motion of the nucleons outside the closed shells (full energy levels) combined with the motion of the paired nucleons in the core. Roughly speaking, the nuclear core may be thought of as a liquid drop on whose surface circulates a stable tidal bulge directed toward the rotating unpaired nucleons outside the bulge. The tide of positively charged protons constitutes a current that in turn contributes to the magnetic

properties of the nucleus. The increase in nuclear deformation; that occurs with the increase in the number of unpaired nucleons accounts for the measured electric quadrupole moment; which may be considered a measure of how much the distribution of electric charge in the nucleus departs from spherical symmetry.

2.2.1 The Vibrational Model

A spherical nucleus can be considered as compressible liquid drop. Its excitation mode arises from small oscillations about the equilibrium spherical shape. The surface of the spherical drop can be written as (see Alder et al. (1956)):

$$R(\Theta,\Phi) = R_0 = \left[1 + \sum_{\lambda\mu} \alpha_{\lambda\mu} Y_{\lambda\mu}(\Theta,\Phi)\right] \quad (2.1)$$

where, R_0 is the average nuclear radius, $\alpha_{\lambda\mu}$ are the deformation variables, λ verify in mode of the nuclear motion, μ is the projection of λ on the Z-axis and $Y_{\lambda\mu}(\Theta,\Phi)$ are the spherical harmonics where Θ and Φ are the polar angles with respect to the arbitrary space-fixed axes. The $\lambda = 0$ mode corresponds to the change in the nuclear radius without any change in the shape, λ = 1 mode corresponds to the translation of the center of mass, λ = 2 is the quadrupole mode of the lowest order of mode and λ = 3 corresponds to the octupole mode related to the higher lying excitation. In the λ = 2 mode the ground state has no phonon while the first excited state has one phonon excitation and is five-fold degenerate, since the azimuthal quantum number μ can take of the integral value -2, -1, 0, 1, 2.

In vibrational model it was assumed that the nucleus performs vibrations around the spherical shape and the Hamiltonian in quadrupole mode can be written as (see Alder et al. (1956) and Bohr and Mottelson (1953):

$$H_v = \frac{1}{2}C\sum_{\mu}\left|\alpha_\mu^2\right| + \frac{1}{2}B\left|\dot{\alpha}_\mu^2\right| \quad (2.2)$$

Where, B and C are the mass parameter and the stiffness parameter respectively. A typical spectrum of the ^{118}Cd isotope, which has the vibrational characteristics, is given by Aprahamian et al. (1987) is shown in Figure 2.1.

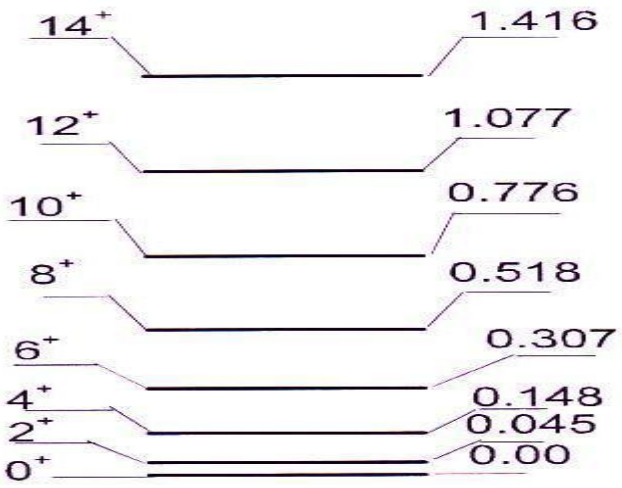

Figure 2.1: Energy levels diagram of $^{238}U_{92}$ nuclei.

2.2.2 Rotational Model

In the rotational model the shape of the nucleus is assumed to be fixed and the nuclear system rotates like a rigid structure. The energy associated with rotation would be purely kinetic and equal to $\frac{1}{2}\Im_0 w^2$. According to the collective model, the $\Im_0$ of nuclei can be determined from the energies of the rotational states. Rotational energy level of an axially symmetric nucleus can be described by three constants of motion: J, the total angular momentum; K, the projection of J on the nuclear symmetric axis (Z-axis); M, the projection of J on the space fixed axis (Z' –axis). The collective rotational angular momentum R is perpendicular to the symmetric axis.

If $\mathfrak{J}$ and $\mathfrak{J}$ are the moments of inertia for rotations about symmetric axis 3 (i.e. Z-axis) and about an axis perpendicular to Z-axis, J_1, J_2 and J_3 are the components of the total angular momentum operator along the body fixed axis. The Hamiltonian given by Bohr and Mottelson (1953) can be written as if $J_1 = J_2 = J$:

$$H_{rot} = \sum_{i=3}^{3} \frac{\hbar^2}{2\Im_i} J_i^2 = \frac{\hbar^2}{2\Im}(J_1^2 + J_2^2) + \frac{\hbar^2}{2\Im_3} J_3^2 \qquad (2.3)$$

$$= \frac{\hbar^2}{2\Im}(J_1^2 - J_2^2) + \frac{\hbar^2}{2\Im_3} J_3^2$$

For H_{rot} the eigenfunctions are the D functions, which are the transformation functions for spherical harmonics under finite rotations,

$$J^2 D^J_{MK} = J(J+1) D^J_{MK}$$
$$J_3 D^J_{MK} = K D^J_{MK} \qquad (2.4)$$
$$J'_z D^J_{MK} = D^J_{MK}$$

and

$$H_{rot}\ D^J_{MK} = \left[\frac{\hbar^2}{2\Im}(J(J+1) - K^2) + \frac{\hbar^2}{2\Im_3} K^2\right] D^J_{MK}\ .$$

The energy Eigen values are:

$$E = \frac{\hbar^2}{2\Im}[J(J+1) - K^2] + K^2 + \frac{\hbar^2}{2\Im_3} K^2 \qquad (2.5)$$

For $K = 0$ the energy expression becomes

$$E = \frac{\hbar^2}{2\Im} J(J+1), \quad J = 0,2,4,6 \ldots\ldots\ldots \qquad (2.6)$$

The energy levels of the ground state rotational band have the relation,

$E(2^+_1) : E(4^+_1) : E(6^+_1) : E(8^+_1)$: … = 1 :10/3 : 7 : 12 : …… (2.7)

Gupta et al. (1990) study the few good examples of rigid rotors such as ^{156}Gd, ^{170}Er, ^{170}Yb and ^{176}W isotopes. The rotational spectrum of the ^{156}Gd isotope is given in the Figure 2.2 and the values of experimental energies are taken from Sakai (1984).

In the presence of the centrifugal stretching, most of the nuclei deviate from the expression (2.8) and this effect can be taken into account by modifying to,

$$E_{rot} = \frac{\hbar^2}{2\Im} J(J+1) - B[J(J+1)]^2 \qquad (2.8)$$

where B is constant parameter for all J and $\Im$.

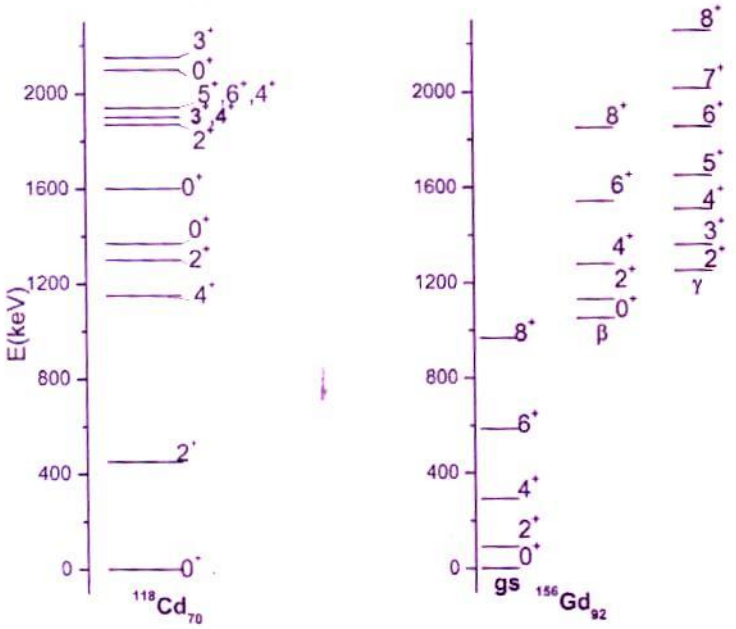

Figure 2.2: The vibrational spectrum of ^{118}Cd isotope and the rotational spectrum of ^{156}Gd isotope.

2.2.3 Rotation Vibration Interaction Model

Fasessler et al. (1965) formulated the rotation vibration interaction model that was a complete form the collective model of Bohr (1952). It assumes the nucleus to be an axially symmetric rotating body undergoing very small amplitude shape vibrations (β_0, equilibrium deformation parameter $\neq 0$; γ_0 asymmetry parameter $= 0$). This extended model allows the diagonalization of the collective Hamiltonian, and the interaction of $\beta-$vibrational, rotational motion, as well as of $\beta-,\gamma-$ vibrational interaction Hamiltonian that can be written as:

$$\hat{H} = \hat{H}_{rot.} + \hat{H}_{vib.} + \hat{H}_{rot-vib.} \tag{2.9}$$

The value of g-, $\beta-$ and $\gamma-$ band, the absolute B(E2) values and B(E2) ratios of a given nucleus can be obtained with the help of four model parameters i.e. the moment of inertia which takes into account the energy of 2_1^+ state: the equilibrium deformation β_0 of the nucleus which can be obtained from the absolute B(E2) value for the first excited 2_1^+ states; the $\gamma-$ vibrational energy E_γ which is fitted to the

energy of the 2_1^+ state, the β −vibrational energy E_β which is taken from the energy of first excited 0^+ state.

2.3 ASYMMETRIC ROTOR MODEL

Davydov and Filippov (1958) investigated the energy levels corresponding to rotation of nucleus which does not change its internal state. They established that the violation of axial symmetry of even nuclei affect the rotation spectrum of axial nucleus with appearance of some new rotational states having total angular moments of 2,3,4,…. If the deviation from axial symmetry is small than these levels lie very high and are not excited. The energy rotation of a non-spherical even-even nucleus is given, in the adiabatic approximation, by the Schrodinger equation:

$$(H - E)\psi = 0 \tag{2.10}$$

where, E is measured in units of $\hbar^2/4B\beta^2$, and the operator H is given by the formula:

$$H = \sum_{k=1}^{3} \frac{A J_k^2}{2sin^2(\gamma_0 - \frac{2\pi k}{3})} \tag{2.11}$$

Here, $A = \hbar^2/4B\beta^2$ is a quantity having dimension of energy, γ_0 varies between 0 and $\frac{\pi}{3}$ and determines the deviation of the nucleus from axial symmetry. The J_k are the operators of the angular momenta on the axis of a coordinate system connected with the nucleus. In eq. (2.29), for $\gamma \neq 0$ or $\frac{\pi}{3}$ the nucleus should be regarded as an asymmetric top. The wave function corresponding to the state with total moment J, can be represented as:

$$\psi_{JN} = \sum_{\lambda \geq 0} |J\lambda > A_\lambda| \tag{2.12}$$

where,

$$|J\lambda> = \left[\frac{2j+1}{16\,\pi^2(1+\delta_{\lambda 0})}\right]^{1/2} \{D^J_{N\lambda} + (-1)^J\ D^J_{N,-\lambda}\} \ldots\ldots\ldots \tag{2.13}$$

The function $D^J_{N\lambda}$ in eq. (2.13) are the functions of the Euler angles that determine the orientation of the principal axis of the nucleus with respect to the laboratory space. It can be shown that the wave functions (2.12) from the basis of totally

symmetric representation of the group D_2 the element of which are the rotation through 180° around each of three principal axes of the nucleus (see Davydov and Filippov (1958); Davydov and Rostovsky (1959)). The wave function of the rotational 2_1^+ states of the non-axial nucleus can be rewritten as (see Davydov and Filippov (1958)):

$$\psi_{21n} = \sqrt{5/8\pi^2}\left[A_1 D^2_{n0} + B_1(D^2_{n2} + D^2_{n,-2})/\sqrt{2}\right], \tag{2.14}$$

$$\psi_{22n} = \sqrt{5/8\pi^2}\left[A_2 D^2_{n0} + B_1(D^2_{n2} + D^2_{n,-2})/\sqrt{2}\right], \tag{2.15}$$

where, the value of A_λ coefficients in the wave function of eq.(2.14, 2.15) can be obtained using the value of γ_0:

$$\begin{aligned}
&A_1 M_1 = -\left[sin\gamma_0 sin3\gamma_0 + 3cos\gamma_0 cos3\gamma_0 + (9 - 8sin^2 3\gamma_0)^{1/2}\right]\\
&B_1 M_1 = 3sin\gamma_0 cos3\gamma_0 - cos\gamma_0 sin3\gamma_0,\\
&M_1^2 = 2\sqrt{(9 - 8sin^2 3\gamma_0)} \times \left[\sqrt{(9 - 8sin^2 3\gamma_0)} + sin\gamma_0 sin3\gamma_0 + 3cos\gamma_0 cos3\gamma_0\right],\\
&A_2 M_2 = \sqrt{(9 - 8sin^2 3\gamma_0)} - sin\gamma_0 sin3\gamma_0 - 3cos\gamma_0 cos3\gamma_0\ , \qquad (2.16)\\
&B_2 M_2 = 3sin\gamma_0 cos3\gamma_0 - cos\gamma_0 sin3\gamma_0,
\end{aligned}$$

$$M_2^2 = 2\sqrt{(9 - 8sin^2 3\gamma_0)} \times \left[\sqrt{(9 - 8sin^2 3\gamma_0)} - sin\gamma_0 sin3\gamma_0 - 3cos\gamma_0 cos3\gamma_0\right]$$

Similarly for 3_1^+ state the wave function can be written as

$$\psi_{3n} = \sqrt{7/16\pi^2}\left(D^3_{n2} - D^3_{n,-2}\right).$$

And spin 4_1^+ wave function is

$$\psi_{41} = \sqrt{9/8\pi^2}D^4_{n0},$$

$$\psi_{42} = \sqrt{9/16\pi^2}\left(D^4_{n2} + D^4_{n,-2}\right)$$

$$\psi_{43} = \sqrt{9/16\pi^2}\left(D^4_{n2} + D^4_{n,-4}\right), \text{ etc.}$$

Putting the eq.(2.30)in eq.(2.28) and making use the value of matrix element of the operator of the rotational energy eq. (2.29) acting on the wave function eq.(2.31)

$$< J\boldsymbol{\lambda}|\mathrm{H}|\mathrm{J}\boldsymbol{\lambda} > = \frac{(\alpha+\beta)}{4}[J(J+1) - \lambda^2] + \frac{\delta_\lambda^2}{2}$$

$$< J\lambda + 2|\mathrm{H}|\mathrm{J}\lambda> = \frac{(\alpha-\beta)}{4}[(1+\delta_{\lambda 0})(J-\lambda)\times(J-\lambda-1)(J+\lambda+1)(J+\lambda+2)]^{1/2}$$

……(2.17)

$$\alpha = sin^{-2}\left(\gamma_0 - \frac{2\pi}{3}\right), \qquad \beta = sin^{-2}\left(\gamma_0 + \frac{2\pi}{3}\right),$$

$$\delta = \quad sin^{-2}\gamma_0 \qquad \delta_{\lambda 0} = \begin{cases} 0, & for\ \lambda \neq 0 \\ 1, & for \lambda = 0 \end{cases}$$

(2.18)

One obtains for each value of J a system of algebraic equations for the coefficients A_λ in the wave function (2.11). For $J = 4$, the Schrodinger eq. (2.10) is reduced to a system of equation as (see Davydov and Rostovsky (1959))

$$\begin{bmatrix} 5(\alpha+\beta)-E & 3/2.\sqrt{5}(\alpha-\beta) & 0 \\ 3/2.\sqrt{5}(\alpha-\beta) & 4(\alpha+\beta)+2\delta-E & \frac{\sqrt{7}}{2}.(\alpha-\beta) \\ 0 & \frac{\sqrt{7}}{2}.(\alpha-\beta) & (\alpha+\beta)+8\delta-E \end{bmatrix} \begin{bmatrix} A_0 \\ A_2 \\ A_4 \end{bmatrix} = \begin{bmatrix} 0 \\ 0 \\ 0 \end{bmatrix}$$

(2.19)

The energy of the corresponding rotational states can be determined from the condition that the system (2.19) has a solution. The three values of E can be obtained the cubic equation,

$$X^3 - \frac{45X^2}{2Sin^2 3\gamma_0} - \left(39t^2 + 117t\frac{cos3\gamma_0}{Sin^2 3\gamma_0} - \frac{81}{Sin^4 3\gamma_0} - \frac{78}{Sin^2 3\gamma_0}\right)\times -70t^2 cos3\gamma_0 + 5\left(42 - \frac{9}{2Sin^2 3\gamma_0}\right)t^2 + 5t\left(81 - \frac{cos3\gamma_0}{Sin^4 3\gamma_0} + 42\right) - \frac{270}{Sin^4 3\gamma_0} - \frac{70}{Sin^2 3\gamma_0} = 0$$

Where

$$X = \left(\frac{E}{\hbar^2 B\beta^2}\right) \quad and \quad t = 4T\beta/(\hbar^2 B\beta^2).$$

For a rough estimate of t, the value of $\gamma = 40MeV$, $\hbar^2 B\beta^2 = 400keV$ and $\beta = 0.2$ gives the value of $t = 80$. Similarly, the energy of $E(2_1^+)$ states can be determined from the,

$$\begin{vmatrix} \frac{3}{2}(a+b) - 6T\beta cos\gamma_0 - E & 6T\beta sin\gamma_0 + (a-b)\sqrt{3/2} \\ 6T\beta sin\gamma_0 + (a-b)\sqrt{3/2} & 6T\beta cos\gamma_0 + \frac{(a+b)}{2} + 2c - E \end{vmatrix} = 0$$

(2.20)

where

$$a = \hbar^2[4B\beta^2 sin^2(\gamma_0 - 2\pi/3)]^{-1},$$
$$b = \hbar^2[4B\beta^2 sin^2(\gamma_0 + 2\pi/3)]^{-1} \quad , \qquad (2.21)$$

$$c = \hbar^2[4B\beta^2 sin^2(\gamma_0)]^{-1}. \tag{2.22}$$

Substituting the values of a, b, c and expending the determinant (2.20) we obtained the second degree equation,

$$X^2 - \frac{9X}{2sin^2 3\gamma_0} - \frac{9t^2}{4} - \frac{27cos3\gamma_0}{4sin^2 3\gamma_0}t + \frac{9}{2sin^2 3\gamma_0} = 0 \tag{2.23}$$

The roots of eq. (2.23) can be written as:

$$E_{21} = \frac{9\left[1 - \sqrt{\left\{1 - \frac{8sin^2(3\gamma_0)}{9}\right\}}\right]}{Sin^2(3\gamma_0)} \tag{2.24}$$

$$E_{22} = \frac{9\left[1 + \sqrt{\left\{1 - \frac{8sin^2(3\gamma_0)}{9}\right\}}\right]}{Sin^2(3\gamma_0)} \tag{2.25}$$

The energy levels of $J = 3$ state is given by Davydov and Filippov (1958):

$$E(3) = \sum_{K=1}^{3} \frac{2}{sin^2\left(\gamma_0 - \frac{2\pi}{3}\lambda\right)} = \frac{18}{sin^2(3\gamma_0)} \tag{2.26}$$

And energies of $J = 5$ states are given

$$E_\tau = \frac{[45 \pm \sqrt{(9 - 8Sin^2 3\gamma_0)}]}{Sin^2 3\gamma_0} \tag{2.27}$$

In eq. (2.26), $\boldsymbol{\tau}$=1 for the minus sign on the square root and $\boldsymbol{\tau}$=2 for the plus sign. The value of asymmetry parameter (γ_0) can be obtained using the eq. (2.24) and (2.25):

$$\gamma_0 = \frac{1}{3}Sin^{-1}\frac{9}{8}\left[1 - \left(\frac{1-R_\gamma}{1+R_\gamma}\right)^2\right]^{1/2} \quad ; \qquad R_\gamma = \frac{E(2_2^+)}{E(2_1^+)} \ . \tag{2.28}$$

In stationary states of the asymmetric top not one of the projections of the total momentum on axes 1, 2, 3 of the body-fixed coordinate system has a definite value and hence the energy levels cannot be specified the values of $K = J_3$. Each value of the total angular momentum in the asymmetric top corresponds to $2J$+1 different energy levels.

These levels can be classified with respect to the irreducible representations of group D_2. In virtue of the symmetry conditions on the wave function in even nuclei of the $2J + 1$ different levels only those energy levels with a given J can exist which correspond symmetric representation of group D_2. Rotation states of the required symmetry will not exist if $J = 1$. Two such states will exist for $J = 2$, one for $J = 3$, three for $J = 4$, two for $J = 6$ etc. The energy of two levels of required symmetry for $J = 2$ are defined by the expressions

$$\varepsilon_1(2) = \frac{9\left[1-\sqrt{\left\{1-\frac{8}{9}sin^2(3\gamma_0)\right\}}\right]}{Sin^2(3\gamma_0)} \tag{2.29}$$

$$\varepsilon_1(2) = \frac{9\left[1+\sqrt{\left\{1-\frac{8}{9}sin^2(3\gamma_0)\right\}}\right]}{Sin^2(3\gamma_0)} \tag{2.30}$$

Energy of a level for J = 3 is given by

$$\varepsilon(3) = \frac{18}{Sin^2(3\gamma_0)} \tag{2.31}$$

The three spin 4 energy levels are the roots of the third degree equation:

$$\varepsilon^3 - \frac{90}{Sin^2(3\gamma_0)}\varepsilon^2 + \frac{48}{Sin^4(3\gamma_0)}[27 + 16Sin^3(3\gamma_0)]\varepsilon - \frac{640}{Sin^4(3\gamma_0)}[27 + 7Sin^2(3\gamma_0)] = 0 \tag{2.3.2}$$

The two spin 5 energy levels are given by the formula

$$E_\tau(5) = \frac{[45 \pm \sqrt{(9-8sin^2(3\gamma_0)}]}{sin^2 3\gamma_0} \qquad \text{where } \boldsymbol{\tau} = 1,2 \tag{2.33}$$

where $\boldsymbol{\tau} = 1$ with negative sign and $\boldsymbol{\tau} = 2$ with positive sign. For $\gamma_0 = 0$ the energy spectrum is identical to that of an axially-symmetric nucleus. For a fixed value of β violation of axial symmetry of the nucleus leads to an increase energy levels belonging to the axial nucleus. This increase in the energy levels corresponds to a decrease of the effective moment of inertia of the nucleus or the effective deformation parameter β_{eff}. For the first excited state of spin 2 the effective deformation parameter can be determined as

$$\beta_{eff} = \left[\frac{4sin^2(3\gamma_0)}{9-\sqrt{(81-72sin^2(3\gamma_0))}}\right] \tag{2.34}$$

The small change of the level energies of an axially symmetric nucleus, violation of axial symmetry of the nucleus leads to the appearance of some new energy levels $\varepsilon_2(2)$, $\varepsilon_2(3)$, $\varepsilon_2(4)$ etc. By using the dependence of $\varepsilon_2(2)$, $\varepsilon_1(2)$ on γ_0 one can determine the corresponding value of γ_0 from the experimental value of the ratio.

2.4 INTERACTING BOSON MODEL

As we move away from closed nuclei, proton and neutron number increases the shell model basis states increases and calculations and explanation becomes complicated. Using quadrupole interactions, basis states reduce and calculations become simple.

Feshbach & Iachello (1973, 1974) described some properties of light mass nuclei in terms of interacting boson. Whereas, Janseen et al. (1974) described the collective quadrupole in terms of SU(6). Arima and Iachello (1975) added s-boson to the d-boson collectively to explain the structure of nuclei as a boson treated as nucleon pair & gives microscopic explanation of collective quadrupole states with large theoretical information Iachello & Arima (1987) and Bonatsos (1989).

Collective excitation of nuclei is explained by boson on the basis of boson creation and annihilation operator of multi-polarity l and z component of m, $b^{\dagger}_{l,m}$ and $b_{j,m}$. On the basis of boson operator, boson model is explained. The low lying collective states of nuclei described in the form of monopole boson having angular momentum an parity $J^{\pi}=0^{+}$ as s-boson and quadrupole boson with $J^{\pi}=2^{+}$ called as d-boson.

$s^{\dagger}d_{\mu}$ (μ= 0, ±1, ±2) (2.35)

$s\ d_{\mu}$ (μ= 0, ±1, ±2) (2.36)

Above relation is following Bose communication relation as:

$$[s\ s^{\dagger}]=1 \quad (2.37)$$

and

$$[d_{\mu}\ d^{\dagger}_{\mu}]=\delta_{\mu\mu'} \quad (2.38)$$

Spherical tensor T^{k}_{k} is created with Boson operator, that transformed basis vectors of (2k+1) dimensions, give Clebsch Gorden Coefficients with product of two operators. Total boson number N is the sum of number of s and d-bosons. i. e., $N= n_s+n_d$, which is conserved.

The Hamiltonian is used to obtain the information about spectrum, which is a combination of energy term (E_0), one and two body interactions term, here creation

operator is equal to the annihilation operator. The Hamiltonian is hermition operator $H^{\dagger}=H$.

$$H = E_0 + \sum \epsilon_s (b_l^{\dagger}.b_l) + \sum \left(\frac{1}{2}\right) u^{L}_{l,l',l'',l'''} \left[\left(b_l^{\dagger} \times b_l^{\dagger}\right)^{L} \times (b_l \times b_l)^{L} \right]^{0}_{0} + \cdots \ldots \ldots \quad (2.39)$$

The H can also expressed as

$$H = E_0 + \Sigma \epsilon s(s^{\dagger}.s) + \Sigma \epsilon_d (d^{\dagger}.d) + \Sigma (1/2)(2L+1)^{\frac{1}{2}} c_L [(d^{\dagger} \times d^{\dagger})^{L} \times (d \times d)^{L}]^{0}_{0} + \frac{v_2}{\sqrt{2}} [\{(d^{\dagger} \times d^{\dagger})^{2} \times (d \times s)^{2}\} + \{(d^{\dagger} \times s^{\dagger})^{2} \times (d \times d)^{2}\}]^{0}_{0} + \frac{v_2}{2} [\{(d^{\dagger} \times d^{\dagger})^{0} \times ((s \times s)^{0}\} + \{(s^{\dagger} \times s^{\dagger})^{0} \times (d \times d)^{0}\}]^{0}_{0} + u_2 [(d^{\dagger} \times s^{\dagger})^{2} \times (d \times s)^{2}]^{0}_{0} + \frac{u_2}{2} [(s^{\dagger} \times s^{\dagger})^{0} \times (s \times s)^{2}]^{0}_{0} \quad (2.40)$$

It consist of two one body terms and seven two body terms c_L(L= 0, 2, 4), v_L(L= 0, 2) and u_L(L= 0, 2).

Electromagnetic transition of multi-polarity in the forms of s and d boson one body interaction is written as.

$$T_0^{E2} = \gamma_0 + \alpha_0 [(s^{\dagger} \times s)]^{0}_{0} + \beta_0 [(d^{\dagger} \times d_l)]^{0}_{0} \quad (2.41)$$

$$T_u^{M1} = \beta_1 [(d^{\dagger} \times d)]^{1}_{u} \quad (2.42)$$

$$T_0^{E2} = \alpha_2 [(d^{\dagger} \times s) + (s^{\dagger} \times d)]^{2}_{u} + \beta_2 [(d^{\dagger} \times d)]^{2}_{u} \quad (2.43)$$

$$T_u^{M3} = \beta_3 [(d^{\dagger} \times d)]^{3}_{u} \quad (2.44)$$

$$T_u^{E4} = \beta_4 [(d^{\dagger} \times d)]^{4}_{u} \quad (2.45)$$

The s and d boson have positive polarity. Operator with multi-polarity one has positive parity as a M1 operator and for negative parity E1 operator. One can construct transition operator with multi polarity four. The constant γ_0, α_L(L=0,2) and β_L(L=0,1,2,3,4) are parameters magnitude and scale of corresponding operator. The cubic term in Hamiltonian consist of three creations and three annihilation operator.

The Hamiltonian is also written as:

$$H = \varepsilon'' n_d + a_0 P^{\dagger} P + a_1 L^2 + a_2 Q^2 + a_3 T_3^{\,2} + a_4 T_4^{\,2} \quad (2.46)$$

Here P, L, Q, T_3 and T_4 are as pairing, angular momentum, quadrupole, octupole and hexadecapole operator. For microscopic calculation same Q is used in transition operator and in Hamiltonian and is known as Q- formalism.

The energy of nuclear states and reduced transition probability in the interacting boson model is calculated by PHINT program which is written by Scholten (1976) where coefficients of Hamiltonian correspond to input parameter as

ε''=EPS (2.47)

a_0= 2 PAIR (2.48)

a_1=ELL/2 (2.49)

a_2=QQ/2 (2.50)

a_3=5 OCT (2.51)

a_4=5 HEX (2.52)

The boson creation ($s^\dagger$ or $d^\dagger$) and annihilation (s or d) operator gives a set two linear operator. As $G_{\alpha\beta}=b_\alpha^\dagger b_\beta$ for (α, β=1, 2,….6) gives 36 operator which satisfies communication unitary algebra in six dimension U(6). The group of transformations is related with each relation. During communication constant is equal to one or zero, called as lie structure constant. Using Racah approach, G operator is as

$G_k^k = \left(b_l^\dagger \times b_l^\dagger\right)_k^k$ for l, l'=0, 2. In terms of s and d boson operator G expanded as $G_0^0(s,s)$, G_0^0 (d,d), G_u^1 (d,d), G_u^2 (d,d), G_u^3 (d,d), G_u^4 (d,d), G_u^2 (d,s) and G_0^2 (s,s) gives 1, 1, 3, 5, 7, 9, 5 and 5 components respectively. The U(6) algebra is classified into three sub group U(5), SU(3) and O(6).

2.4.1 Sub-group U(5)

The operators G_0^0d,d), G_u^1 (d,d), G_u^2 (d,d), G_u^3 (d,d) and G_u^4 (d,d) gives 25 component as a O(5) group. The operator G_u^1 (d,d) gives 3 component s a O(3). The operator G_u^3 (d,d) gives one component as a O(2) rotation group. The chain of Boson subalgebra is U(6) ⊃ U(5) ⊃ O(5) ⊃ O(3) ⊃ O(2). The quantum number for the chain is $N, nd, (v, n\Delta), L$ and M_L.

2.4.2 Sub-group SU(3)

Boson sub algebra II consist 9 components having a linear combination of G_0^0, G_u^1, G_u^2 for s and d pair with 1,3 and 5 component. The G_u^2 term is proportional to the electrical quadrupole operator gives information about deformations of the

nucleus with positive (negative) quadrupole moments. The operator $G_u^1$and G_u^2 give sub group SU(3) of U(6) having 3 and 5 components. The G_u^1 give sub-group O(3) of SU(3) with 3 components and G_0^1gives 1 component as a O(2) rotation group. The chin of boson sub-algebra II is is U(6) ⊃ U(5) ⊃ O(3) ⊃ O(2). The quantum number for the chain is $N, (\lambda, v)\chi$, L and M_L.

2.4.3 Sub-group O(6)

Boson sub-algebra III consistG_u^1, G_u^3 and G_u^2 having 3,7 and 5 terms as a sub group O(6) of U(6) with 15 terms. The operators G_u^1andG_u^3gives 10 terms as a sub-group O(5). The operator G_u^1gives 3 terms as a sub-group O(3) and G_u^1gives one term as a sub-group O(2). The chain of boson sub-algebra is U(6) ⊃ O(6) ⊃ O(5) ⊃ O(3) ⊃ O(2). The quantum number for the chain is $N, \sigma, (\tau, v\Delta), L \text{ and } M_L$.

The Hamiltonian in the form of Casimier operators gives energy spectrum, electric quadrupole operator for each symmetry with individual properties. Most of the nuclei do not show properties as like symmetry exactly. Then Hamiltonian H can be written by the operator of two chains. The classification of nuclei as (shown in Fig. 2.3):

1. Class A, nuclei with properties intermediate between I and II.
2. Class B, nuclei with properties intermediate between II and III.
3. Class C, nuclei with properties intermediate between III and I.
4. Class D, nuclei with properties intermediate between all three limits.

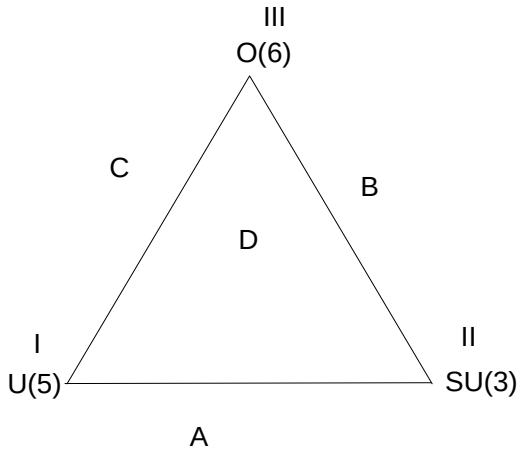

Fig. 2.3 Casten's symmetry triangle.

2.5 VARIOUS INDEPENDENT PARAMETERS

2.5.1 NpNn Product

It is the product of number of valence protons Np and the number of valence neutrons Nn. On taking it as independent parameter; we studied the variation of other dependent quantities on NpNn product.

2.5.2 P-factor

P-factor defined as it is the ratio of product of Np and Nn to the sum of number of valence proton (Np) and the number of valence neutrons (Nn). It is the normalised value of NpNn. It is represented by:

$$P=\frac{NpNn}{Np+Nn}$$

2.5.3Energy Ratio (R_4)

It is the ratio of energy of (4^+_1) and (2^+_1) levels of ground state bands. For vibration nuclei, it lies from $2 \leq R_4 \leq 2.4$, for transitional nuclei it lies as $2.4 \leq R_4 \leq 3$ and rotational nuclei it lies as $3 \leq R_4 \leq 3.33$.This ratio is also observed with other calculated quantities.

CHAPTER -III

SYSTEMATIC DEPENDENCE OF ASYMMETRIC PARAMETER FOR EVEN Z EVEN N NUCLEI IN LIGHT AND MEDIUM MASS REGION

3.1 INTRODUCTION

The study of collective nuclear structure with N, Z, N_B (=Np+Nn) and N_pN_n provide detailed information of nuclear interactions involved. Several studies have been carried out to study the collectivity, deformation and systematic dependence of other nuclear properties on N_pN_n. de-Shalit & Goldhaber (1953) pointed out the important role of valence nucleons. Talmi (1953) noted the constancy of nuclear level structure in semi-magic isotones/isotopes. Hamamoto (1965) observed that the protons (p^+) and neutrons (n^0) both are required for producing the nuclear deformation. In interacting boson model-I (IBM-1) Casten (1990), the structure of nuclei depends on the total boson numbers N_B. The concept of F-spin multiplets was based on this and was well explained by von Brentano et al. (1985). Casten (1985) noted that the E_{2g}+ have smooth dependence on N_pN_n. Other studies have been carried out by Casten and Zamfir (1996) to study the collectivity, deformation and systematic dependence of various nuclear observables on the product N_pN_n.

Gupta (1986) observed that $1/\alpha$ was linearly dependent on N_pN_n, where the coefficient α contributes for rotational part of energy in the SU(3) symmetry limit of IBM Casten (1990) as,

$$\mathbf{E([N](\lambda, \mu)\ KLM) = \alpha\ L(L+1) + \beta\ C(\lambda, \mu).} \qquad (3.1)$$

The B(E2; $2_1^+ \rightarrow 0_1^+$) values were also related with N_pN_n. Gupta et al.(1990a) noted a systematic dependence of γ–g B(E2) ratios on the N_pN_n in different parts of the major shell space Z=50–82, N<82 and N=82–126. Casten (1985) presented a review on the

evolution of nuclear structure based on N_pN_n product. The N_pN_n scheme was further modified to use P- factor Gupta et al. (1990a).

In this chapter, we study the role of valence nucleons and holes on the nuclear structure, through N, N_B and N_pN_n. Casten (1985) and Casten and Zamfir (1996) covered the various regions, viz., A=100, 130, 150 (Z<64, Z>64) and A=190. We present our results for 50≤Z≤82 and 82≤N≤126 region on *quadrant wise basis*. The systematic dependence of asymmetry parameter on N, N_B and N_pN_n has been studied. The role of Z=64 subshell effect for N≤90 region Casten (1985) is also taken care in this work.

3.2 LITERATURE REVIEW

The values of asymmetry parameter (γ_0) are calculated for 50≤Z≤82 and 82≤N≤126 region and the whole data is divided into four quadrants as suggested by Gupta et al. (1990b).

3.2.1 Calculation of Asymmetric Parameter

The values of asymmetry parameter (γ_0) of asymmetric rotor model (ARM) Davydov and Filippov (1958) are evaluated using the experimental energies $E2_2^+$ and $E2_1^+$ states. The experimental data is taken from the website of Brookhaven National Laboratory *http://www.nndc.bnl.gov* (2015). The energy ratio $R\gamma = E_{22} / E_{21}$ and γ_0 is:

$$\gamma_0 = \frac{1}{3}\sin^{-1}\{\frac{9}{8}[1-\left(\frac{R_\gamma - 1}{R\gamma + 1}\right)^2\}^{1/2}. \qquad (3.2)$$

It can be evaluated using:

(a) The energy ratio $R_4=(E_{4g}/E_{2g})$ but only the nuclei with 2.8≤R4≤3.33 will be allowed as noted by Sharma (1989) and Gupta and Sharma (1989).

(b) The B(E2) values which are very small and available with uncertainties. Therefore the values from energy ratio Rγ are more reliable. The calculated values of asymmetry parameter (γ_0) are listed in Table 3.1 and Table 3.2 for light and medium mass region, respectively.

3.3 RESULT AND DISCUSSIONS

The whole observed data of asymmetry parameter is divided into four quadrants. The Quadrant I (Q-I) is for $50 \leq Z \leq 66$ and $82 \leq N \leq 104$ shell space with particle like proton-bosons and neutron-bosons and it is forming the p-p space. The Quadrant II (Q-II) is for $66 \leq Z \leq 82$ and $82 \leq N \leq 104$ shell space, with hole like proton-bosons space and particle like neutron-bosons space and it is forming the h-p space. The Quadrant III (Q-III) is for $66 \leq Z \leq 82$ and $104 \leq N \leq 126$ region shell space, with hole like proton-bosons and neutron-bosons and it is forming h-h space. The quadrant IV (Q-IV) is for $50 \leq Z \leq 66$ and $104 \leq N \leq 126$ shell space with particle like proton-bosons and hole like neutron-bosons and it is forming the p-h space. Therefore, the quadrant I and III have p-p and h-h bosons space, respectively and quadrant II and IV for h-p and p-h bosons space respectively. It has been observed that there are no nuclei in quadrant IV. The division of the $50 \leq Z \leq 82$ and $82 \leq N \leq 126$ shell space had been suggested by Gupta et al. (1990b) to study the concept of F-spin multiplets. Further this concept of four quadrant used by Kumar (2013), Kumar et al. (2012) and Sharma and Kumar (2010) to study the systematic dependence of various nuclear observables and it was found that this concept gives deep information of nuclear structure.

3.3.1 The variation of asymmetry parameter (γ_0) in quadrant- I for $50 \leq Z \leq 66$ and $82 \leq N \leq 104$ region:

The systematic variation of asymmetry parameter γ_0 versus N, N_B and NpNn for quadrant-I are shown in Fig. 3.1, Fig. 3.2 and Fig. 3.3, respectively. It is evident from Fig. 3.1 that the γ_0 decreases sharply from 30^0 to 9^0 as N increases from 82 to 90 indicating the shape phase transition from Vibrational (VM) to rotational (RM) limit of collective model of Bohr and Mottelson (1975) and also SU(5) or O(6) limit to SU(3) limit of IBM Casten (1990). If N is increased beyond 92 the γ_0 does not change and becomes almost saturated indicating that the full nuclear core deformation is achieved even at about 9^0 - 12^0 for each isotopes example for Sm, Gd and Dy. It is clear from the Fig. 3.1 that there is little scattering of data for fixed values of N i.e. the asymmetry parameter is having smooth dependence on N.

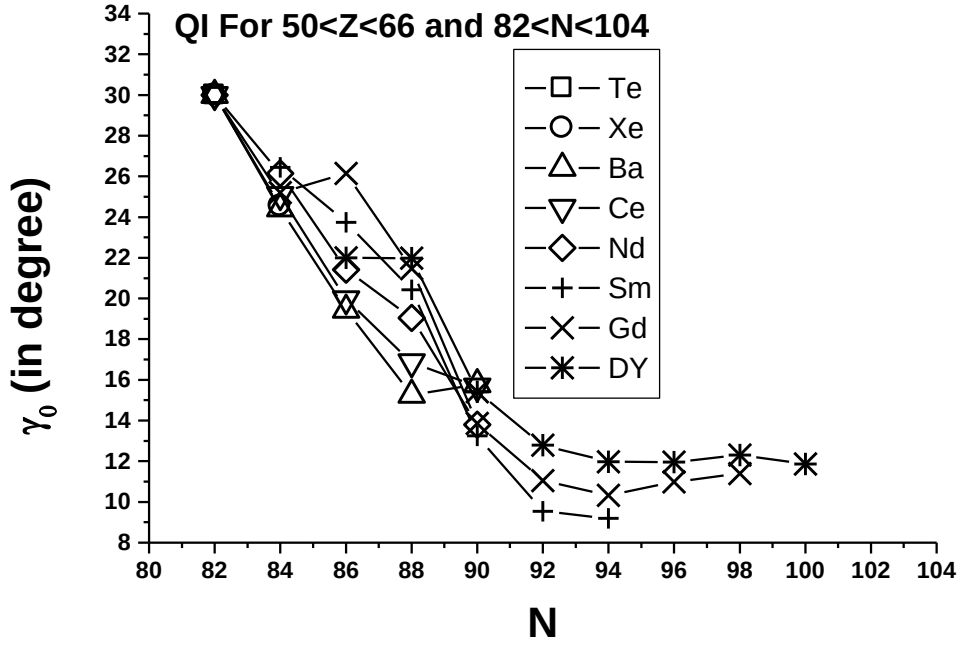

Fig.3.1 The variation of asymmetry parameter (γ_0) vs. Neutron number (N) for Quadrant I for 50≤Z≤66 and 82≤N≤104 region.

However, the data points of asymmetry parameter have much scattering for a fixed values of N_B, for example for a fixed value of N_B = 6 there is variation in the values of γ_0 from 15^0 to 26^0 (see Fig.3.2) and indicating very week dependence of asymmetry parameter on N_B. The asymmetry parameter rises for N=84, 86 and 88 with little increasing slop for N=84 and fast increasing slop for N=86 and 88 with increasing N_B and for N=90 there is a small fall instead, and which finally saturates for N≥92, that is for N_B≥12 (see Fig. 3.2). It is also evident that the asymmetry parameter decreases sharply on increasing the value of N_B from 2 to 12 for each value of Z with almost same slope for Xe, Ba, Ce, Nd, Sm, Gd and Dy elements for 82≤N≤90 region. But the individual curve of each element has been shifted towards right while Z is increased.

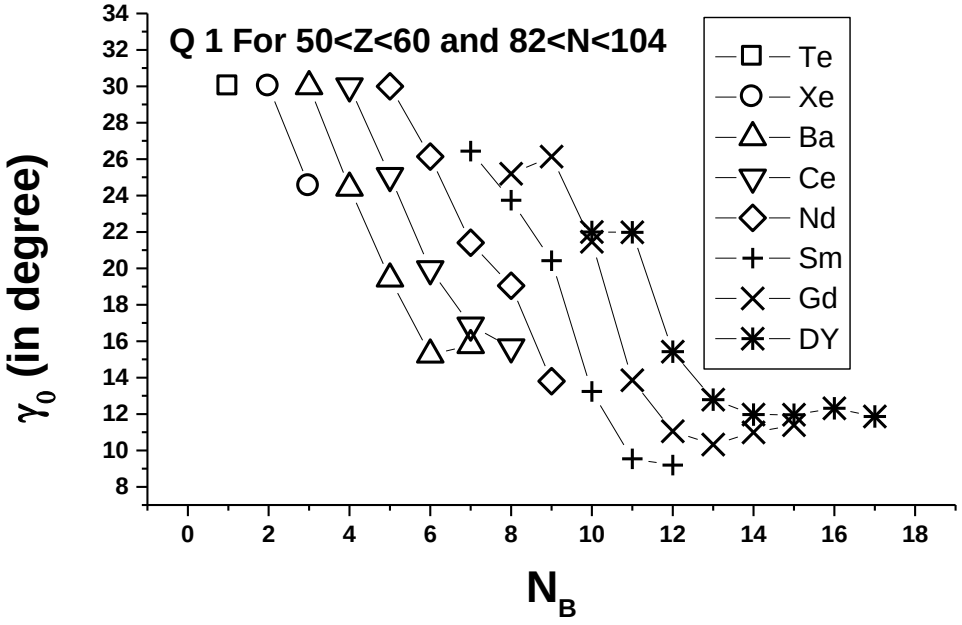

Fig.3.2 The variation of asymmetry parameter (γ_0) vs. Boson number (N_B) for Quadrant I for 50≤Z≤66 and 82≤N≤104 region.

The variation of asymmetry parameter γ_0 versus Np.Nn has been shown in Fig. 3.3. The γ_0 decreases from a maximum value of 30° for $N_pN_n = 0$ (i.e. SU(5) limit of IBM Casten (1990) to a minimum values of about 9° (i.e. SU(3) limit of IBM). The γ_0 saturates for $N_pN_n \geq 30$. It is evident that the asymmetry parameter also rises for N=84, 86 and 88 isotones with little increasing slop for N=84 and fast increasing slop for N=86 and 88 with increasing NpNn and for N=90 there is a small fall instead, and finally γ_0 saturates for N≥92, that is for NpNn ≥30. The same feature was observed for the E_{2g} in quadrant I by Kumar (2013) and Kumar et al. (2012). But this effect was in reverse order for the ground state moment of Inertia ($\theta_g = 1/ E_{2g}$) and energy ratio R_4 (= E_{4g}/ E_{2g}) by Kumar (2013) and Kumar et al. (2012).

These variations in rising slopes of N=84, 86 and 88 versus the product NpNn in Fig. 3.3 arise on account of the Z=64 proton subshell gap. Ogawa et al.(1978) noted the Z=64 sub-shell effect in ^{146}Gd. The role played by the Z=64 subshell effect in Nd-Sm-Gd-Dy nuclei had been stressed earlier by Casten (1985), Casten et al. (1996) and Gupta (1993). It is evident here that the smooth dependence of asymmetry parameter γ_0 on NpNn is confined to N>90 region (see Fig. 3.3), where

the Z=64 subshell effect disappears, unless one uses the effective proton bosons Np number for N<90.

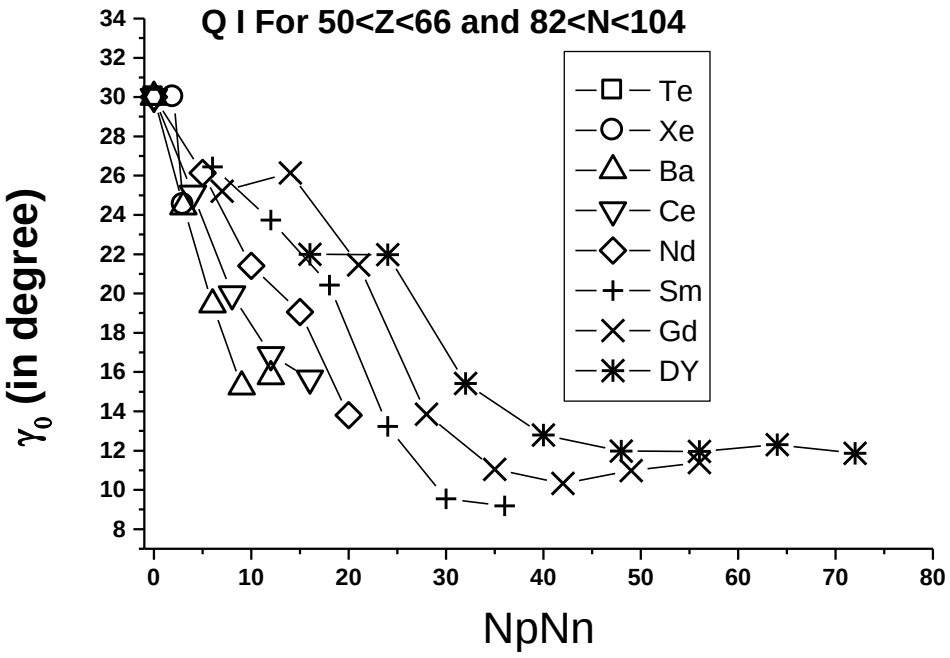

Fig.3.3 The variation of asymmetry parameter (γ_0) vs. N_pN_n for Quadrant I for 50≤Z≤66 and 82≤N≤104 region.

This shows non-dependence of γ_0 with N_pN_n because for a fixed value of N_pN_n the γ_0 is having varying values. It is clear from the Figs. 3.1-3.3 that the asymmetry parameter γ_0 vividly display the formation of isotonic multiplets in quadrant-I which supports the observation of Gupta et al. (1990b) who had illustrated it in a different way and Kumar (2013), Kumar et al. (2012).

3.3.2 The variation of asymmetry parameter γ_0 for quadrant-II for 66≤Z≤82 and 82≤N≤104:

The systematic variation of asymmetry parameter γ_0 versus N, N_B and NpNn for quadrant –II are shown in Fig. 3.4, Fig. 3.5 and Fig. 3.7, respectively. It is evident from Fig. 3.4 that the γ_0 decreases sharply from 30^0 to 12^0 as N increases from 82 to 94 for Dy, Er and Yb isotopes indicating that the shape phase transition takes place from Vibrational (VM) to rotational (RM) limit of collective model of Bohr and

Mottelson (1975) and also SU(5) or O(6) limit to SU(3) limit of IBM Casten (1990) as observed in quadrant-I. If N is increased from 94 to 98, γ_0 does not change and remains saturated indicating that the full deformation is achieved even at about $\approx 12^0$ and $\approx 13^0$ for each isotopes example for Dy and Er isotopes, respectively. However, for Yb and Hf isotopes the nature of the asymmetry parameter γ_0 is different because it goes on decreasing 21^0 to 8^0 for Yb and from 18^0 to 10^0 for Hf while N increases from 90 to 104 for Yb and from 94 to 104 for Hf isotopes. It indicates that for Yb and Hf isotopes the asymmetry parameter γ_0 goes on decreasing i.e. nuclear core deformation increases when the neutrons number (N) is increased from 82 to 104, i.e. till the shell is half filled. The point of Os and Pt are away from the line of general trend. It is clear from the Fig. 3.4, that there is much scattering of data points for fixed values of N i.e. the asymmetry parameter is not having smooth dependence on N.

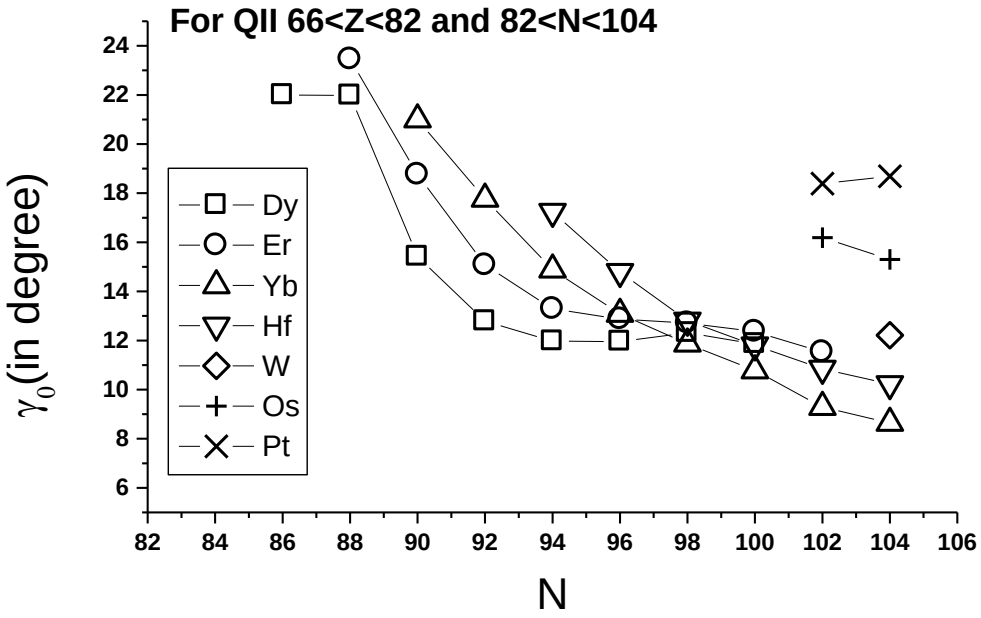

Fig. 3.4 The variation of asymmetry parameter (γ_0) vs. Neutron number (N) for Quadrant II for 66≤Z≤82 and 82≤N≤104 region.

The data points of asymmetry parameter are overlapping on each other for Dy - W isotopes (see Fig. 3.5) for N_B = 12 and 13. For N_B= 11 to16 the data points of Yb and Hf isotopes are overlapping on each other and the value of asymmetry parameter for these nuclei goes on decreasing till N_B approaches 16. The data points of Dy and

Er are also overlapping for N_B=13-17 and the value of asymmetry parameter are independent of N_B. It indicates that the Dy and Er nuclei have different nature of nuclear deformation than Yb and Hf isotopes for this region. The Os and Pt data points are above the uniform pattern curve indication different nature of these nuclei. For this region (quadrant-II), the data points of asymmetry parameter have less scattering for a fixed value of N_B in comparison to quadrant-I (see Fig. 3.2). The Fig. 3.5 is indicating a week dependence of asymmetry parameter on N_B.

The variation of asymmetry parameter γ_0 vs. Np.Nn has been shown in Fig. 3.6. The γ_0 decreases fast at first and gradually later while NpNn is increasing; and remains unchanged for NpNn≥45 for Dy and Er isotopes for which the proton boson pair Np decreases from 8 to 7; and decreases for Yb and Hf on increasing NpNn beyond 45 for which the proton boson pair Np decreases from 6 to 5. The two data points of Os and one of W are lying on the smooth curve while for Pt the data point are slightly below the uniform curve.

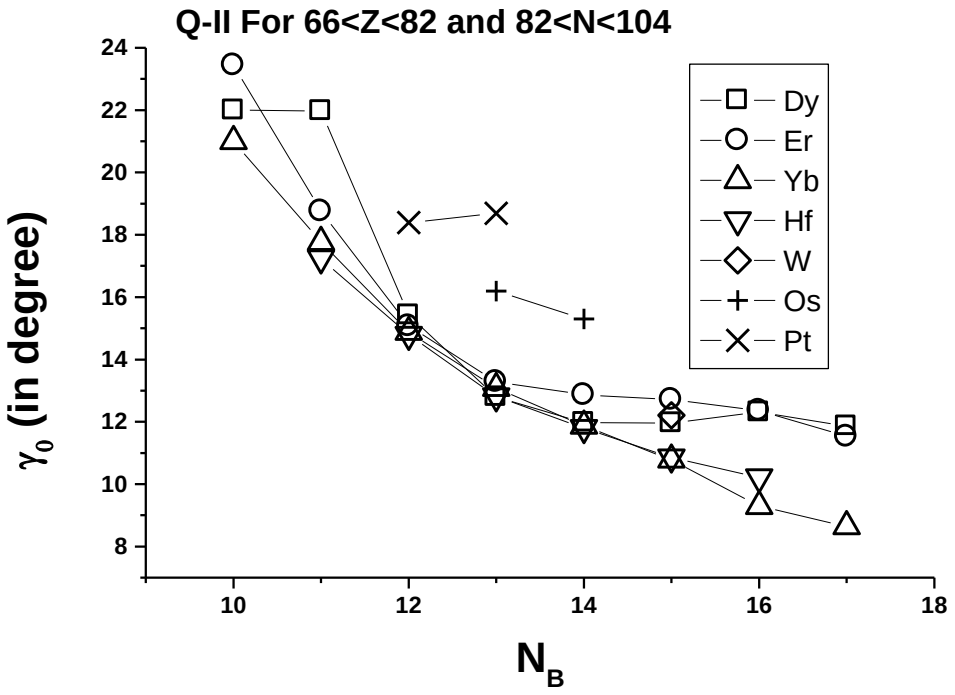

Fig. 3.5 The variation of asymmetry parameter (γ_0) vs. Boson number (N_B) for Quadrant II for 66≤Z≤82 and 82≤N≤104 region.

One important point is to be noted here that the asymmetry parameter γ_0 is calculated from the values of E_{2g} and $E_{2\gamma}$ and the nature of variation of $E_{2\gamma}$ verses N is different for Dy and Er isotopes than Yb and Hf as shown in Fig. 3.6. The $E_{2\gamma}$ remains almost constant for Dy and Er isotopes for N=88-102 but for Yb and Hf it increases sharply as N increases from N=94-104 and becomes maximum for N=104. This effect is reflected here and the value of asymmetry parameter remains constant and (i.e. above the usual trend) for Dy and Er isotopes for NpNn≥45 as stated above. The same feature of $E_{2\gamma}$ state had been observed with NpNn by Kumar (2013). There is a smooth dependence of asymmetry parameter γ_0 with NpNn in quadrant –II.

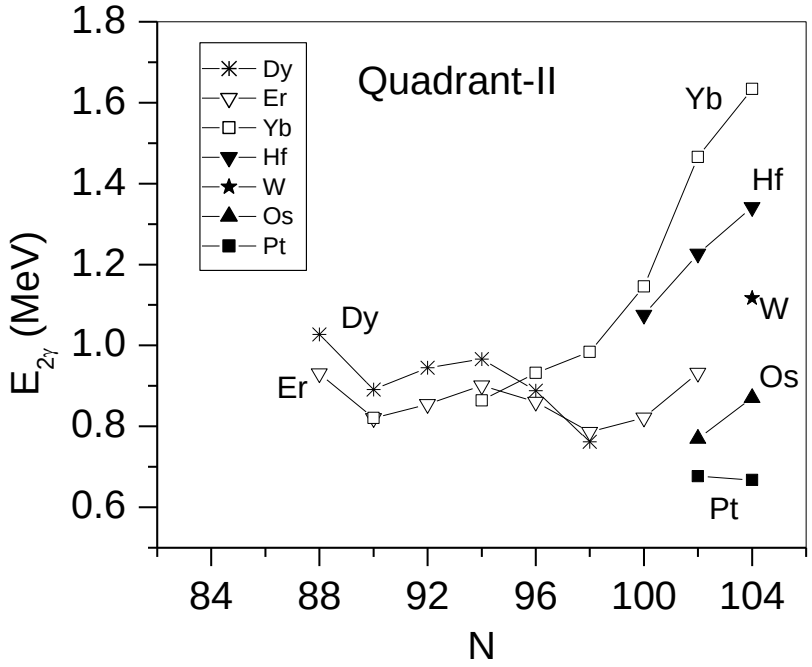

Fig. 3.6 The variation of the energy of E2γ state vs. N for Quadrant II for 66≤Z≤82 and 82≤N≤104 region.

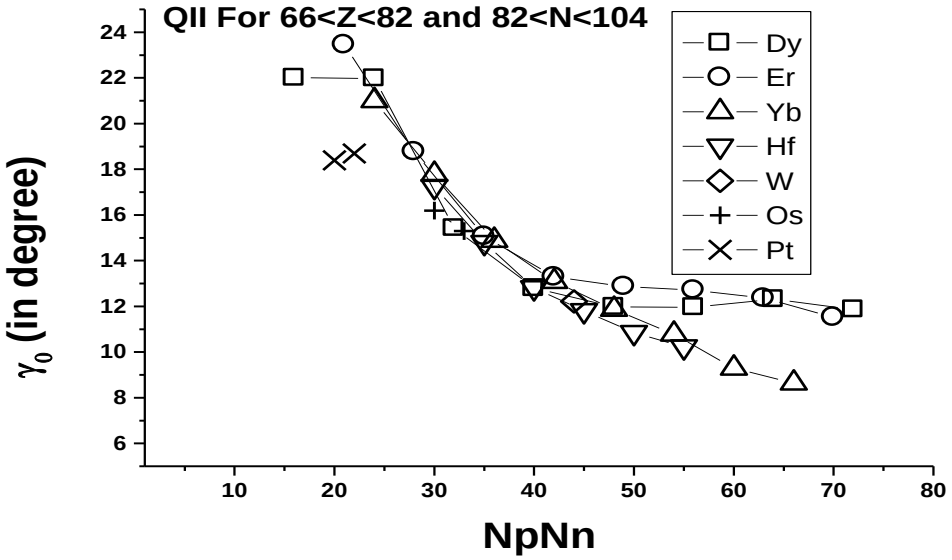

Fig. 3.7 The variation of asymmetry parameter (γ_0) vs. N_pN_n for Quadrant II for 66≤Z≤82 and 82≤N≤104 region.

3.3.3 The variation of asymmetry parameter γ_0 for quadrant-III for 66≤Z≤82 and 104≤N≤126:

The variation of asymmetry parameter γ_0 versus N, N_B and NpNn for quadrant –III are shown in Fig. 3.8, Fig. 3.9 and Fig. 3.10, respectively. In Fig. 3.8, the asymmetry parameter increases/decreases with increasing N in different style for different value of proton number Z. For Yb and Hf the curves are almost horizontal with little curvature. In W (Z=74, Np=4) and Os (Z=76, Np=3) the curve fall very slowly for N=104 to 108 (attains minimum value of γ_0 at N=108) and rises significantly when N increases beyond 108. In case of Os the asymmetry parameter decreases while N increases from 116 to 118. The nature of curve is different for Pt (Z=78, Np=2) it initially increases sharply while N increases from 104 to 112 and becomes horizontal for N=110-122. For Hg (Z=80, Np=1) the curve is almost horizontal with little curvature for N=108-116 beyond that it significantly decreases while N increasing from 116 to 120 and again increases while N increases from 120 to 122. The feature of E_{2g} vs. N had been reported for W isotopes for quadrant –III by Kumar (2013).

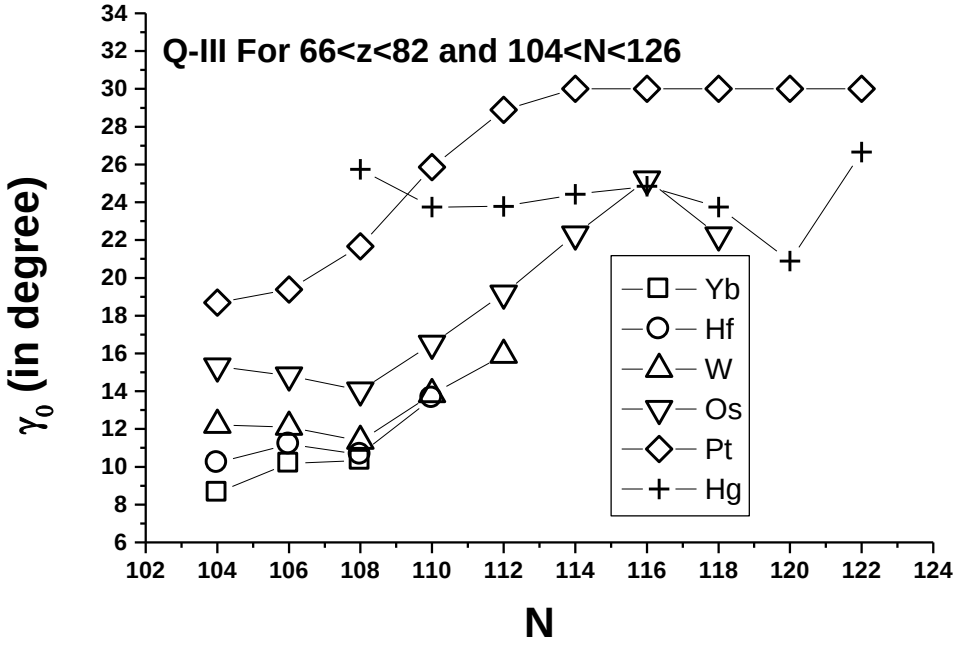

Fig. 3.8 The variation of asymmetry parameter (γ_0) vs. Neutron number (N) for Quadrant III for 66≤Z≤82 and 104≤N≤126 region.

The variation of asymmetry parameter γ_0 versus N_B is shown in Fig. 3.9. The γ_0 decreases with increasing N in different style for different value of proton number Z. For Pt, the γ_0 is independent of N_B for $4 \leq N_B \leq 10$ the curve is horizontal (with $\gamma_0 = 30^0$) and γ_0 decreases sharply on increasing N_B beyond 10. The curve for Pt is lying above the observed curve for other isotopes except Hg for which the curve is almost horizontal with little curvature except for N_B =4. For Yb – Os isotopes the asymmetry parameter has N_B dependence with little scattering for Os and W isotopes as discussed above.

The variation of asymmetry parameter γ_0 versus NpNn is shown in Fig. 3.10. The value of γ_0 decreases with increasing NpNn (going towards the mid shell) and provide a single broken curve (except for Hg isotopes with Z=80, Np=1) indication that the values of γ_0 are slightly different for different Z. For quadrant –III, the Nn and Np both are the hole boson pairs and the value of both decreases as we go towards closed shell i.e., right to left in Fig. 3.9. The strong dependence of asymmetry parameter with NpNn is evident in the quadrant-III.

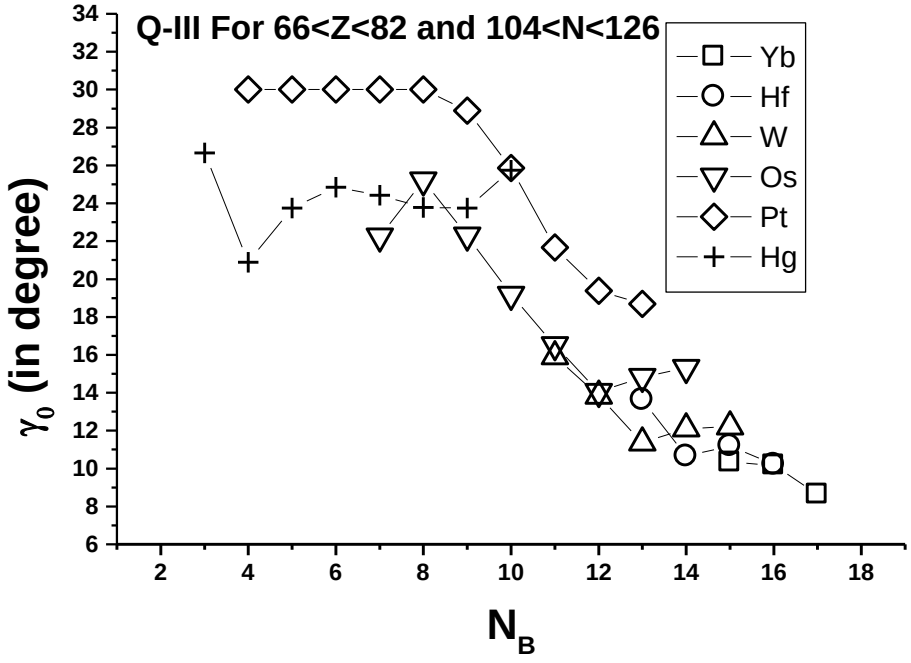

Fig. 3.9 The variation of asymmetry parameter (γ_0) vs. Boson number (N_B) for Quadrant III for 66≤Z≤82 and 104≤N≤126 region.

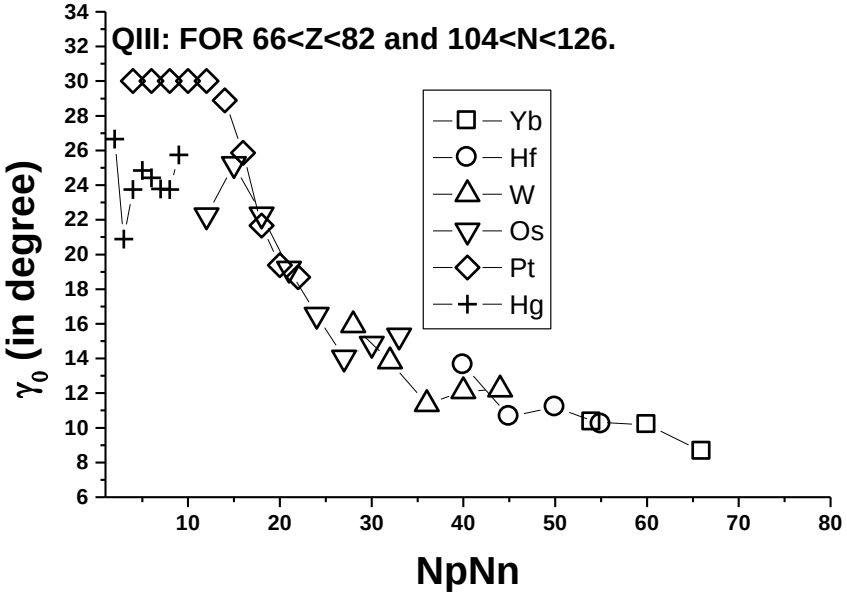

Fig. 3.10 The variation of asymmetry parameter (γ_0) vs. N_pN_n for Quadrant III for 66≤Z≤82 and 104≤N≤126 region.

3.4 CONCLUSION

The NpNn scheme is very useful in considering the systematic behavior of asymmetry parameter (γ_0) which gives the information of nuclear structure of atomic nuclei in a medium and light mass region, i.e. change in product NpNn are correlated with the change in nuclear structure. The NpNn product is a good measure of its effect in producing the deformation in atomic nuclei. This product is also an indicator of the n-p interaction among the valance proton and/or neutron nucleons causing the deformation of nuclear core.

In quadrant-I for $50 \leq Z \leq 66$ and $82 \leq N \leq 104$ and quadrant-II for $66 \leq Z \leq 82$ and $82 \leq N \leq 104$ region, the asymmetry parameter γ_0 decreases from 30^0 in Q-I and from 22^0 in Q-II to 9^0- 10^0 with increasing N from 82 to 104 (i.e. the mid of N=82 to 126 neutron shell), signifying that the nuclear deformation (β) is increasing, while the energy ratio R_4 increase from 2.0 (for harmonic vibrators or SU(5) type nuclei) to 3.33 (for good rotors or SU(3) type nuclei). This indicates that in this region the nuclear structure depends much more on Z. The values of asymmetry parameter in Q-I, shows shape phase transition at N=88-90 and regions (QII-III) have a systematic dependence with N, but having different patterns. Partial results of this study have been presented in the DAE Symposium on Nuclear Physics Kaushik and Sharma (2014).

In quadrant-I, the asymmetry parameter is having more correlated dependence on the neutron number N, rather than on the product NpNn. In this quadrant- I, the Z=64 sub-shell effect for $N \leq 90$ nuclei affect the variation of asymmetry parameter with N and NpNn product. Casten (1985) and Casten et al. (1996) obtained a smooth dependence of various observables with NpNn by adopting effective numbers proton bosons Np for $N \leq 90$ nuclei. This was a very useful procedure for obtaining the universal smooth curves for various regions with NpNn. The present studies also confirm the observations of Gupta et al. (1990b), Kumar (2013), Kumar et al. (2012) and Sharma and Kumar (2010) i.e. the existence of isotonic multiplets in quadrant-I.

The existence of X(5) symmetry in N=90 isotones established in recent works supports the formation of isotonic multiplets in this work. The calculated values of asymmetry parameter are almost constant for N=90 isotones e.g. 13.8^0 for Nd, 13.24^0 for Sm and 13.86^0 for Gd; which support the findings of Gupta (2012a); who gave the microscopic explanation for the constant structure of N=90 isotones. This is certainly different from the universal NpNn scheme Casten (1985) and Casten and Zamfir (1996) and found to be very useful for most of the atomic nuclei throughout the periodic table as noticed by Casten and Zamfir (1996). This special condition for N=90 isotones is made more explicit in the present work for Q-I and supports the findings of Casten and Zamfir (1996).

The systematic dependence of asymmetric parameter on NpNn has strong dependence in quadrant-II. In Q-II, the line of β- stability runs nearly diagonally, i.e. parallel to N_B (where, N_B is the sum of proton hole bosons and neutron particle bosons) and leading to the formation of F-spin multiplets. The same feature had been observed earlier for E_{2g} by Kumar et al. (2012) and Sharma and Kumar (2010).

In quadrant-III, for $66 \leq Z \leq 82$ and $104 \leq N \leq 126$ region, the variation of asymmetry parameter is different from quadrant I and II because the asymmetry parameter γ_0 increases sharply from 9^0 - 10^0 to 30^0 with increasing N from 104 to 126. This is signifying that the nuclear deformation (β) is decreasing and the nuclear structure changes from pure rotor SU(3) type to vibrational SU(5) or γ-unstable O(6) type. Further, the asymmetry parameter for different elements has smooth curve with NpNn with almost same slopes except for Hg isotopes.

The graphs of asymmetry parameter against N_pN_n vividly display the formation of isotonic multiplets in quadrant-I, strong dependence on N_pN_n in quadrant-II and weak constancy with Z in quadrant-III is illustrated and support the findings of Gupta (2012b). Also in every case the role of N, Z is well evident. This also agrees with known variation of nuclear deformation in the light and medium mass region. The quadrant wise presentation of asymmetry parameter is very useful as in case of other observables of collectivity and deformation i.e. the energy of first excited state E_{2g}, the energy ratio R_4, the B(E2; $0_1^+ \rightarrow 2_1^+$) value and ground state band moment of inertia ($\theta_g = 3/E_{2g}^+$) as noted by Kumar (2013), Kumar et al. (2012) and Sharma and Kumar (2010).

Table 3.1: The calculated values of asymmetric parameter (γ_0) for Te to Ce nuclei using equation 3.2.

N	Te	Xe	Ba	Ce
82	30	30	30	30
84		24.52	24.42	25.07
86			19.43	19.95
88			15.26	16.86
90			15.78	15.66

Table 3.2: The calculated values of asymmetric parameter (γ_0) for Nd to Pt nuclei using equation 3.2.

N	Nd	Sm	Gd	Dy	Er	Yb	Hf	W	Os	Pt	Hg
82	30.0										
84	26.14	26.44	25.2								
86	21.41	23.74	26.14	22							
88	19.05	20.42	21.46	21.98	23.45						
90	13.8	13.24	13.86	15.42	18.76	21					
92		9.54	11.05	12.79	15.07	17.77					
94		9.19	10.32	11.97	13.29	14.88	17.24				
96			10.98	11.96	12.87	13.08	14.79				
98			11.39	12.31	12.71	11.87	12.81				
100				11.86	12.36	10.78	11.8				
102					11.53	9.29	10.85		16.19	18.39	
104						8.64	10.22	12.21	15.3	18.69	
106						10.18	11.19	12.1	14.83	19.39	
108						10.33	10.66	11.37	14.04	21.67	25.74
110							13.63	13.83	16.5	25.87	23.74
112								15.91	19.16	28.89	23.78
114									22.3	30	24.42
116									25.21	30	24.85
118									22.24	30	23.74
120										30	20.89
122										30	26.65

CHAPTER-IV

SYSTEMATIC STUDY OF B(E2; 4g→2g)/ B(E2;2g→0g) BRANCHING RATIO USING ASYMMETRY ROTOR MODEL AND ITS VARIATION WITH N AND Z

4.1 INTRODUCTION

The concept of collectivity in atomic nuclei is one of the most fundamental findings in history of nuclear structure physics. The macroscopic, microscopic and geometrical nuclear models have been applied to describe this collective behavior of nuclei. The geometrical models depicting the atomic nucleus as a liquid drop with a given nuclear shape and algebraic models, take into account the pairs of proton and/or neutron only. Despite the often very dissimilar theoretical approaches, most of the collective models have some common basic features, such as predictions of energies of g- band, β- band, γ- band and other higher multi-phonon bands or B(E2) values and B(E2) ratios for inter and intra band transitions, which have been observed in a wealth of nuclei away from closed shells.

The energy ratio R_4 (=E_{4g}/ E_{2g}) is a key observables which can be used to assess the collectivity of nuclei and it is equal to 2.0 for an ideal spherical harmonic vibrator i.e., SU(5) limit and 3.33 in an axially symmetric deformed rotor, i.e. SU(3) limit of interacting boson model (IBM) of Iachello and Arima (1987) and Casten (1990). Bohr and Mottelson (1975) pointed out that the inter/ intra band transition rates provide another good measure of nuclear collectivity, which is less sensitive to anharmonicities than energies of various bands. The B(E2;4_g→2_g)/B(E2;2_g→0_g) branching ratio is a particularly good example, as it is 2.0 in the spherical limit or SU(5) and 1.42 in the deformed limit or SU(3) of IBM Iachello and Arima (1987). Significant deviations from these two limiting values can be found; if one considers very small numbers of valence neutrons (Nn) and/or protons (Np), which are used in

the IBM; also in asymmetric rotor model (ARM) of Davydov and Filippov (1958) where asymmetric parameter (γ_0) changes from 0^0 to 30^0 which corresponds to above mentioned two limits of IBM i.e. SU(3) and SU(5) respectively.

In the present chapter, we have compiled the experimental data of $B(E2;4_g \rightarrow 2_g)/B(E2;2_g \rightarrow 0_g)$ branching ratio from the website of Brookhaven National Laboratory(http://www.nndc.bnl.gov) for medium mass region (Nd - Hg) and listed in Table 4.1. The observed data is compared with the ARM predictions for asymmetric parameter (γ_0) equals to 0^0 to 30^0. The SU(3) and SU(5) limits are also included to get new information about the structure. The systematic dependence of $B(E2;4_g \rightarrow 2_g)/B(E2;2_g \rightarrow 0_g)$ with N and Z are also carried out to find out a definite conclusion regarding nuclear structure.

4.2 ASYMMETRIC ROTOR MODEL

Davydov and Filippov (1958) investigated the energy levels corresponding to rotation of nucleus which does not change its internal state. They established that the violation of axial symmetry of even –even nuclei affect the rotation spectrum of axial nucleus with appearance of some new rotational states having total angular momentum of 2, 3, 4,⋯. If the deviation from axial symmetry is small, then these levels lie very high and are not excited. The energy of rotation of a non-spherical even-even nucleus is given, in the adiabatic approach, by Schrödinger eq.:

$$(H - E)\Psi = 0 \tag{4.1}$$

where E is measured in units of $\frac{\hbar^2}{4B\beta^2}$, and the operator H is given by the formula:

$$H = \frac{1}{2}\sum_{\lambda=1}^{3} J_\lambda^2 \, sin^{-2}(\gamma_0 - \frac{2\pi\lambda}{3}) \tag{4.2}$$

where J_λ are the projection of the total angular momentum along the axes of a coordinate system fixed in the nucleus. The wave function corresponding to the state with total moment J, can be represented as:

$$\psi_{JM} = \Sigma_{K\geq 0} |JK\rangle \, A_K \tag{4.3}$$

$$\text{where } |jk\rangle = [\frac{(2J+1)}{16\pi^2}(1+\delta_{KO})]^{\frac{1}{2}} \{D^J_{MK} + (-1)^J D^J_{M,-K}\} \tag{4.4}$$

The function D^{J}_{MK} in eq. (4.4) is the function of the Euler angles that determine the orientation of the principal axis of the nucleus with respect to the laboratory space. It can be shown that the wave functions (4.3) from the basis of totally symmetric representation of the group D_2, the elements of which are the rotation through 180^{o} around each of three principal axes of the nucleus Davydov and Filippov(1958) and Davydov and Rostovsky (1959).

The values of first excited state E_{21} and second 2+ state i.e. E_{22} can be written as (in unit of $\hbar^2/4B\beta^2$):

$$E_{21} = \frac{9\left[1-\sqrt{\left\{1-\frac{8sin^2(3\gamma_0)}{9}\right\}}\right]}{Sin^2(3\gamma_0)} \tag{4.5}$$

$$E_{22} = \frac{9\left[1+\sqrt{\left\{1-\frac{8sin^2(3\gamma_0)}{9}\right\}}\right]}{Sin^2(3\gamma_0)} \tag{4.6}$$

The value of asymmetry parameter can be obtained using the Eqs. (4.5) and (4.6) and the asymmetric parameter (γ_0) become:

$$\gamma_0 = \frac{1}{3}\sin^{-1}\{\frac{9}{8}[1-\left(\frac{R_\gamma-1}{R\gamma+1}\right)^2\}^{1/2}, \text{ where } R_\gamma = \frac{E_{22}}{E_{21}} \tag{4.7}$$

4.2.1 Reduced Transition Probabilities

The reduced transition probability B(E2; $I_i \rightarrow I_f'$) between two numbers of the same rotational band with quantum number K is expressed as:

$$B(E2; I_K \rightarrow I'_K) = \frac{5}{16\pi} e^2 Q_0^2 |\langle I_2 K_0 | I' K\rangle|^2 \tag{4.8}$$

where we have used

$$\sum_{m1\ m2\ m3} |\langle I_1 I_2 M_1 M_2 | IM\rangle|^2 = (2I+1) \quad . \tag{4.9}$$

For Coulomb excitation, the B(E2), reduced transition probability in the case of symmetric rotor (even-even nuclei) is expressed;

$$B(E2; I_K \rightarrow I'_K) = \frac{5}{16\pi} e^2 Q_0^2 |\langle I_{200} | I'+2, 0\rangle|^2$$

$$B(E2; I_K \rightarrow I'_K) = \frac{5}{16\pi} e^2 Q_0^2 \frac{(I+1)(I+2)}{(2I+1)(2I+3)} \tag{4.10}$$

The non-spherical nuclei have rotational levels which are due to very fast electric quadrupole transition probability B(E2; I→I′). According to equation (4.10), B(E2;

$I_i \rightarrow I_f'$) increases as the value of intrinsic quadrupole moment Q_0 increases. If the transition takes place between the ground state (I=0) and the first excited state (I=2) of nuclei, then

$$B(E2) = \frac{5}{16\pi} e^2 Q_0^2 \quad (4.11)$$

For transition between rotational level of spin I=2 and I=0, the BE(2) value can be expressed (in unit of $e^2Q_0^2/16\pi$):

$$B(E2;2_1 \rightarrow 0_1) = B(E2; 2_1 \rightarrow 0_1)/ e^2Q_0^2/16\pi = (1/2)\{1+ [(3-2\sin^2(3\gamma_0)/ (9-8\sin^2(3\gamma_0)^{1/2}]\} \quad (4.12)$$

Where the intrinsic quadrupole moment of an axial nucleus with nuclear core deformation β is:

$$Q_0 = 3ZR^2\beta/ (5\pi)^{1/2}. \quad (4.13)$$

Also the B(E2) value for other transitions can be written as:

$$B(E2;4_i \rightarrow 2_f) = 5/126 [\cos\gamma_0 (6A_{0i} A_f + \sqrt{35}A_{2i} B_f) + \sin(\sqrt{15}A_{2i}A_f + A_{0i}B_f + \sqrt{35}A_{4i}B_f)]^2$$

where, A_f and B_f are the coefficients that determine the wave functions of spin 2_1^+ and A_λ coefficients determine the wavefunction of spin 4_{1+}. Using the values of coefficients determined the wavefunctions, one can calculate the probabilities of electric quadrupole transitions between various rotational states of the nucleus. The ARM $B(E2;4_g \rightarrow 2_g)/B(E2;2_g \rightarrow 0_g)$ branching ratio is deduced from eqs. (4.12, 4.14) using asymmetric parameter (γ_0) from equation (4.7).

4.2.2.Calculation of Asymmetric Parameter (γ_0)

The values of asymmetry parameter (γ_0) are evaluated using eq. (4.7) by puting the the experimental energies of $E2_2^+$ (=E_{22}) and $E2_1^+$ (=E_{21}) states which are taken from the website http://www.nndc.bnl.gov . It can also be evaluated using:

(a) The energy ratio $R_4=(E_{4g}/E_{2g})$ but only the nuclei with $2.8 \leq R4 \leq 3.33$ will be allowed Sharma (1989) and Gupta and Sharma (1989).

(b) The B(E2) values which are very small and available with uncertainties.

Therefore the values from energy ratio Rγ are more reliable. The calculated values of asymmetry parameter (γ_0) for all nuclei of medium mass region are used to calculate the $B(E2;4_g \rightarrow 2_g)/B(E2;2_g \rightarrow 0_g)$ branching ratio.

4.3 RESULT AND DISCUSSIONS

4.3.1 Variation of ARM $B(E2;4_g \rightarrow 2_g)/B(E2;2_g \rightarrow 0_g)$ ratio versus asymmetry parameter (γ_0)

The variation of B(E2;4g→2g)/ B(E2; 2g→0g) ratio from ARM vs. γ_0 is shown in Fig. 4.1. The ARM data points are shown by hollow circles and the vibrational or SU(5) limit at 2.0 and rotational or SU(3) limit at 1.4 are shown by dotted lines for useful comparison. It is clear from the figure that the ARM predictions are very close to the SU(3) limiting value and also it is increases very slowly on increasing γ_0 from 0^0 to 20^0 forming a peak at 20^0 and decreases slowly beyond 20^0 approaches 1.4 which is SU(3) limiting value at $\gamma_0 \approx 27^0$. The ARM ratio is away from vibration model limit of 2.0 this shows that it cannot explain the vibrational nature of the nuclei.

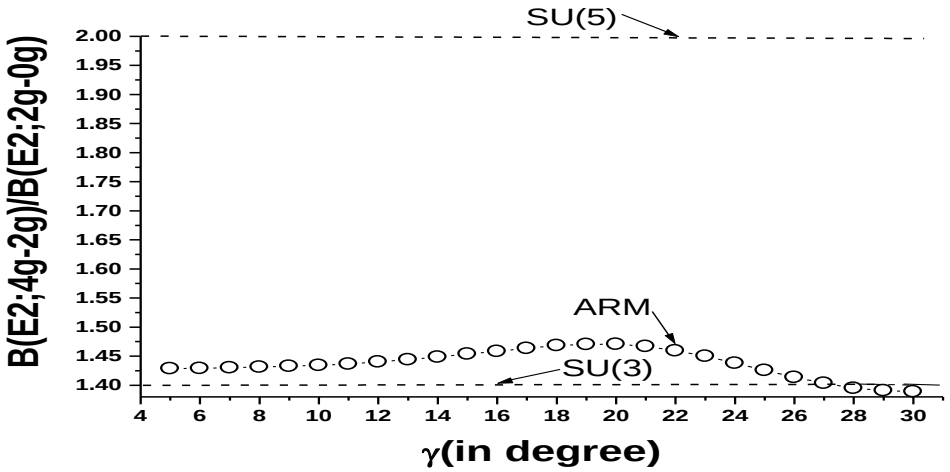

Fig.4.1 The Variation of B(E2;4g→2g)/ B(E2; 2g→0g) ratio from ARM (shown by hollow circles) vs. asymmetry parameter (γ_0) in degree. The vibrational limit SU(5) at 2.0 and rotational limit SU(3) at 1.4 are shown by dotted lines for comparison.

4.3.1.1 Variation of Experimental and ARM $B(E2;4_g \rightarrow 2_g)/B(E2;2_g \rightarrow 0_g)$ ratio versus Asymmetry Parameter (γ_0)

The variation of B(E2) ratio from experiment and ARM with γ_0 is shown in Fig.4.2. The ARM data points are shown by solid triangles and SU(5) limit at 2.0 and SU(3) limit at 1.4 are shown by dotted lines. Two nuclei are having B(E2) ratio anomalously more than 2.0 and not shown in the Fig.4.2, e.g. ^{182}Hg and ^{184}Hg for them the $B(E2;4_g \rightarrow 2_g)/B(E2;2_g \rightarrow 0_g)$ ratios are 4.6(3) and 2.8(8) respectively. There are some other nuclei in medium mass region those are having this ratio anomalously lesser than 1.4 i.e. SU(3) limiting value e.g., ^{150}Nd, ^{164}Dy, ^{164}Er, 168W, ^{182}W, ^{184}W, ^{192}Os, ^{180}Pt and ^{198}Hg having values 1.31(10), 1.30(7), 1.18(13), 1.1(3), 1.386(20), 1.30(9), 1.22(4), 0.92(22) and 0.375(18) respectively. It is noted that in medium mass region (Nd-Hg), this B(E2) ratio is smallest in case of ^{198}Hg [=0.375(18)] which is non magic nucleus with only two vacancy of protons for Z=82. This ratio is also very small in case of $^{144}Nd_{84}$ [=0.73(9)]; which is also a non- magic nucleus; which has only two valence neutrons outside N=82. It supports the findings of Cakirli et al (2004) that the value of this B(E2) ratio is anomalously small in non magic nuclei, as it cannot be explained with collective approaches. The values of $B(E2;4_g \rightarrow 2_g)/B(E2;2_g \rightarrow 0_g)$ ratios for N=88 isotones (Nd, Sm, Gd, Er) are lying between SU(3) and SU(5) limits indicating the shape phase transition for these nuclei. However the nature of the Dy_{88} is different and its value is close to SU(3) limit. Other data points are lying between SU(5) and SU(3) limits. While the ARM predictions are very close to the SU(3) limit.

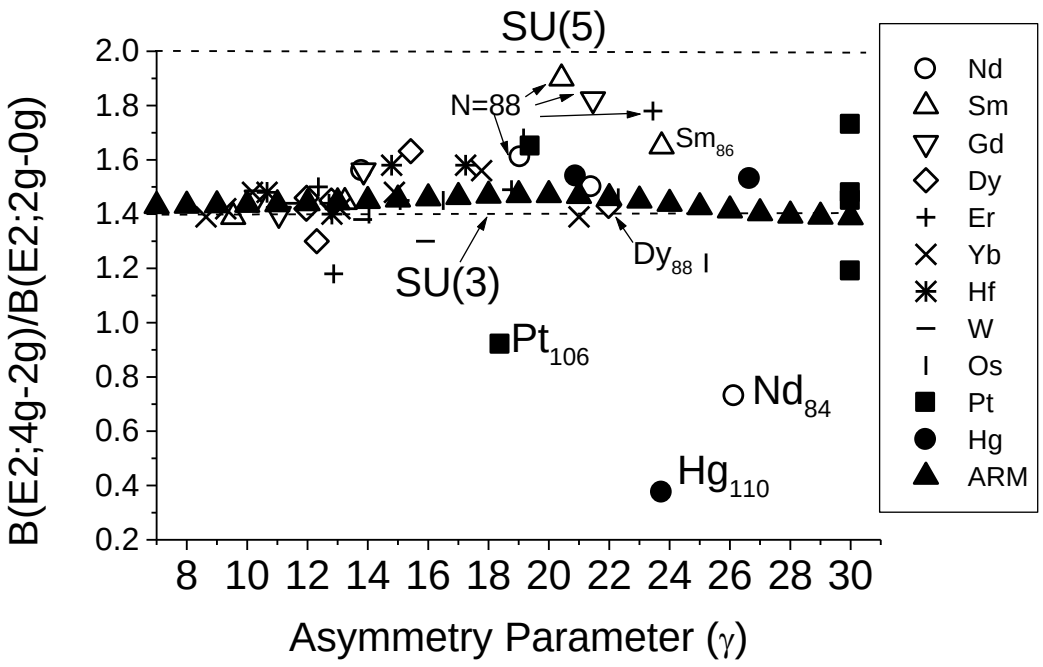

Fig.4.2 The Variation of experimental B(E2;4g→2g)/ B(E2; 2g→0g) ratio vs. asymmetry parameter (γ_0) in degree. The vibrational limit SU(5) at 2.0 and rotational limit SU(3) at 1.4 are shown by dotted lines for comparison. The ratio from ARM is shown by solid triangles.

4.3.1.2 Conclusions

The predictions of asymmetric rotor model (ARM) of Davydov and Filippov(1958) for B(E2;4g→2g)/B(E2;2g→0g) branching ratio are compared with the experimental data in medium mass region. It is found that the observed data point of this ratio for N=88 isotones (Nd, Sm, Gd, Er) are indicating the shape phase transition from an ideal spherical harmonic vibrator or SU(5) to an axially symmetric deformed rotor or SU(3). It is also noted that this B(E2) ratio is anomalously small in case of two non- magic nuclei i.e., $^{198}_{80}Hg_{118}$ [=0.375(18)] and $^{144}_{60}Nd_{84}$ [=0.73(9)] with only two vacancy of protons for Z =82 and two valence neutrons outside N=82, respectively; which supports the findings of Cakirli et al (2004). The data points for other nuclei are lying between SU(5) and SU(3) limits. The calculated B(E2) ratios of ARM are very close to the SU(3) limit of IBM indicating that it can

explain the structure of only well deformed nuclei. Therefore the ARM is partially successful in explaining this branching ratio.

4.3.2 SYSTEMATIC DEPENDENCE OF B(E2; 4g→2g)/ B(E2;2g→0g) BRANCHING RATIO ON N AND Z

4.3.2.1 Result And Discussions

4.3.2.1.1 The variation of experimental B(E2;4g→2g)/ B(E2; 2g→0g) ratio verses neutron number (N)

To avoid the overlapping of experimental data of the nuclei and to have a clear picture for a definite conclusion about the dependence of B(E2;4g→2g)/B(E2;2g→0g) ratio on N, the whole data is divided into two parts and shown in two figures i.e. Fig. 4.3 for Nd- Er nuclei and in Fig. 4.4 for Yb- Hg nuclei. The vibrational model or SU(5) limit at 2 and rotational model or SU(3) limit at 1.4 are shown in the Fig 4.3 and Fig. 4.4. The data points are joined for same value of Z, so that the effect of N will be visible.

For Nd, this ratio increases sharply from 0.73 to 1.61(maximum value at N=88) as N increases from 84 to 88 and if N is further increased from 88 to 92 it decreases slowly from 1.61 to 1.31(see Fig. 4.3). The same feature is observed for Sm, where this ratio increases from 1.65 to 1.9 on increasing N from 86 to 88 and beyond N=88 it drops sharply and approaches to Alaga value of 1.4 for N=92. In case of Gd, the BE(2) ratio decreases from 1.82 to 1.46 as N increases from 88 to 94. Also in Er, this ratio decreases from 1.78 to 1.5 as N increases from 88 to 100 and minimum value of 1.18 at N=96. Therefore, for N=88 (Sm, Gd and Er) isotones, this ratio ≈1.8 is very close to the VM limit of 2.0 indication vibrational nature. However for Dy (N=88, 92, 94, 96) this ratio is close to Alaga value indication deformed rotor nature and for N=90; Dy indicating transitional nature because this ratio (=1.63) is lying in between SU(5) and SU(3) limiting value (see Fig. 4.3).

For Yb and Hf nuclei, BE(2) ratio is ranging between 1.4 to 1.6 for different values of N and close to SU(3) limit (see Fig. 4.4). In case of W, the ratio increases sharply from 1.1(3) to 1.74(15) on increasing N from 94 to 100 and decreases very slowly on increasing N from 108 to 112 (almost remains around Alaga value).

For N=96 the data point of Os is close to the other N=96 isotones (Yb, Hf, W) data points. When N increases from 108 to 112, the ratio for Os increases from 1.4(4) to 1.68(11) and when N is increased from 112 to 116 the B(E2) ratio decreases from 1.68(11) to 1.22(4) indicating prolate to oblate shape-phase-transition as observed by Kumar and Baranger (1968).

For N=98, the B(E2) [=1.87(24)] for Pt is close to VM value and for N=102 the ratios is minimum [=0.92(22)]. The B(E2) ratio for Pt decreases from 1.65 to 1.56 when N increases 106 from 114 and again increases from 1.56 to 1.73 as N increases from 114 to 116(attains maximum value =1.73(11) at 116). If N is increased from 116 to 120 this ratio drops linearly with the same slope as observed for Os (N=112 to 116).This indicates the similar nature of Pt and Os nuclei for this region.

For two nuclei; ^{182}Hg and ^{184}Hg; the B(E2) ratio is 4.6(3) and 2.8(8) respectively; which are anomalously more than VM limiting value and not included in the Fig.2. The B(E2) ratio is smallest in case of ^{198}Hg; which is non magic nucleus; has only two vacancy of p+ for Z =82. This ratio is also very small in case of $^{144}Nd_{84}$ [=0.73(9)] (see Fig.4.3); which is also a non- magic nucleus; which has only two valence n^0 outside N=82. It supports the findings of Cakirli et al. (2004), that the B(E2;4g→2g)/B(E2;2g→0g) ratio is anomalously small in non magic nuclei, as it cannot be explained with collective approaches.

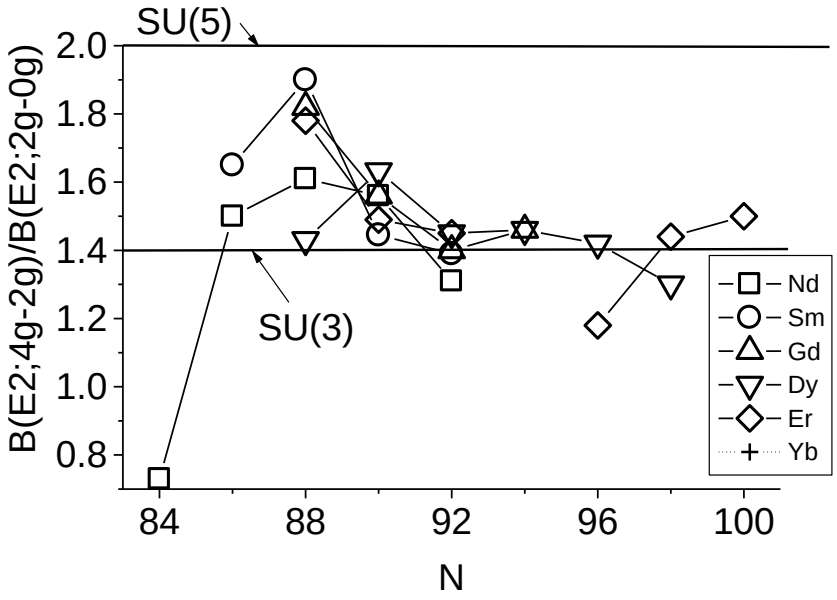

Fig.4.3: The variation of experimental B(E2;4g→2g)/B(E2;2g→0g) ratio vs. neutron number (N) for Nd- Er nuclei. The vibrational limit SU(5) at 2.0 and rotational limit SU(3) at 1.4 are shown by dotted lines for comparison.

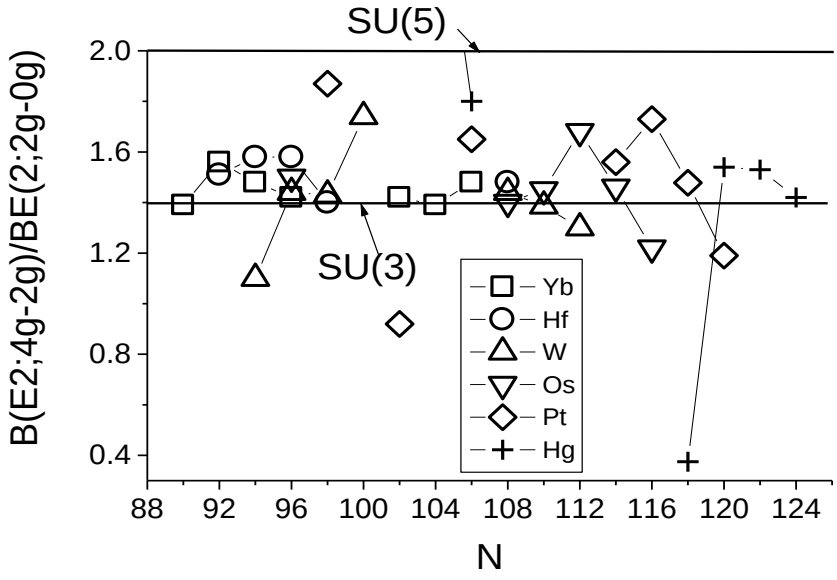

Fig.4.4: The variation of experimental B(E2;4g→2g)/B(E2;2g→0g) ratio vs. neutron number (N) for Yb- Hg nuclei. The vibrational limit SU(5) at 2.0 and rotational limit SU(3) at 1.4 are shown by dotted lines for comparison.

4.3.2.1.2 The variation of experimental B(E2;4g→2g)/ B(E2; 2g→0g) ratio verses proton number (Z).

The variation of observed B(E2;4g→2g)/ B(E2; 2g→0g) ratio with proton number (Z) is shown in Fig. 4.5, 4.6 and 4.7 for N=84 to 92, N=94 to 102 and N= 104 to 124 isotones respectively and the experimental points are joined for same value of N to observe the effect of Z. The vibrational limit (VM) or SU(5) at 2 and rotational limit or SU(3) at 1.4 are also shown by dotted lines for useful comparison in each figure.

It is evident from Fig. 4.5, that the BE(2) ratio for N=88 isotones increases on increasing Z from 60 to 62 (attains the maximum values for Sm_{88}) and decreases for Gd and Dy (attains minimum value close to SU(3) limit for Dy_{88}) and again for Er it increases. For N=88, the B(E2) ratio is close to SU(5) limiting value for Sm, Gd and Er while Dy reflects SU(3) nature and Nd in between these two limits. Also, the Sm_{88} is least deformed and Dy_{88} is most deformed. For N=86 isotones the B(E2) data is available only for two nuclei and it is increasing on increasing N from 60 to 60 as in the case of N=88.

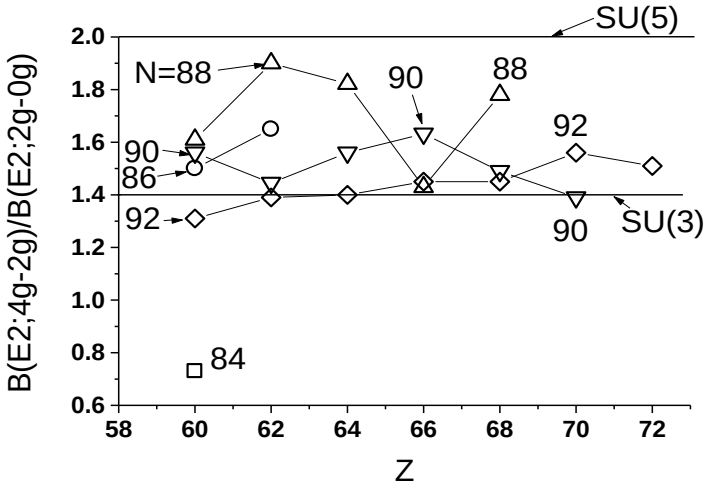

Fig.4.5: The variation of experimental B(E2;4g→2g)/ B(E2; 2g→0g) ratio vs. proton number (Z). The vibrational limit SU(5) at 2.0 and rotational limit SU(3) at 1.4 are shown by dotted lines for comparison. The experimental points are joined for same value of N to observe the effect of Z on this B(E2) ratio for each isotones for N=84-92.

For N=90 isotones the behavior of B(E2) is just opposite to N=86 and 88; the B(E2) ratio initially decreases as N increases from 60 to 62 and increases as N increases from 62 to 66 just opposite to N=88. It is evident from the figure that the gap is maximum between the two curves for N=88 and 90 around Z= 64 indication the subshell effect at Z=64 for N<90. It is supporting the findings of Casten (1985) and Casten and Zamfir (1996).

In general, for N=90 isotones, the B(E2) ratio is somewhat independent of Z indicating constant structures because the values of this ratio are ranging between 1.45 to 1.6 and it support the findings of Gupta (2012). For N=90 isotones, this B(E2) ratio initially decreases on increasing Z from 60 to 62 (attains minimum values which is close to SU(3) limiting value for Sm_{90} unlike Sm_{88} for which this ratio is close to SU(5) limiting value) and increases slowly on increasing Z from 62 to 66; and attains maximum value(=1.6) for Dy_{90}; and beyond Z=66 the BE(2) decreases linearly on increasing Z from 66 to 70 (and approaches 1.4 value for Hf_{90}). It is clear from Fig. 4.5 that Sm_{90} and Hf_{90} are most deformed in comparison to other N=90 isotones.

For N=92 isotones, this ratio goes on increasing very slowly from 1.31 to 1.56 on increasing Z from 60 to 74 and is close to SU(3) limiting value of 1.4. However for N=94, this ratio is almost constant because its values are 1.46±0.05, 1.46±0.07, 1.48±0.07, 1.58±0.10 and 1.1±0.3 for Gd, Dy, Yb, Hf and W isotopes respectively indication Z independency. For N=94, 96 and 98 isotones (see Fig. 4.6) the ratio is close to SU(3) limiting value indicating deformed nature. For other isotones the B(E2) ratio is lying between SU(5) and SU(3) or O(6) limiting values (see Fig. 4.7) as predicted by the asymmetry rotor model Sharma and Kaushik (2015a).

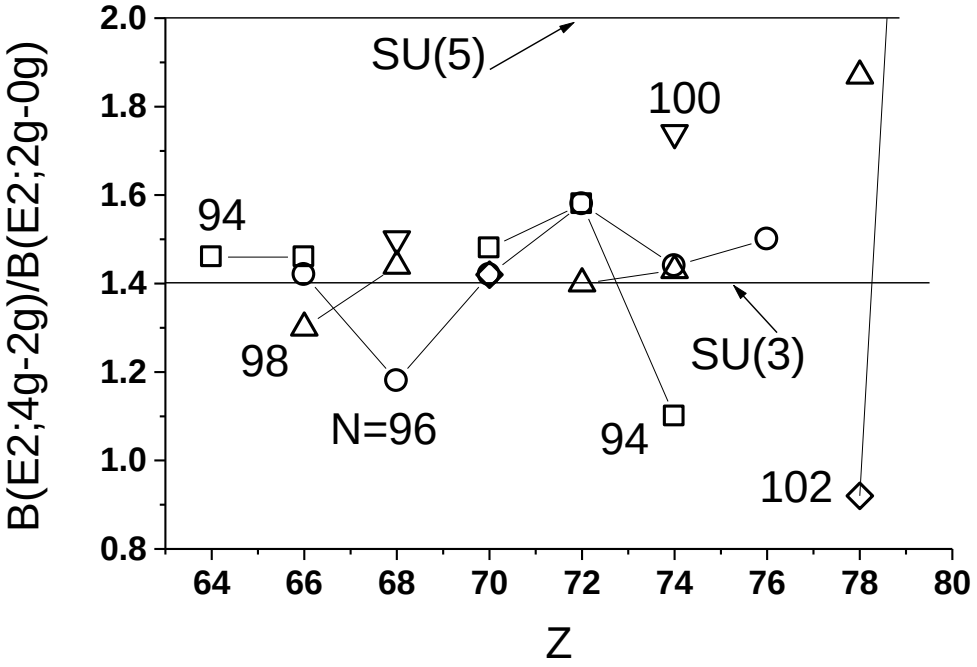

Fig.4.6: Same as Fig.3 for N=94 to 102.

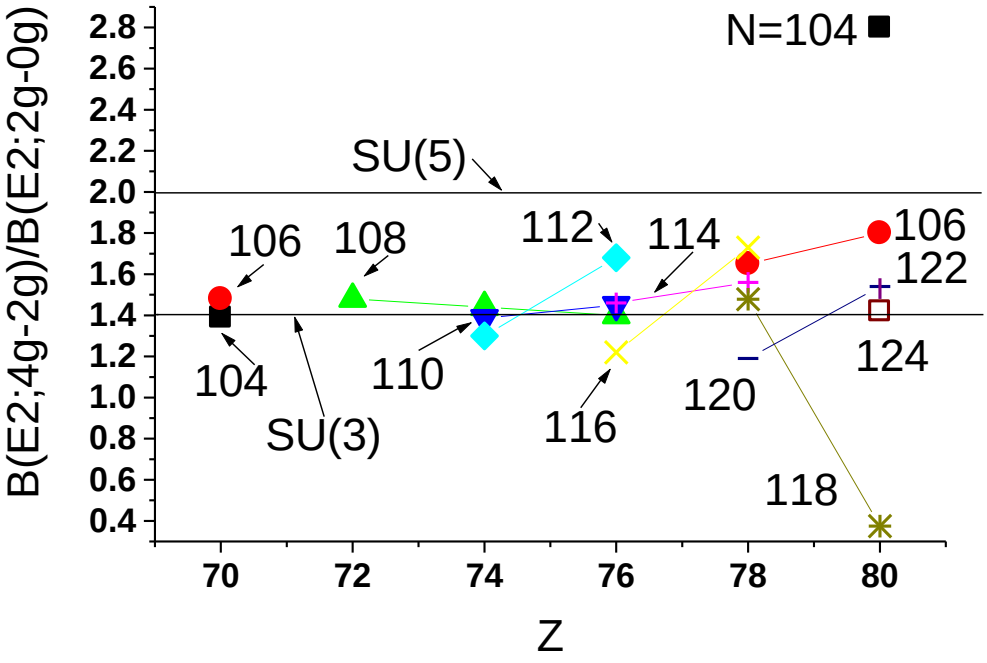

Fig.4.7: Same as Fig.3 for N=104 to 124.

4.3.2.1.3 Conclusion

The variation of B(E2; 4g→2g)/ B(E2;2g→0g) ratio with N and Z is shown for Nd – Hg nuclei. It is found that the there is shape phase transition for N=88 and 90 isotones (Nd, Sm, Gd, Er) from an ideal spherical harmonic vibrator or SU(5) to an axially symmetric deformed rotor or SU(3). Also B(E2) ratio is anomalously small for two nuclei i.e., $^{198}_{80}Hg_{118}$ (=0.375±0.018) and $^{144}_{60}Nd_{84}$ (=0.73±0.090) with only two vacancy of p+ for Z =82 and two valence n^0 outside N=82, respectively; which supports the findings of Cakirli et al. (2004). The present study supports the subshell effect around Z=64, for N≤ 90 as observed by Casten (1985) and Casten and Zamfir (1996). The B(E2; 4g→2g)/ B(E2;2g→0g) ratio for N=90 isotones is almost constant indicating that the nuclear structure is constant for these nuclei and it is supporting the findings of Gupta (2012). Partial results have been published recently Sharma and Kaushik (2015a, 2015b).

Table 4.1: The experimental values of B(E2; 4g→2g)/ B(E2;2g→0g) branching ratio taken from http://www.nndc.bnl.gov. The error is also mentioned with each value after a gap shown by *italic*.

A	Nd	Sm	Gd	Dy	Er	Yb	Hf	W	Os	Pt	Hg
Z	60	62	64	66	68	70	72	74	76	78	80
144	0.73 *9*										
146	1.5 *4*										
148	1.61 *9*	1.65 *21*									
150	1.56 *4*	1.9 *3*									
152	1.31 *10*	1.445 *22*	1.82 *2*								
154		1.39 *3*	1.56 *6*	1.43 *15*							
156			1.40 *3*	1.632 *24*	1.78 *12*						
158			1.46 *5*	1.45 *10*	1.49 *8*						
160				1.46 *7*	1.45 *8*	1.39 *14*					
162				1.42 *6*		1.56 *8*					
164				1.30 *7*	1.18 *13*	1.48 *7*	1.51 *22*				
166					1.44 *6*	1.42 *9*	1.58 *10*				
168					1.50 *5*		1.58 *11*	1.1 *3*			
170							1.4 *4*	1.44 *15*			
172						1.42 *10*		1.43 *16*	1.50 *17*		
174						1.39 *7*		1.74 *15*			
176						1.48 *15*				1.87 *24*	
178											
180							1.48 *20*		1.6 *5*	0.92 *22*	
182								1.44 *8*			4.6 *3*
184								1.386 *20*	1.4 *4*	1.65 *9*	2.8 *8*
186								1.30 *9*	1.45 *7*		1.8 *8*
188									1.68 *11*		
190									1.46 *9*		
192									1.22 *4*	1.56 *9*	
194										1.73 *11*	
196										1.478 *23*	
198										1.19 *13*	0.375 *18*
200											1.54 *3*

CHAPTER V

STUDY OF $^{152, 154}$SM USING INTERACTING BOSON MODEL-I

5.1 INTRODUCTION

The interacting boson model-1 (IBM-1) of Arima and Iachello (1984), Iachello and Arima (1987) and Casten (1990) has been successful in describing the collective nuclear properties of even- even nuclei. In IBM-1, the nuclear structure is assumed to be a function of total boson number N_B (=N_p+ N_n), where N_p and N_n are the valance proton and neutron particle or hole boson number respectively. This model is based on group theory and provides a useful theoretical explanation of various experimentally observed nuclear properties.

In even- even nuclei, the energy ratio R_4 (= E_{4g}^{+} / E_{2g}^{+}) is good measure of deformation and it helps in categorizing the atomic nuclei as per details given below (see Fig. 5.1):

For vibrational or SU(5) type nuclei	R_4= 2.00
For E(5) symmetry	R_4= 2.20
For γ-soft nuclei or O(6)	R_4= 2.50
For X(5) symmetry	R_4= 2.90
For rotational nuclei or SU(3)	R_4 = 3.33

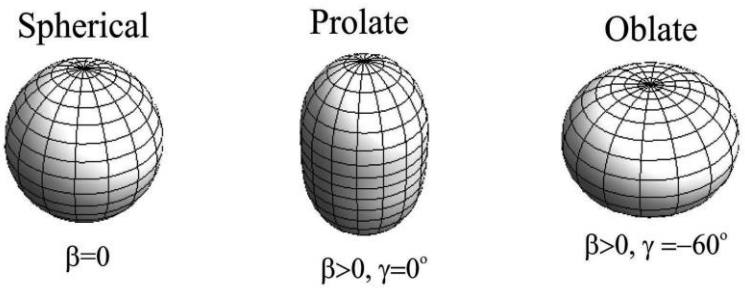

Figure 5.1: The shape of nucleus for different values of β and γ. For spherical nuclei $R_4 = 2.0$ and β =0, transitional nuclei $R_4 \approx 2.3$ to 2.8 and for deformed nuclei [prolate (β>0 and $\gamma = 0^0$) and oblate (β>0 and $\gamma = -60^0$) shape] $R_4 > 2.8$.

5.2 LITERATURE REVIEW

In past years, several systematic studies of $^{146\text{-}154}$Sm isotopes have been performed using IBM-1 by Scholten et al. (1978), Scholten (1980), Castanõs et al. (1982), Chuu et al. (1984), Yen et al. (1984), Hsieh et al. (1986), Chuu and Hsieh (1990) Han et al. (1990), Stewart et al. (1990), Kracikova et al. (1984a) and Kracikova et al. (1984b), dynamic pairing-plus-quadrupole (DPPQ) model by Kumar (1974), Kumar (1976) and Gupta (1983), boson expansion model (BEM) by Tamura et al. (1979), rotational vibrational interaction model (RVM) by Bhardwaj et al. (1983) and Bhardwaj (1983). These theories were partial successful in explaining the complex nuclear structure of $^{146\text{-}154}$Sm isotopes.

The work of Scholten et al. (1978) and Scholten (1980) was limited to the lower bands i.e. g-, β- and γ- bands only. Castanõs et al. (1982) used an effective Hamiltonian of IBA for describing only the low lying energy spectrum of Xe, Ba, Sm, Gd and U isotopes and pointed out that the effective IBM results were in agreement with those projected from IBM calculations of Scholten (1980). Chuu et al. (1984), used an effective H_{IBA} for N = 88 and 90 (Ba-Yb) isotones and obtained a unified E2 transition operator to reproduce the observed B(E2) values and Q_{2+} moments. These attempts of Chuu et al. (1984) were aimed to find a common set of IBM parameters for a group of nuclei (isotopes/ isotones) so that the varying nuclear structure with N, Z may be obtained by varying N_B. Gupta- Hamilton- Rammaya

(1980) observed that the g-band spectra of the isotonic multiplets in the first quadrant of the Z=50-82, N=82-126 major closed shell vary slowly with Z and a common set of parameters should be easier to obtain. Mittal and Gupta (1990) pointed out that the approach of Chuu et al. (1984) did not reproduce the correct variation of the $E_{2\gamma}$ and $E_{0\beta}$ states with Z. Also for N=90 isotones, Chuu et al. (1984) results were not satisfactory for B(E2) values for transition between different bands. In addition, the energy spacing in the H_{IBA} calculation of Chuu et al. (1984) were not in agreement with the observed data in β- and γ– bands (Fig. 3 of Chuu et al. (1984) for ^{152}Sm) and some states were even in reverse order in the γ –band of ^{152}Sm. The DPPQ model of Kumar (1975) had limitations for production the energies of various bands for Sm and other isotopes, because it does not have any fitting procedure of energies like other models (e.g. IBM-1). Also the energy scale is not linear in the g-band versus other bands Gupta (1983).

At present the large amount of experimental data is available from the radio-active decay, coulomb excitation and the reaction work of Lederer and Shirley (1978), Raman et al. (1987), Peker (1989), Venkova and Andrejtischeff (1981), Peker (1987), Sakai (1984) and www.nndc.bnl.gov (2015). Three quasi-bands in ^{154}Sm and four in ^{152}Sm are well established up to higher spins, which requires more detailed theoretical analysis for complete explanation of the observed collective properties. Since all the previous works were performed only for lower members of the three lower bands i.e. g-, β-, and γ-bands, it is interesting to see what the results are of a study of higher bands.

In this chapter, the IBM Hamiltonian is used for $^{152\text{-}154}$Sm isotopes to study the nuclear properties of lower and higher bands up to high spins, which includes the energy spectrum, absolute B(E2) values and B(E2) branching ratios. The absolute B(E2) values and B(E2) branching ratios are sensitive to the wave function and provide more stringent test of a model.

5.3 THE INTERACTING BOSON MODEL AND CALCULATIONS

The two bodies effective Hamiltonian within the boson has two forms

$$H = \varepsilon_s (s^+.s\tilde{}) + \varepsilon_d (d^+.d\tilde{}) + \sum_{L=0,2,4} (1/2)\ (2L+1)^{1/2}\ c_L\{[\ d^+ x\ d^+]^{(L)} x\ [d\tilde{} x\ d\tilde{}]^{(L)}\}^{(0)}$$

$$+ (1/\sqrt{2})\ \tilde{v}_2\ \{[\ d^+ x\ d^+]^{(2)} x\ [d\tilde{} x\ d\tilde{}]^{(2)} + [\ d^+ x\ d^+]^{(2)} x\ [d\tilde{} x\ d\tilde{}]^{(2)}\}^{(0)}$$

$$+ (\tfrac{1}{2})\ \tilde{v}_0\ \{[\ d^+ x\ d^+]^{(0)} x\ [s\tilde{} x\ s\tilde{}]^{(0)} + [s^+ x\ s^+]^{(0)} + [d\tilde{} x\ d\tilde{}]^{(0)}\}^{(0)}$$

$$+ u_2\ \{[\ d^+ x\ s^+]^{(2)} x\ [d\tilde{} x\ s\tilde{}]^{(2)}\}^{(0)} + (\tfrac{1}{2})\ u_0\ [s^+ x\ s^+]^{(0)} + [s\tilde{} x\ s\tilde{}]^{(0)}\}^{(0)} \quad . \qquad (5.1)$$

Where, ε_s and ε_d are the single-boson energies and c_L, $\tilde{v}_L$ and u_L describe the two-boson interaction. Also,

$$H' = \varepsilon'' n_d + a_0 (P^+.P) + a_1 (L.L) + a_2(Q.Q) + a_3 (T_3.T_3) + a_4(T_4.T_4) \qquad (5.2)$$

where,

$n_d = (d^+.\ d\tilde{})$,

$P = (\tfrac{1}{2})\ (d\tilde{}.\ d\tilde{})\ - (\tfrac{1}{2})\ (s\tilde{}.\ s\tilde{})$,

$L = \sqrt{10}\ (d^+ x\ d\tilde{})^{(1)}$,

$Q = [d^+\ x\ s\tilde{}\ + s^+ x\ d\tilde{}]^{(2)}$,

$T_3 = [d^+\ x\ d\tilde{}]^{(2)}$ and

$T_4 = [d^+\ x\ d\tilde{}]^{(4)}$.

A least square fitting technique is used to find out the optimized values of the four parameters i.e ε'', a_0, a_1 and a_2; while a_3 and a_4 are kept zero in equ. 5.2. The PHINT programme of Scholten (1979a) is used to fit the observed energy spectra of $^{152\text{-}154}$Sm isotopes. All levels with reliable spin assignment ($I^{\pi} \leq 10^+$) are included up to the point that the first level with an uncertain spin assignment appears. In fitting of the energy spectra, we first determine the four parameters of H' as discussed above, that reproduce the best lower and higher bands.

The optimized values of these four boson- boson interaction parameters are listed in Table 5.1. These four parameters with E2SD (= α_2) and E2DD (= $\sqrt{5}\beta_2$) are the

input for the FBEM programme of Scholten (1979b). The E2 transition operator depends upon two parameters α_2 and β_2 as given below:

$$T(E2) = \alpha_2 [d^+ \tilde{s} + s^+ \times \tilde{d}]^{(2)} + \beta_2[d^+ \tilde{d}]^{(2)} \quad (5.3)$$

Where, α_2 is called the boson effective charge, simply the scaling parameter and affecting the B(E2) values and β_2 accounts for nuclear shape transition. The ratio E2DD/ E2SD is equal to -2.958 in the SU(3) limit and reduced to zero in the O(6) limit. The FBEM gives the B(E2) values and ratios.

Table 5.1: The Interacting Boson Model-1 parameters (all in keV) for $^{152-154}$Sm.

Parameter	^{152}Sm	^{154}Sm
N_B	10	11
EPS	503.8	411.5
PAIR	13.1	0.1
ELL	0.5	-0.8
QQ	-26.2	-41.8
OCT	0.0	0.0
HEX	0.0	0.0
E2DD	-250.0	-250.0
E2SD	160.0	140.0
E2DD/E2SD	-1.56	-1.786

5.4 RESULT AND DISCUSSION

For $^{146-154}$Sm isotopes, experimental values of energy ratio R_4, R_γ (=$E2_\gamma/E2_g$), R_β (=$E0_\beta/E2_g$), $R_{0,6,\beta,g}$ (=$E0_\beta/E6_g$), $R_{2,0,\beta,g}$ [=$(E2_\beta-E0_\beta)/E2_g$], $R_{4,2,\beta,g}$ [=$(E4_\beta-E2_\beta)/(E4_g-E2_g)$] and $R_{4,2,\gamma,g}$ [=$(E4_\gamma-E2_\gamma)/(E4_g-E2_g)$] are calculated and given in Table 5.2. The experimental values of energies to calculate these ratios are taken from the website of Brookhaven National Laboratory, www.nndc.bnl.gov (2015). It is evident that ^{146}Sm

(R_4= 1.85) and ^{148}Sm (R_4= 2.14) nuclei are the spherical in nature i.e. SU(5) type because their R_4 is close to 2. The ^{150}Sm nucleus (R_4= 2.31) is a transitional one i.e. lying on transition from SU(5) to SU(3) symmetry. The ^{152}Sm is a best example of X(5) symmetry because its experimental value of R_4 is 3.01 compared to X(5) symmetry value 2.9, R_γ is 8.9 compare to X(5) value 8.16, R_β is 5.62 compared to X(5) value 5.65 and the values of other energy ratios i.e., $R_{0,6,\beta,g}$, $R_{2,0,\beta,g}$, $R_{4,2,\beta,g}$ and $R_{4,2,\gamma,g}$ are near to the X(5) values. The ^{154}Sm is rotor type i.e. close to SU(3) symmetry. The $^{152\text{-}154}$Sm isotopes are lying on transition from SU(5) to SU(3) and ^{152}Sm is close to X(5) symmetry (see Casten's symmetry triangle Fig. 5.2). For ^{152}Sm, the present IBM calculation gives the energy ratio $E0_\beta/E6_g$ equal to 0.9509 compared to observed value of 0.9685 and X(5) value 1.0405. Hence present IBM calculation is supporting the X(5) nature of ^{152}Sm.

The variation of experimental values of ratios R_4 and $R_{0,6,\beta,g}$ versus A for $^{146\text{-}154}$Sm is shown in Fig. 5.3. The corresponding values of these ratios in X(5) limit are shown for useful comparison. It is clear from the Fig. 5.3 that the ratio R_4 increases from 1.85 to 3.25 as A increases from 146 to 154 and ^{152}Sm is very close to X(5) limiting value. However, the ratio $R_{0,6,\beta,g}$; decreases initially when A increases from 146 to 150; increases while A increases from 150 to 154 and for ^{152}Sm is very close to X(5) limiting value (see Fig. 5.3).

Table 5.2: The experimental values of energy ratio R_4 (=E4g/E2g), R_γ (=$E2_\gamma/E2_g$), R_β (=$E0_\beta/E2_g$), $R_{0,6,\beta,g}$ (=$E0_\beta/E6_g$), $R_{2,0,\beta,g}$ (=$E2_\beta$-$E0_\beta/E2_g$), $R_{4,2,\beta,g}$ (=$E4_\beta$-$E2_\beta$/ $E4_g$-$E2_g$) and $R_{4,2,\gamma,g}$ (=$E4_\gamma$-$E2_\gamma$/ $E4_g$-$E2_g$) are given for $^{146-154}$Sm isotopes. The experimental values are taken from www.nndc.bnl.gov (2015). The IBM calculated ratios for $^{152-154}$Sm are shown for comparison in last rows as Present Work.

A	R_4	R_γ	R_β	$R_{0,6,\beta,g}$	$R_{2,0,\beta,g}$	$R_{4,2,\beta,g}$	$R_{4,2,\gamma,g}$
146	1.8486	2.2059	1.9433	0.8014	0.2124	-	1.2471
148	2.1446	2.6427	2.5919	0.7483	0.4325	0.3669	1.0425
150	2.3157	3.5748	2.2172	0.5789	0.9155	0.91723	1.02137
152	3.0102	8.9146	5.6215	0.9685	1.0325	0.8679	1.1675
154	3.2532	17.5701	13.414	2.02039	0.9576	1.04591	1.19207
X(5)	2.904	8.16	5.649	1.0405	1.801	1.701	1.071
152 Present Work	2.8121	7.8281	5.0563	0.9509	1.1536	1.3969	1.7088
154 Present Work	3.3138	19.1755	14.531	2.1062	1.4202	1.2798	1.2374

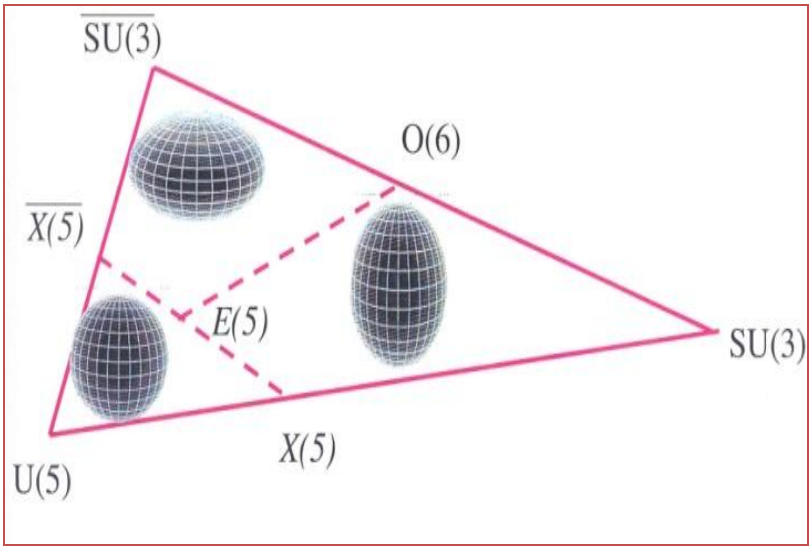

Figure 5.2 Casten's symmetry triangle.

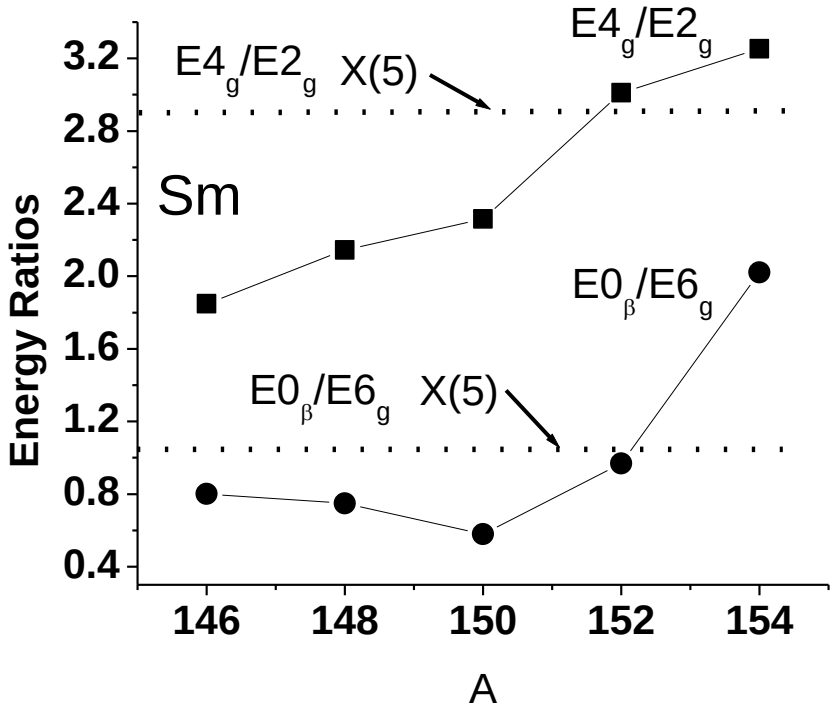

Fig. 5.3: The variation of experimental values of ratio R_4 and $R_{0,6,\beta,g}$ versus A for $^{146\text{-}154}$Sm. The data points of R_4 are shown by solid squares (■) and $R_{0,6,\beta,g}$ by solid circles(●). The corresponding values of these ratios in X(5) limit are shown by dotted lines(--) for useful comparison. The experimental values are taken from www.nndc.bnl.gov (2015).

The variation of experimental values of ratios R_γ and R_β versus A for $^{146\text{-}154}$Sm is shown in Fig. 5.4. The corresponding values of these ratios in X(5) limit are shown for useful comparison. It is clear from the Fig. 5.4 that the ratios R_γ and R_β both; increases as A increases from 146 to 148; decreases slowly as A increases from 148 to 150 and increases sharply as A increases from 150 to 154 indicating shape phase transition from SU(5) to SU(3). Both the experimental ratios for ^{152}Sm is very close to X(5) limiting values indication the X(5) character. In the present IBM calculation, the R_γ and R_β ratios for ^{152}Sm are close to X(5) values (see Table 5.2) and our calculation is supporting X(5) nature of ^{152}Sm.

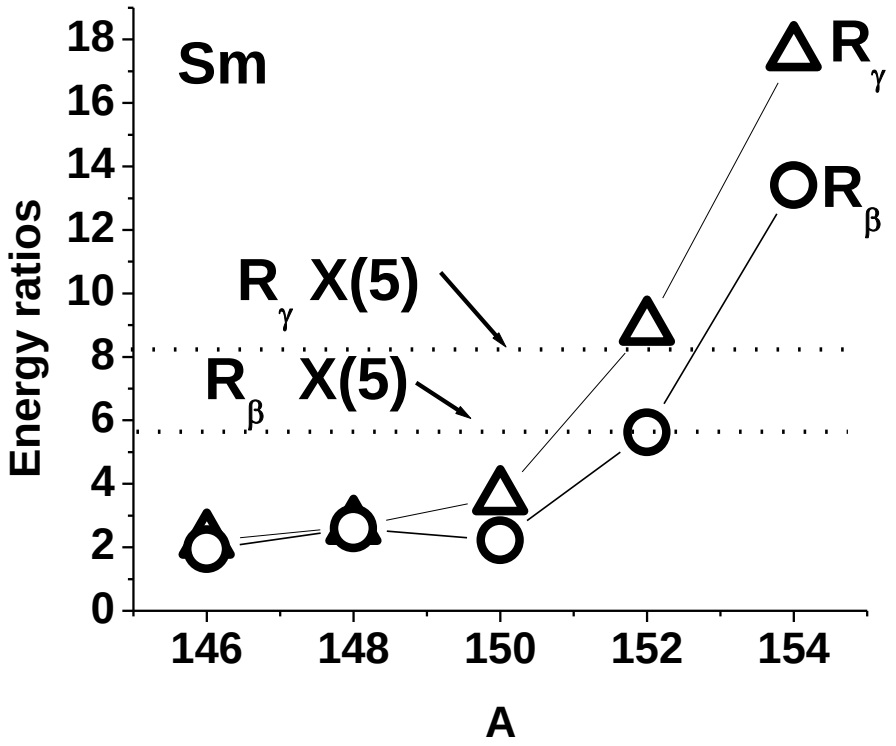

Fig. 5.4: Same as Fig. 5.3 for ratio R_γ and R_β versus A. The data points of R_γ are shown by hollow triangles (Δ) and R_β by hollow circles (○). The corresponding values of these ratios in X(5) limit are shown by dotted lines (--) for useful comparison. The experimental values are taken from www.nndc.bnl.gov (2015).

The experimental values of B(E2;4g→2g)/B(E2;2g→0g), B(E2;$2_\gamma \rightarrow 0_g/2_g$) and B(E2;$2_\beta \rightarrow 0_g/2_g$) branching ratio are given in Table 5.3 for $^{146\text{-}152}$Sm isotopes. The corresponding values of Np, Nn, N_B (=Np+Nn) and NpNn are also given. The values for X(5) symmetry of IBM, vibrational model (VM) and rotor model (RM) are also given for useful comparison. The experimental ratios are taken from www.nndc.bnl.gov (2015). It is noted that for ^{152}Sm, the observed value of B(E2;4g→2g)/ B(E2;2g→0g) ratio is close to X(5) limiting values and our calculated value is 1.499 indicating X(5) nature.

Table 5.3: The experimental values of energy ratio B(E2;4g→2g)/ B(E2;2g→0g), B(E2; $2_\gamma \rightarrow 0_g/2_g$) and B(E2; $2_\beta \rightarrow 0_g/2_g$).The corresponding values of Np, Nn, N_B (=Np+Nn) and NpNn are also listed for $^{146\text{-}152}$Sm isotopes. The values for X(5) symmetry of IBM, vibrational model (VM) and rotor model (RM) are also given.

A	Np	Nn	NB	NpNn	B(E2;4g→2g)/ B(E2;2g→0g)	B(E2; $2_\gamma \rightarrow 0_g/2_g$)	B(E2; $2_\beta \rightarrow 0_g/2_g$)
146	6	1	7	6	1.7941[a] ≥1.27(26)[b] ≥1.30[g]	0.0012(4)[b] >0.01[g]	0.066(13)[b] 0.02[g]
148	6	2	8	12	1.6598[c] 1.65(21)[a]	0.11 [c] 0 .067[h]	0.07[c] 0 .086[h]
150	6	3	9	18	1.856[d] 1.9(3)[a]	0.26[h] 0 .33(8)[d]	0.012(2)[d] 0.012[h]
152	6	4	10	24	1.5574[e] 1.445(22)[a]	0.38(1)[e] 0.40(1)[i]	0.17(1)[e] 0.169(7)[i]
154	6	5	11	30	1.60465[f] 1.39(3)[a]	0.60(11)[f]	0.44[f]
X(5)					1.6	0.666	0.429
VM					2.0	0	0
RM					1.42	0.7	0.7

[a]www.nndc.bnl.gov [b]Kracikova et al. (1984a) [c]Peker (1990)
[d]Mateosian (1986) [e]Peker (1989) [f]Peker (1987)
[g]Peker (1984) [h]Lederer and Shirley (1978) [i]Stewart et al. (1990)

5.4.1 The B(E2) Branching Ratios in the SU(5) and SU(3) Limit

In the SU(5) limit, the one d-boson excitation $n_d = 1$ is 2^+_1 state, the $n_d = 2$ d-boson excitation is a triplet of 0^+_2 , 2^+_2 and 4^+_1 states and nd = 3 boson excitation is a quintuplet of 0^+_3 , 2^+_3 , 3^+_1 , 4^+_2 and 6^+_1 . The $\Delta n_d = 0, \pm 1$ transitions are allowed and $\Delta n_d = \pm 2, \pm 3$, etc. transitions are prohibited.

In the SU(3) limit, these states are regrouped into different bands. The absolute B(E2) values for (γ→g) and (β→g) transitions depend on the intrinsic matrix elements and geometrical factors Bohr and Mottelson (1975). The B(E2) branching ratio for two transitions from a particular level in a given band to the two states of other band i.e. (Ii→If/If') depends on the Alaga value Bohr and Mottelson (1975). In the SU(3) limit these rules are slightly modified because the (γ→g) and (β→g) transitions are prohibited, but in the slightly broken symmetry the (γ→g) transition should be faster that (β→g) transition. The observed B(E2) ratios are obtained from the γ–ray spectrum data, using the relation Alaga et al. (1955),

$$B(E2; I_i \rightarrow I_f / I_{f'}) = [I\gamma / I\gamma'] \{E\gamma' / E\gamma\}^5, \qquad (5.4)$$

where E_γ and E_γ' are the γ – ray energies for ($I_i \rightarrow I_f$) and ($I_i \rightarrow I_f$') transitions; I_γ and I_γ' are the intensities, respectively.

5.4.2 The ^{152}Sm isotope

5.4.2.1 Energy spectrum

In ^{152}Sm the members of g-band and β_1-band are available up to 14^+, for β_2 up to 2^+ and γ_1 up to 5^+ (see Sakai (1984). The experimental energy values of Sakai (1984) and Peker (1989) are compared with the present calculation and DPPQ Gupta (1983) in Table 5.4. In the present calculation the band-head of the g-, β- and γ–bands are very close to the experiment and the spacing of different members in the different bands is also like in the experiment Sakai (1984) and Peker (1989). For $K^{\Pi}= 0^+_3$ band the calculated 0^+ state lies at 1.496 MeV compared to the 1.0829 MeV in experiment. The variation of E_I with spin I^+ for different bands is presented in Fig. 5.5. The slopes of E_I versus I^+ of different bands in experiment are similar to the theoretical slopes.

Table 5.4: The values of energy (in MeV) for ^{152}Sm. The theoretical result from present IBM calculation and DPPQ Gupta (1983) are also shown.

State	K^{π}	Expt. [a]	Present	DPPQ [b]
2_g	0_1^+	0.1218	0.1315	0.121
4_g	0_1^+	0.366648	0.3698	0.361
6_g	0_1^+	0.70694	0.6992	
8_g	0_1^+	1.12537	1.1097	
0_β	0_2^+	0.6847	0.6649	1.000
2_β	0_2^+	0.81047	0.8166	1.211
4_β	0_2^+	1.02296	1.1495	
6_β	0_2^+	1.31051	1.5402	
8_β	0_2^+	1.66648	1.9983	
2_γ	2_1^+	1.08589	1.0294	1.556
3_γ	2_1^+	1.23388	1.1005	
4_γ	2_1^+	1.37175	1.4366	
5_γ	2_1^+	(1.5595)	1.4807	
6_γ	2_1^+	1.7283[c]	1.9086	
7_γ	2_1^+	19458 [c]	1.9312	
8_γ	2_1^+	2.1397 [c]	2.4472	
$0_{\beta 2}$	0_3^+	1.08286	1.4960	
$2_{\beta 2}$	0_3^+	(1.2928)	1.5890	

[a] Sakai (1984), [b] Gupta (1984), [c] Peker (1989)

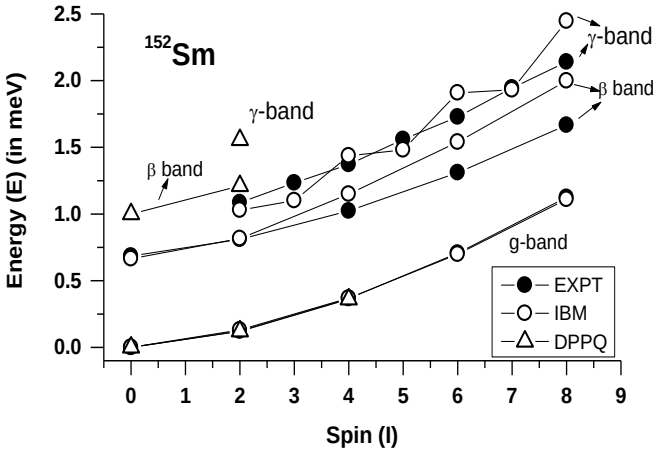

Fig 5.5: The variation of E_I with spin I^+ for different bands in ^{152}Sm.The experimental data Sakai (1984) and Peker (1989), points are shown by solid circles (●), present calculation IBM by hollow circles (○) and DPPQ Gupta (1984) by hollow triangles (Δ).

5.4.2.2 B(E2)values

For ^{152}Sm, the observed and calculated B(E2) values are listed in Table 5.5 for (g→g), (β→g) and (γ→g) transitions.

Table 5.5: The B (E2; Ii→If) values (in e^2b^2 unit) in ^{152}Sm.

$I_i \rightarrow I_f$	Expt.	Present	BEM4	BEM6	DPPQ	RVM1	RVM2	IBM
Ref.	A		c	c	d	e	e	F
$2_g \rightarrow 0_g$	0.6806	0.6806	0.673	0.673	0.64	0.669	0.669	0.75
$4_g \rightarrow 2_g$	1.06(4)	1.02	0.99	0.98	0.96	1.057	1.057	1.0
$6_g \rightarrow 4_g$	1.18 [b]	1.14	1.12	1.09	--	--	--	0.97
$8_g \rightarrow 6_g$	1.36 [b]	1.17	1.17	1.11	--	--	--	0.83
$10_g \rightarrow 8_g$	1.6[b]	1.14	--	--	--	--	--	--
$2_\beta \rightarrow 2_g$	0.026(3)	0.14	0.031	0.025	0.029	0.062	0.069	--
$2_\beta \rightarrow 4_g$	0.0909(8)	0.0108	0.05	0.07	0.089	0.283	0.274	--
$2_\beta \rightarrow 0_g$	0.0046(3)	0.0172	0.005	0.007	0.002	0.019	0.022	--
$0_\beta \rightarrow 2_g$	0.176(11) [c]	0.0092	0.156	0. 12	0.166	0.314	0.347	--
$4_\beta \rightarrow 2_g$	0.0053(35)	0.0027	0.004	0.005	0.001	0.003	0.006	--
$4_\beta \rightarrow 4_g$	0.037(23) [c]	0.1091	0.026	0.016	0.026	0.07	0.08	--
$2_\gamma \rightarrow 0_g$	0.0176(8)	0.0153	0.049	0.05	0.023	0.015	0.016	--
$2_\gamma \rightarrow 2_g$	0.028(10) 0.042(4) [c]	0.0012	0.05	0.053	0.048	0.031	0.032	--
$2_\gamma \rightarrow 4_g$	0.004(3) [c]	0.085	0.007	0.006	0.006	0.0069	0.007	--
$4_\gamma \rightarrow 2_g$	0.0035(13)	0.0052	0.034	0.026	0.009	0.0046	0.0078	--
$4_\gamma \rightarrow 4_g$	0.0037(1) [c]	0.0034	0.068	0.076	0.047	0.017	0.013	--

[a]Peker (1989), [b]Venkova and Andrejtscheff (1981), [c] Tamura et al. (1979), [d] Gupta (1983)[e] Bhardwaj et al. (1983) and Bhardwaj (1983), [f] Chuu et al. (1984)

The variation of B(E2;Ig→Ig-2) values with spin Ig is shown in Fig. 5.6. It is observed that the experimental B(E2) values of Peker (1989) and Venkova and Andrejtscheff (1981), increases rapidly on increasing Ig from 2^+ to 10^+ indicating the sharp change in the nuclear shape (see Fig.5.6). In the IBM calculation of Chuu et al. (1988), the B(E2) values first increases when Ig increases from 2^+ to 4^+ and it decreases while Ig increasing from 4^+ to 8^+ *unlike* the observed trend. But in the present IBM work, the B(E2) values follow the observed trend and values the more

closer than other theoretical data. The BEM6 Tamura et al. (1979) data points are much below the observed data points. However, the BEM4 Tamura et al. (1979) values are close to present calculation (see Fig 5.6). Only two data points are available for DPPQ Gupta (1983), RVM1 and RVM2 Bhardwaj et al. (1983) and Bhardwaj (1983) to find any definite conclusion.

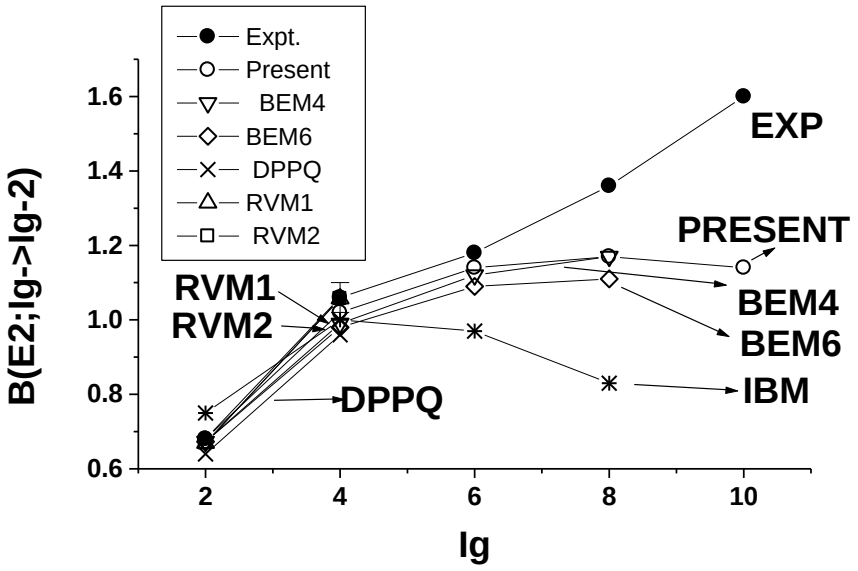

FIG 5.6: The variation of B(E2;Ig→Ig-2) values with spin Ig for ground bands for ^{152}Sm.The experimental data points of Peker (1989) and Venkova and Andrejtscheff (1981) are shown by solid circles (●), present IBM calculation by hollow circles (○), BEM4 Tamura et al. (1979) by inverted hollow triangle(▽), BEM6 Tamura et al. (1979) by hollow diamond (◊), DPPQ Gupta (1984) by cross (x), IBM Chuu et al. (1984) by star (*), RVM1 Bhardwaj et al. (1983) and Bhardwaj (1983) by upright triangle (Δ) and RVM2 Bhardwaj et al. (1983) and Bhardwaj (1983) by hollow square (□).

The theoretical results of vibrational model (VM), SU(5), O(6) and SU(3) limiting values, present calculation and IBM calculation of Chuu et al. (1988) along with the experimental data for B(E2) values of Peker (1989) and Venkova and Andrejtscheff (1981) are shown in Fig. 5.7. It is clear from the Fig. 5.7 that the observed data is quite below from the VM limiting values and is lying between SU(5) and S(3) limiting values. The B(E2) values from present calculation and BEM4 Tamura et al.

(1979) are very close to the experimental data point and also present IBM calculation produces the observed slop of this ratio with I_g. There are only two data points from RVM1 and RVM2 Bhardwaj et al (1983) and Bhardwaj (1983) and DPPQ Gupta (1984) not shown in the Fig. to avoid overlapping?

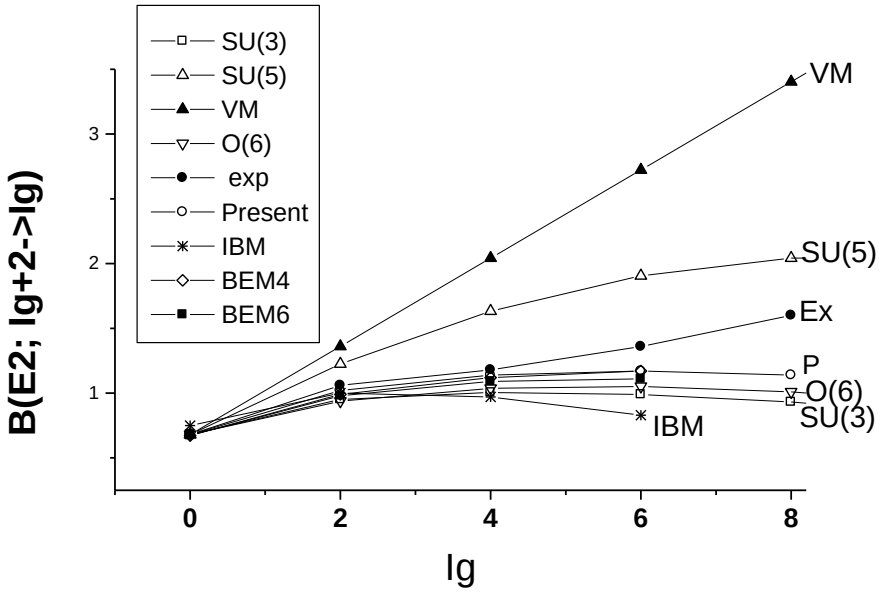

FIG 5.7: The variation of B(E2;Ig→Ig-2) values with spin Ig for ground state rotational bands for ^{152}Sm.The experimental data points of Peker (1989) and Venkova and Andrejtscheff (1981) are shown by solid circles (●), present IBM calculation by hollow circles (○), BEM4 Tamura et al. (1979) by hollow diamond (◊), BEM6 Tamura et al. (1979) by solid square (■), IBM Chuu et al. (1984) by star (*). The vibrational model (VM) is shown by solid triangle (▲), SU(5) limiting values by hollow upright triangle (Δ), O(6) limiting values by hollow inverted triangle (∇) and SU(3) limiting values by hollow square (□). There are only two data points from RVM1 and RVM2 Bhardwaj et al (1983) and Bhardwaj (1983) and DPPQ Gupta (1984) not shown in the Fig. to avoid overlapping.

The B(E2) values for six (β→g) and five (γ→g) transitions are also compared (see Table 5.5) with the present calculation, boson expansion model (BEM4 and BEM6 version) of Tamura et al (1979), dynamic pairing plus quadrupole (DPPQ) model of Gupta (1983), rotational vibrational model (RVM1 and RVM2) of Bhardwaj et al

(1983) and Bhardwaj (1983) and interaction boson model –1 (IBM-1) of Chuu et al. (1988). It is evident that the present calculation gives the satisfactory results.

5.4.2.3 The B(E2) branching ratios for β– band

In the β–decay of ^{152}Eu, 13 new transitions and 5 new levels were reported by Stewart et al. (1990), which are included in the present work for useful discussion.

In Table of Isotopes of Lederer and Shirley (1978), the B(E2) ratio for ($2_\beta \rightarrow 0_g/2_g$) transition is 0.84 which is more than the SU(3) limiting value 0.7. This ratio may be large due to 0.2% M1 and 4% E0 mixing in the ($2_\beta \rightarrow 2_g$) 0.6886 MeV γ–ray. In a recent compilation work of Peker (1989) this ratio is 0.17(1) compared to the theoretical value 0.12 & DPPQ value Gupta (1983) 0.076 (see Table 5.6).

The ($2_\beta \rightarrow 4_g$) 0.444 MeV γ–ray was overlapping with ($2^- \rightarrow 3_\gamma$) transition and gives B(E2; $2_\beta \rightarrow 2_g/4_g$) = 0.35 (the intensity of ($2^- \rightarrow 3\gamma$) γ–ray was 12 which gives this ratio 0.56) Lederer and Shirley (1978). But in the recent compilation of Peker (1989) this ratio is 0.30(3) and in decay of ^{152}Eu work of Stewart et al. (1990) ratio is 0.030(1).

In the Table of Isotopes Lederer and Shirley (1978); the ($4_\beta \rightarrow 4_g$) 0.6565 MeV γ–ray had 16% M1 and 5% E0 mixing, which gave the B(E2;$4_\beta \rightarrow 2_g/4_g$) = 0.11 and B(E2;$4_\beta \rightarrow 4_g/6_g$) = 0.76, but Peker (1989) gave these ratios equal to 0.21(2) and 3.6(22); Stewart et al (1990) gave 0.11(2) and 0.08(2); and in the present work these ratios are 9.3 and 231 respectively (see Table 5.6).

For ($6_\beta \rightarrow 4_g/6_g$), ($8_\beta \rightarrow 6_g/8_g$) and ($10_\beta \rightarrow 8_g/10_g$) transitions; the observed B(E2) ratios lie away from the respective Alaga values and theoretical values are close to the observed values. It is also evident that the (β→β) transitions are stronger than (β→g) which is supported by present IBM calculation (see Table 5.6).

Table 5.6: The B(E2) ratios for ^{152}Sm.

$I_i \rightarrow I_f / I_{f'}$	Expt	Expt	Present	DPPQ	BEM 4	BEM 6	RVM (I)	RVM (II)	RM
Ref.	a	b		c	d	d	e	e	
$2_\beta \rightarrow 0_g/2_g$	0.17(1)	0.169(7)	0.12	0.08	0.16	0.26	0.31	0.32	0.7
$2_\beta \rightarrow 2_g/4_g$	0.30(3)	0.030(1)	12.94	0.33	0.62	0.36	0.22	0.25	0.56
$2_\beta \rightarrow 0_\beta/0_g$	406(77)	829(113)	12.5	291	91	69	--	--	--
$2_\beta \rightarrow 4_g/0_g$	19.8(23)	--	0.63	40.5	10.1	10.8	--	--	0.8
$4_\beta \rightarrow 2_g/4_g$	0.21(2)	0.11(2)	9.32	0.023	0.17	0.32	0.04	0.08	1.1
$4_\beta \rightarrow 4_g/6_g$	3.6(22)	0.08(2)	231	--	0.37	0.34	--		0.57
$4_\beta \rightarrow 2_\beta/2_g$	291(27)	--	186	--	180	126	--	--	--
$4_\beta \rightarrow 2_\beta/4_g$	1385.7	--	20	43	27.7	3.9	10.9	9.12	1.1
$4_\beta \rightarrow 2_\beta/3_\gamma$	350(170)	--	1.3	123	1831	--	--	---	--
$6_\beta \rightarrow 4_g/6_g$	0.078(5)	--	0.012	--	--	--	--		1.24
$6_\beta \rightarrow 4_\beta/4_g$	50(17)	--	694	--	--	--	--	--	--
$8_\beta \rightarrow 6_g/6_g$	0.012(1)	--	0.008	--	---	--	--		1.3
$8_\beta \rightarrow 6_\beta/6_g$	2374(309)	--	1415	--	---	--	--	--	--
$10_\beta \rightarrow 8_g/10_g$	0.05(1)	--	0.007	--	---	--	--	--	--
$10_\beta \rightarrow 8_\beta/8_g$	440(55)	--	2106	--	---	--	--	--	--
$2_\gamma \rightarrow 0_g/2_g$	0.38(1)	0.40(1)	12.8	0.48	0.98	0.94	0.49	0.5	0.07
$2_\gamma \rightarrow 2_g/4_g$	12.4(6)	9.8(4)	0.014	8	7.57	9.14	4.5	4.57	19.07
$2_\gamma \rightarrow 2_\beta/2_g$	1208(68)	3.9(6)	267	2.5	--	2.64	0.25	0.28	--
$2_\gamma \rightarrow 0_\beta/0_g$	--	--	16.8	0.42	0.37	0.42	--	--	--
$3_\gamma \rightarrow 2_g/4_g$	0.94(3)	0.93(3)	0.78	--	2.83	2.68	--	--	2.5
$3_\gamma \rightarrow 2_\beta/2_g$	0.025(3)	0.05(1)	9.74	0.026	0.33	0.4	--	--	--
$3_\gamma \rightarrow 2_\gamma/2_g$	69(5)	80(10)	8.1	25	9.06	8.9	--	--	--
$3_\gamma \rightarrow 2_\gamma/2_\beta$	2779(575)	1555(553)	0.83	961	27.5	22.3	--	--	--
$4_\gamma \rightarrow 2_g/4_g$	0.096(8)	0.095(9)	1.53	0.19	0.5	0.34	0.26	0.60	0.34
$4_\gamma \rightarrow 4_g/6_g$	4.36(55)	5.9(26)	0.03	--	8.5	38	--	--	11.3
$4_\gamma \rightarrow 2_\beta/2_g$	0.31(8)	--	0.92	0.2	0.31	1.65	--	--	--
$4_\gamma \rightarrow 2_\gamma/2_g$	97(17)	110(50)	98	--	--	--	--	--	--
$4_\gamma \rightarrow 2_\gamma/2_\beta$	314(96)	--	106	--	--	--	--	--	--
$5_\gamma \rightarrow 4_g/6_g$	0.33(2)	--	0.39	--	--	--	--	--	1.75
$5_\gamma \rightarrow 3_\gamma/4_g$	25.8(88)	--	20.9	--	--	--	--	--	0.6
$5_\gamma \rightarrow 3_\gamma/6_g$	8.5(29)	--	8.2	--	--	--	--	--	1.05
$6_\gamma \rightarrow 4_g/6_g$	0.04(2)	--	0.8	--	--	--	--	--	0.27
$7_\gamma \rightarrow 6_g/8_g$	0.24(2)	--	0.25	--	--	--	--	--	1.5
$7_\gamma \rightarrow 5_\gamma/6_\gamma$	0.164(7)	--	4.91	--	--	--	--	--	--
$7_\gamma \rightarrow 6_\gamma/6_g$	455(41)	--	10	--	--	--	--	--	2.15
$9_\gamma \rightarrow 8_g/10_g$	0.14(5)	--	0.17	--	--	--	--	--	1.37
$9_\gamma \rightarrow 7_\gamma/10_g$	23.6(37)	--	14.6	--	--	--	--	--	--
$2_{\beta 2} \rightarrow 0_g/2_g$	1.74(17)	1.69(45)	0.13	--	--	--	--	--	--
$2_{\beta 2} \rightarrow 2_g/4_g$	0.042(3)	--	16.7	--	--	--	--	--	--
$2_{\beta 2} \rightarrow 2_\beta/2_\beta$	0.18(1)	--	0.24	--	--	--	--	--	--
$2_{\beta 2} \rightarrow 2_\beta/2_g$	63.7(74)	56.3(188)	3.7	--	--	--	--	--	--
$2_{\beta 2} \rightarrow 4_\beta/2_g$	14.8(4)	--	253	--	--	--	--	--	--

[a]Peker (1989), [b]Stewart et al. (1990), [c]Gupta (1983), [d]Tamura et al. (1979), [e]Bhardwaj et al. (1983) and Bhardwaj (1983)

5.4.2.4 The B(E2) branching ratios for γ–band

The experimental data was available for 21 ratios, for transition from γ–band (see Table 5.6). It is evident from the observed data that the (γ→β) transitions are stronger than (γ→g); and (γ→ γ) transitions are stronger are than (γ→β). Theory supports these aspects. Most of the B(E2) ratios lie on the transition from SU(5) to SU(3).

The theoretical B(E2) ratios for the transition from 5_γ, 6_γ, 7_γ and 9_γ states were not available from the earlier from any previous work Gupta (1983), Tamura et al. (1979), Bhardwaj et al. (1983) and Bhardwaj (1983). The present study is extended for these four states along with three other lower states i.e. 2_γ, 3_γ and 4_γ states for calculating the B(E2) ratios. The B(E2) ratios for the transition from 2_γ, 3_γ, 4_γ 5_γ, 6_γ, 7_γ and 9_γ states are compared with the present work and found that most of the theoretical values are close to the observed values (see Table 5.6).

5.4.2.5 The B(E2) branching ratios for $K^\pi = 0^+_3$, β_2 –band

The five B(E2) ratios were available for transition from $2\beta_2$ state, the experimental data is compared for all these transitions and there is agreement between theory and experiment (see Table 5.6).

5.4.3 The ^{154}Sm isotope

5.4.3.1 Energy spectrum

In Table 5.7 the energy values are compared with the present work and DPPQ model. The calculated spectrum is good and the band-head of β– and γ –bands are close to the observed spectrum.

Table 5.7: The values of energy (in MeV) for ^{154}Sm.

State	Expt.[a]	Present	DPPQ[b]
2g	0.08198	0.0752	0.086
4g	0.2667	0.2492	0.270
6g	0.5443	0.5188	
8g	0.9031	0.8811	
10g	1.3333	1.3330	
0_β	1.0997	1.0927	1.096
2_β	1.1782	1.1995	1.198
2_γ	1.4404	1.4420	1.537
3_γ	(1.5400)	1.5361	
4_γ	(1.6606)	1.6573	

[a]Sakai (1984) [b]Gupta (1983)

5.4.3.2 B(E2) values

There are 10 B(E2) values available from the experiment for (g→g), (β→g), and (γ→g) transitions. The 24 B(E2) values are listed and compared with the previous work i.e. DPPQ of Gupta (1983), BEM of Tamura et al. (1979), effective IBA of Chuu et al. (1988) and RVM1and RVM2 of Bhardwaj et al. (1983) and Bhardwaj (1983) (see Table 5.8).

The observed B(E2) values of Tamura et al. (1979) and Peker (1987) for (β→g) and (γ→g) transitions are also compared with the present work and previous work of Chuu et al. (1988), Han et al. (1990), Kumar (1974), Kumar (1976) and Gupta (1983) for useful comparison in Table 5.8. The IBM-1 yields satisfactory results.

5.4.3.3 The B(E2) branching ratios for β-band

The experimental data of Tamura et al. (1979) and Peker (1987) for (2β→0g/2g), (2β→4g/2g) and (4β→2g/4g) transitions indicate that ^{154}Sm lies close to the SU(3)

limit. The present calculation gives these ratios close to observed values. Theory gives satisfactory results (see Table 5.9).

5.4.3.4 B(E2) branching ratios for γ –band

The B(E2) ratios for (2γ→0g/2g) is 0.60(11) compared to the Alaga value 0.7. For (2γ→2g/4g), (3γ→2g/4g) and (4 γ→2g/4g) transitions the Alaga values are 19.07, 2.5 and 0.34; and theoretical values are 11.2, 1.58 and 0.24 respectively (see Table 5.9). For other transitions the theoretical values are compared with BEM-4 and BEM-6 of Tamura et al. (1979), DPPQ of Gupta (1983), effective IBA of Han et al. (1990) and RVM of Bhardwaj et al. (1983) and Bhardwaj (1983) calculations. There is agreement between theory & previous work.

Table 5.8: The absolute B(E2) values (in e^2 b^2 unit) for ^{154}Sm.

$I_i \rightarrow I_f$	Expt. a	Present	DPPQ b	BEM4 c	BEM6 c	IBM-1 d	IBM-1 e
$2_g \rightarrow 0_g$	0.86(4)	0.808	0.79	0.909	0.881	0.978	1.026
$4_g \rightarrow 2_g$	1.38(22)	1.141.17	1.26	1.25	1.364	1.445	
$6_g \rightarrow 4_g$	1.37	1.22	---	1.37	1.35	--	1.547
$8_g \rightarrow 6_g$	1.50	1.219	--	1.41	1.38	1.416	1.549
$10_g \rightarrow 8_g$	1.49	1.175	--	--	--	1.333	1.492
$0_\beta \rightarrow 2_g$	--	0.015	0.094	0.054	0.054	--	--
$2_\beta \rightarrow 0_g$	0.006(41)[c]	0.001	0.0055	0.008	0.001	--	0.0068
$2_\beta \rightarrow 2_g$	0.012[c]	0.004	0.021	0.014	0.01	--	--
$2_\beta \rightarrow 4_g$	0.024[c]	0.009	0.062	0.033	0.008	--	0.007
$4_\beta \rightarrow 2_g$	--	0.0004	0.003	0.011	0.018	--	--
$4_\beta \rightarrow 4_g$	--	0.0058	0.020	0.01	0.003	--	--
$4_\beta \rightarrow 6_g$	--	0.0074	--	0.029	0.014	--	--
$2_\gamma \rightarrow 2_g$	0.02[c]	0.0242	0.039	0.037	0.047	0.018	0.003
$2_\gamma \rightarrow 4_g$	0.0008[c]	0.0022	0.0046	0.001	0.00001	0.0012	--
$4_\gamma \rightarrow 2_g$	--	0.0062	0.0093	0.020	0.021	--	--
$2_\gamma \rightarrow 4_g$	--	0.0256	0.043	0.043	0.040	--	--
$4_\gamma \rightarrow 6_g$	--	0.0191	--	0.002	0.002	--	--
$2_\beta \rightarrow 0_\beta$	--	0.057	0.084[f]	0.68	0.62	--	--
$4_\beta \rightarrow 2_\beta$	--	0.81	1.3[f]	0.96	0.86	--	--
$3_\gamma \rightarrow 2_\gamma$	--	1.08	--	1.30	1.28	--	--
$4_\gamma \rightarrow 3_\gamma$	--	0.76	--	0.98	0.98	--	--
$5_\gamma \rightarrow 4_\gamma$	--	0.57	--	0.69	0.62	--	--

[a] Peker (1987)

[b] Venkova and Andrejtscheff (1981)

[c] Tamura et al. (1979)

[d] Han et al. (1990)

[e] Chuu et al. (1984), [f] Kumar (1974) and Kumar (1976)

Table 5.9: The B(E2; $I_i \rightarrow I_f/I_{f'}$) ratios for ^{154}Sm.

$I_i \rightarrow I_f/I_{f'}$	Expt. *a*	Present	DPPQ *b*	BEM4 *c*	BEM6 *c*	RVM1 *d*	RVM2 *d*	IBM1 *e*
$2_\beta \rightarrow 0_g/2_g$	0.44	0.25	0.26	0.61	010	0.49	0.82	--
$2_\beta \rightarrow 4_g/2_g$	2.04	2.33	2.95	2.36	0.86	2.77	2.71	--
$2_\beta \rightarrow 0_\beta/0_g$	--	569	159	82.3	616	--	--	--
$4_\beta \rightarrow 2_g/2_g$	0.9(5)	0.07	0.16	1.10	6.48	0.42	0.42	--
$2_\beta \rightarrow 2_\beta/4_g$	--	140	66	99	318	--	--	--
$4_\beta \rightarrow 2_\beta/2_g$	--	2032	6500	87.3	47.8	--	--	--
$4_\beta \rightarrow 2_\beta/3_\gamma$	--	18.7	4.15	--	--	--	--	--
$2_\gamma \rightarrow 0_g/2_g$	0.60(11)	0.6	0.56	0.72	0.45	0.56	0.59	0.38
$2_\gamma \rightarrow 2_g/4_g$	4.8(32)	11.2	8.48	37	39.6	9.5	8.5	--
$2_\gamma \rightarrow 0_\beta/0_g$	--	0.45	0.001	0.63	0.8	---	---	---
$2_\gamma \rightarrow 2_\beta/2_g$	---	2.2	1.11	0.7	0.7	---	---	---
$2_\gamma \rightarrow 0_\beta/2_\beta$	---	0.12	---	0.63	0.51	---	---	---
$3_\gamma \rightarrow 2_g/4_g$	1.45(77)	1.58	1.53	3.57	3.45	---	---	---
$3_\gamma \rightarrow 2_\beta/2_g$	---	0.41	33.0	0.54	0.63	---	---	---
$3_\gamma \rightarrow 2_\gamma/2_g$	--	44.5	0.003	26.0	33.7	---	---	---
$3_\gamma \rightarrow 2_\beta/2_\gamma$	--	0.009	11000	0.02	0.019	---	---	---
$4_\gamma \rightarrow 2_g/4_g$	0.055	0.24	0.22	0.47	0.51	0.24	0.308	0.11
$4_\gamma \rightarrow 2_\gamma/2_g$	--	57.1	0.18	--	--	---	---	---
$4_\gamma \rightarrow 2_\beta/2_g$	--	0.048	--	0.99	2.77	---	---	---
$4_\gamma \rightarrow 4_\beta/2_\beta$	--	146.7	--	1.26	017	---	---	---
$4_\gamma \rightarrow 3_\gamma/2_\gamma$	--	2.14	--	2.33	2.63	---	---	---
$4_\gamma \rightarrow 4_\beta/4_g$	--	1.71	--	0.56	0.24	---	---	---

[a]Peker (1987)

[b]Gupta (1983)

[c]Tamura et al. (1979)

[d] Bhardwaj et al. (1983) and Bhardwaj (1983)

[e]Han et al. (1990)

[f] Kumar (1974) and Kumar (1976)

5.5 CONCLUSIONS

In this Chapter, the systematic study has been carried out for the lower and higher states of lower and higher bands, absolute B(E2) values and B(E2) branching ratios of $^{152\text{-}154}$Sm nuclei. The mass-dependent IBM-1 Hamiltonian is used to test its validity for explaining the large amount of experimental data for energy spectra, B(E2) values and B(E2) ratios. The present IBM-1 calculation is quite successful in explaining the observed properties.

In β–decay of ^{152}Eu, 13 new transitions and 5 new levels were reported by Stewart et al. (1990) for ^{152}Sm, which were included in the present work and present IBM-1 calculated results for the B(E2) branching ratios for β– band are close to observed data points (see Table 5.6). Present IBM-1 calculation also supports the X(5) character of ^{152}Sm (N=90).

The observed B(E2:Ig+2→Ig)) values increases rapidly on increasing Ig from 2^+ to 10^+ indicating the sharp change in the nuclear shape of ^{152}Sm which is supported by present IBM work (see Fig.5.6). The BEM6 Tamura et al. (1979) data points are much below the observed data points. However, the BEM4 Tamura et al. (1979) values are close to present calculation. But, IBM calculation of Chuu et al. (1988) gives *opposite* trend.

The calculated energy spectrum, B(E2) values and B(E2) ratios present a coherent and varied picture of the change in nuclear shape and dynamics with n^0 number N in $^{152\text{-}154}$Sm isotopes. It is found that the inclusion of energy states up to higher spins in the PHINT programme provides the proper transition from SU(5) to SU(3) limit. The results of our phenomenological calculations indicate that the mass-dependent Hamiltonian in IBM-1 is an encouraging approach than the effective boson approach with or without inclusion of Z = 64 subshell effect.

CHAPTER VI

SUMMARY AND CONCLUSIONS

The medium mass region provides a rich ground of testing the understanding of collective nuclear structure of doubly even nuclei. The collective nuclear structures of these nuclei have been analyzed, using empirical studies, phenomenological, geometrical, group theoretical models.

The values of asymmetry parameter (γ_0) of asymmetric rotor model are calculated using the experimental energies of $E2_2^+$ and $E2_1^+$ states for $50 \leq Z \leq 82$ and $82 \leq N \leq 126$ region. The whole calculated data is divided into four quadrants. The systematic dependence of γ_0 on N, N_B and NpNn has been carried out on *quadrant wise basis* to find out the role of valence nucleons and holes on nuclear structure. The role of Z=64 subshell effect for N≤90 region is discussed. In quadrant-I and quadrant-II, the γ_0 decreases; from 30^0 in Q-I and from 22^0 in Q-II to 9^0- 10^0; with increasing N from 82 to 104 (i.e. the mid of N=82 to 126 neutron shell), signifying that the nuclear deformation (β) is increasing, while the energy ratio R_4 increases from 2 (for harmonic vibrators or SU(5) type nuclei) to 3.33 (for good rotors or SU(3) type nuclei). This indicates that in this region the nuclear structure depends much more on Z. Asymmetry parameter shows the shape phase transition at N=88-90 in Q-I. In Q-II and Q-III; γ_0 has a systematic dependence with N, but with different patterns. In quadrant-I, the γ_0 is having more correlated dependence on N, rather than on NpNn. Also in quadrant- I, the Z=64 sub-shell effect for N≤90 nuclei affect the variation of γ_0 with N and NpNn product. The existence of X(5) symmetry in N=90 isotones established in recent works supports the formation of isotonic multiplets in this work. The calculated values of γ_0 are almost constant for N=90 isotones e.g. 13.8^0 for Nd, 13.24^0 for Sm and 13.86^0 for Gd; which supports the constant nuclear structure findings for N=90 isotones. The present work confirms the existence of isotonic multiplets in quadrant-I as reported earlier. In quadrant-III, the variation of γ_0 is different from quadrant I and II because the γ_0 increases sharply from 9^0 - 10^0 to 30^0 with increasing N from 104 to 126. This is signifying that the nuclear

deformation (β) is decreasing and the nuclear structure changes from pure rotor SU(3) type to vibrational SU(5) or γ-unstable O(6) type. Further, the asymmetry parameter for different elements has smooth curve with NpNn with almost same slopes except for Hg isotopes.

The predictions of asymmetric rotor model for B(E2;4g→2g)/B(E2;2g→0g) ratio are compared with the experimental data. It is also noted that this B(E2) ratio is anomalously small in case of two non- magic nuclei i.e., $^{198}_{80}Hg_{118}$ and $^{144}_{60}Nd_{84}$ with only two vacancy of protons for Z =82 and two valence neutrons outside N=82, respectively. The data points for other nuclei are lying between SU(5) and SU(3) limits. The calculated B(E2) ratios of ARM are very close to the SU(3) limit of IBM indicating that it can explain the structure of only well deformed nuclei. Therefore the ARM is partially successful in explaining this branching ratio. The variation of experimental B(E2; 4g→2g)/ B(E2;2g→0g) branching ratio with N and Z is carried out for Nd–Hg nuclei. It is found that there is shape phase transition for N=88 and 90 isotones (Nd, Sm, Gd, Er) from an ideal spherical harmonic vibrator or SU(5) to an axially symmetric deformed rotor or SU(3). The present study supports the subshell closer effect around Z=64, for N≤ 90 and the constant nuclear structure of N=90 isotones.

The interacting Boson Model-1 is used to study the nuclear structure of ^{152}Sm (a best example of X(5) symmetry) and ^{154}Sm (a best example of SU(3) symmetry). The level structure of ^{152,154}Sm is well reproduced and is in agreement with the experiment. The B(E2) branching values and B(E2) branching ratios are calculated for inter-band and intra-band transitions for g-, β-, γ- and β_2- bands and the calculated results are in good agreement with experimental data. Present calculation supports that ^{152}Sm is as a best example of X(5) symmetry and ^{154}Sm is a SU(3) type in nature.

REFERENCES

Alaga G., Alder K., Bohr A. and Mottelson B. R., Dan. Mat, -Fys. Medd. Danske Vid. Selsk 29, no.9, 1955.

Alder, K., Bohr, A., Huus, T., Mottelson, B. and Winter, A., Study of nuclear structure by electromagnetic excitation with accelerated ions, Rev. Mod. Phys., 28, p. 432-542, 1956.

Aprahamian, A., Brenner, D.S., Casten, R.F., Gill, R.L. and Piotrowski, A., First observation of a near-harmonic vibrational nucleus, Phys. Rev. Lett., 59, p. 535-538, 1987.

Arima, A. and Iachello, F., Collective nuclear states as representations of a SU(6) group, Phys. Rev. Lett., 35, 1069-1072, 1975.

Arima A. and Iachello F., Interacting boson model of collective states I. The vibrational limit, Ann. Phys. (N.Y), 99, p. 253-317, 1976.

Arima A. & Iachello F., Advances in Nuclear Physics (ed. J. W. Negele and E. Vogt), Vol. 13, p. 139, (Plenum Press, New York), 1984.

Iachello F. and Arima A., The Interacting Boson Model (Cambridge University Press, Cambridge, 1987).

Baranger M. and Kumar K., Nuclear deformations in the pairing-plus-quadrupole model: (I). The single-j shell*, *Nucl. Phys. A 62, 113, 1965

Baranger M. and Kumar K., Nuclear deformations in the pairing-plus-quadrupole model: (II). Discussion of validity of the model, Nucl. Phys. A110, 490, 1968a.

Baranger M. and Kumar K., Nuclear deformations in the pairing-plus-quadrupole model: (VI). Theory of collective motion, Nucl. Phys. A 122, 241, 1968b.

Bhardwaj S. K., Ph. D. thesis, Agra University, Agra, India, 1983.

Bhardwaj S. K., Gupta K. K., Gupta J. B. and Gupta D. K, Rotation-vibration description and transitional nuclei, Phys. Rev. C27, 872, 1983.

Bohr, A. and Mottelson, B.R., Mat Fys. Medd. K. Dan. Videask Selsk., 24, No. 16, 1953

Bohr A. and Mottelson B. R., Nuclear Structure, Vol. II, (W.A. Benjamin, New York), 1975.

Bonatsos, D., Interacting boson models of nuclear structure, (Clarendon Press, Oxford), 1989.

Brookhaven National Laboratory http://www.nndc.bnl.gov , 2015.

Cakirli R. B., Casten R. F., Jolie J., and Warr N., Highly anomalous yrast B(E2) values and vibrational collectivity, Phys. Rev. C70, p. 047302, 2004.

Castaños O., Federman P., Frank A. and Pittel S., Study of the effective hamiltonian interacting boson approximation, Nucl. Phys. A379, 61, 1982.

Casten R. F., NpNn systematics in heavy nuclei, Nucl. Phys. A443, p. 1, 1985.

Casten R. F., Nuclear Structure from a Simple Perspective, Oxford University Press, New York, 1990.

Casten R. F. and Zamfir N. V., The evolution of nuclear structure: the NpNn scheme and related correlations, J. Phys. G Nucl. Part. Phys. 22, p.1521, 1996.

Chadwick, J., The existence of a neutron, Proc. Roy. Soc. Lond. A 136 (830), 692, 1932.

Chuu D. S., Han C. S., Hsieh S. T. and Yen M. M. King, Structures of N=88 and N=90 isotones in the interacting boson approximation, Phys. Rev. C30, p.1300-1309, 1984.

Chuu D. S. and Hsieh S. T., IBA-1 studies of strongly deformed nuclei near A=150,

J. Phys. G: Nucl. Phys. 16, 583, 1990.

Davydov A. S., Bull. Acad. Sci. USSR 23, 783, 1959.

Davydov A. S. and Rostovsky V. S., Relative transition probabilities between rotational levels of non-axial nuclei, Nucl. Phys., Vol. 12, 58, 1959.

Davydov A. S. and Filippov G. F., Rotational states in even atomic nuclei, Nucl. Phys. 8, 237, 1985.

De Shalit A. and Goldhaber M., Mixed configurations in nuclei, Phys. Rev. 92, p.1211-1218,1953.

Fasessler, A., Greiner, W. and Sheline, R.K., The coriolis anti-pairing and blocking effects in deformed even nuclei, Nucl. Phys., 62, p.241-253, 1965.

Feshbach, H. and Iachello, F., The interacting boson model structure of ^{16}O, Phys. Lett. 45B, p.7-11, 1973.

Feshbach, H. and Iachello, F., The interacting boson model, Ann. Phys. (NY) 84, p.211-231, 1974.

Gupta J. B., Nuclear structure of $^{146-154}Sm$ in the dynamic pairing-plus-quadrupole model, Phys. Rev. C28, 1829, 1983.

Gupta, J. B., Unbroken SU(3) symmetry and the relation of interacting-boson model parameters with the shell model, Phys. Rev. C33,1505, 1986.

Gupta J. B., *Z*=64 subshell gap in the shell model and the effective boson number in the interacting boson model, Phy. Rev. C47, 1489, 1993.

Gupta J. B., A microscopic explanation of the isotonic multiplet at N=90, Workshop on "Frontiers in Gamma ray Spectroscopy" at Inter University Accelerator Centre, New Delhi, March 05, 2012a.

Gupta J. B., A microscopic explanation of the isotonic multiplet at N = 90 and of the F-spin multiplet in Dy-Hf, Eur. Phys. J. A. 48, p.1-6, 2012b.

Gupta J. B., Mittal H. M., Hamilton J. H. and Ramayya A. V., Systematic dependence of the γ-g B(E2) ratios on the NpNn product, Phys. Rev. C42**,** 1373, 1990a.

Gupta J. B., Hamilton J. H. and Ramayya A.V., A comparison of the F-spin and NpNn schemes with global empirical systematics, Int. J. of Modern Physics A, vol 5, No. 6, 1155-1164, 1990b.

Gupta J. B. and Sharma S., Interband B (E2) ratios in the rigid triaxial model, a review, Physica Scripta, 39, p.50, 1989.

Gupta R. K., Nuclear-softness model of ground-state bands in even-even nuclei, Phys. Lett. 36B, 173, 1971.

Hamamoto I., Empirical data concerning the electric quadrupole moments, Nucl. Phys. **73,** p.225-233, 1965.

Han C. S., Chuu D. S. and Hsieh S.T., Effective boson number calculations near the *Z*=64 subshell, Phys. Rev. C42, 280,1990.

Heisenberg, W., On the Structure of Atomic Nuclei, *Z. Phys.* 77, 1, 1932.

Hsieh S. T., Chiang H. C., Yen M. M. King and Chuu D. S., Effective boson calculations on Sm isotopes, J. Phys. G: Nucl. Phys. 12, L167, 1986.

T I Kracikova, M Finger, J Konicek, N A Lebedev, V A Deryuga, P O Lipas, E Hammaren and P Toivonen, Nuclear orientation study of the decay of ^{148}Eu, J. Phys. G: Nucl. Phys. 10, 667, 1984.

Iachello F. and Arima A., The Interacting Boson Model (Cambridge University Press) 1987.

Johnson A., Ryde H. and Sztarkier J., Evidence for a "singularity" in the nuclear rotational band structure, Phys. Lett. 34B, 605, 1971,

Janseen D., Jolos R. V. and Donau F., An algebraic treatment of the nuclear quadrupole degree of freedom, Nucl. Phys. A224, p.93-115, 1974.

Reetu Kaushik , S. Sharma and J. B. Gupta, Systematic dependence of asymmetric parameter in light and medium mass region, Proceedings of the DAE Symposium on Nuclear Physics (India), Vol. 59 (2014) p 300-301.

Kumar K, Collective Hamiltonian derived from the pairing-plus-quadrupole model: Modification and application to the transitional nuclei, $^{150, 152}$Sm, Nucl. Phys. A231, 189, 1974.

Kumar K., The Electromagnetic Interaction in Nuclear Spectroscopy, edited by W. D. Hamilton (North-Holland, Amsterdam), p.55, 1975.

Kumar K., Collective potential energy and shape fluctuations of even nuclei: (I). Dynamical effects in ^{154}Sm, Nucl. Phys. A92, p.653-672, 1967.

Kumar K., Nuclei off the Line of Stability, ACS Symposium Series 324 (ed. Meyer R. A. and Brenner D. S., American Chemical Society), p. 85, Washington, DC, 1986.

Kumar Rajesh, *Study of collective nuclear structure of some light and medium mass nuclei,* Ph. D. Thesis, U. P. Technical University, Lucknow, India (2013) unpublished.

Kumar K. and Baranger M., Nuclear deformations in the pairing-plus-quadrupole model (V): Energy levels and electromagnetic moments of the W, Os and Pt nuclei, Nucl. Phy. A 122, p. 273-324, 1968.

Kracikova T. I., Finger M., Pavlov V. N., Deryuga V. A., Lipas P. O., Hammaren E. and Toivonen P., Nuclear orientation study of the decay of ^{146} Eu, J. Phys. G: Nucl. Phys. 10, 571, 1984a.

Kracikova T. I., Finger M., Konicek J., Lebedev N. A., Deryuga V. A., Lipas P. O., Hammaren E. and Toivonen P., Nuclear orientation study of the decay of ^{148}Eu, J. Phys. G: Nucl. Phys. 10, 667, 1984b.

Kumar Rajesh, Sharma S. and Gupta J. B., Study of ground band about the nuclear structure variation of N Z chart A= 100–200 mass region, Armenian Journal of Physics, vol. **5**, issue 2, 62, 2012.

Lederer C. K. and Shirley V. S., Table of Isotopes, 7th edn. (New York: Wiley), 1978.

Mateosian E. der, Nuclear Data Sheets for A=150, Nucl. Data Sheets 48**,** 345, 1986.

Mayer M. G., On Closed Shells in Nuclei. II, Phys. Rev. 75, 1969, 1949.

Mayer M. G., Nuclear configurations in the spin-orbit coupling model. II. Theoretical considerations, Phys. Rev., **78,** 2223, 1950.

Ogawa M., Broda R., Zell K., Daly P. J. and Kleinheinz P., Lowest 2^+ state in $^{146}Gd_{82}$ and the energy gap at Z=64**,** Phys. Rev. Lett. **41**, 289, 1978

Peker L. K., Nuclear Data Sheets for A = 156, Nuclear Data Sheets 51, 1, 1987.

Peker L. K., Nuclear Data Sheets for A = 146, Nuclear Data Sheets 41, 195, 1984.

Peker L. K., Nuclear Data Sheets for A = 152, Nuclear Data Sheets 58, 93, 1989.

Peker L. K., Nuclear Data Sheets for A = 148, Nuclear Data Sheets 59, 393, 1990.

Raman S., Malarkey C. H., Milner W. T., Nestor C. W. Jr. and Stelson P. H., Transition probability, B(E2)↑, from the ground to the first-excited 2^+ state of even-even nuclides, Atomic Data & Nuclear Data Table **36**, 1, 1987.

Rutherford, E., The Scattering of α and β Particles by Matter and the Structure of the Atom, Philos. Mag., 6(21), p.669-688, 1911.

Sakai M**.,** Quasi-Bands in Even-Even Nuclei, Atomic Data & Nuclear Data Table 36, 399, 1984.

Scholten O., Iachello F. and Arima A., Interacting boson model of collective nuclear states III. The transition from SU(5) to SU(3), Ann. Phys. (N.Y.) 115, p. 325-366,1978.

Scholten O., Programme PHINT, KVI internal report 63, 1979a.

Scholten O., Programme FBEM, KVI internal report 63, 1979b.

Scholten O., Ph. D. thesis, University of Groningen, 1980.

Satpathy M. and Satpathy L., Shape-fluctuation model of ground-state bands in even-even nuclei, Phys. Lett 34B, 377, 1971.

Sharma S., Ph. D. Thesis, *Study of Nuclear Structure of some medium mass nuclei*, University of Delhi, 1989.

Sharma Satendra and Kaushik Reetu, Test of Asymmetry Rotor Model for the B(E2;4g→2g)/B(E2;2g→0g) Branching Ratio in Medium Mass Region, International Journal of Computer & Mathematical Sciences, Vol. 4, Special Issue, p. 160-167, 2015a.

Sharma Satendra and Kaushik Reetu, The systematic dependence of B(E2;4g→2g)/B(E2;2g→0g) ratio on N and Z for Nd - Hg nuclei, International Journal of Advanced Technology in Engineering and Science, Volume No 03, Special Issue No. 01, p. 1348- 1353, 2015b.

Sharma S. and Kumar Rajesh, Systematic dependence of E_{2g} and energy ratio R_4 on NpNn product for light and medium mass nuclei, Adv. Studies Theor. Phys. Vol. 4, no 3,109, 2010.

Stewart N. M., Eid E., El-Daghmah M. S. S. and Jabber J. K., Levels in ^{152}Gd and ^{152}Sm populated by the decay of ^{152}Eu, Z. Phys. A335, 13,1990.

Takahashi T., Yoshinaga N. and Higashiyama K., Backbending phenomena in $Ce^{132,134,136}$ with a pair-truncated shell model, Phys. Rev. C71, 014305, 2005.

Talmi I., Effective interactions and coupling schemes in nuclei, Rev. Mod. Phys. 34, 704, 1953.

Tamura T., Weeks K. and Krishimoto T., Sixth-order boson expansion calculations applied to samarium isotopes, Phys. Rev. C20, 307, 1979.

Venkova Ts. and Andrejtscheff W., Transition strengths B(E2) in the yrast bands of doubly even nuclei, Atomic Data and Nuclear Data Table 26, 93, 1981.

Von Brentano P., Gelberg A., Harter H. and Sala P., F-spin multiplets in rare-earth nuclei, J. Phys. G11, L85, 1985.

Yen M. M. King, Hsieh S. T., Chiang H. C. and Chuu D. S., Even samarium isotopes in the interaction boson approximation, Phys. Rev. C29, 688,1984.

Curriculum Vitae

Personal Information:

Name	Reetu Kaushik
Date of Birth	December 01, 1978
Father Name	Mr. Rajendra Sharma
Mother Name	Mrs. Saroj Bala Sharma
Permanent Address	82/12, New Multan Nagar, Meerut
Contact No.	91 9528217521
E-mail id	kaushikreetu19@gmail.com
Nationality	Indian
Gender	Female

Educational Qualification:

- B. Sc. (PCM) with 2nd division from C.C.S. University, Meerut in 1999.
- M. Sc. (Physics) with 1st division from C.C.S. University, Meerut in 2002.
- M. Phil. (Physics) with 1st division from Global Open University, Nagaland in 2010. Topic of Dissertation: *Study of Electromagnetic Waves & its Effect on Human Body.*

Research Publications:

- Paper published in International Journals : 02
- Paper in International Journals (under process) : 01
- Paper published in International/ National Symposia : 07
- National/ International Conferences Attended : 02

(REETU KAUSHIK)

LIST OF PUBLICATIONS

Publication in Referred Journal/s [International]

1. *"Test of Asymmetry Rotor Model for the B(E2; 4g→2g)/ B(E2;2g→0g) Branching Ratio in Medium Mass Region" - Satendra Sharma and Reetu Kaushik,* *International Journal of Computer & Mathematical Sciences, Vol. 4, Special Issue, March 2015, p. 160-167. ISSN: 2347 – 8527, DIIF Impact Factor Value 2.58.*
http://www.academicscience.co.in/admin/resources/project/paper/f20150305142554 4120.pdf

2. **"**The Systematic Dependence of B(E2;4g→2g)/B(E2;2g→0g) Ratio on N and Z for Nd -Hg Nuclei"- Satendra Sharma and Reetu Kaushik**.**

International Journal of Advanced Technology in Engineering and Science, Vol. No 03, Special Issue No. 01, March 2015, p 1348 – 1353. ISSN: 2348 – 7550. Impact factor = 1.012

http://ijates.com/images/short_pdf/1427120036_1144.pdf

3. "Systematic Dependence of Asymmetric Parameter for Even Z Even N Nuclei in Light and Medium Mass Region" - Satendra Sharma and Reetu Kaushik **(Under Process).**

Publication in Proceeding of Conferences/ Symposium [International]

1. "Systematic dependence of B(E2)↑ on asymmetry parameter γ_0"- Rajesh Kumar, Reetu Kaushik, S. Sharma, ***Proc. of the International Symposium on Nuclear Physics*** *(India)* Vol. 58 (2013) p 236-237. **ISBN 81-8372-070-6.** http://sympnp.org/proceedings/58/A94.pdf

2. ***"Test of Asymmetry Rotor Model for the B(E2; 4g→2g)/ B(E2;2g→0g) Branching Ratio in Medium Mass Region",*** 2nd International Conference on Emerging Trends of Engineering, Science, Management and its Applications**, JNU, New Delhi, March 1, 2015, paper ID: JNU/ 469.**

3. ***"The Systematic Dependence of B(E2;4g→2g)/B(E2;2g→0g) Ratio on N and Z for Nd -Hg Nuclei"- Satendra Sharma and Reetu Kaushik,*** International Conference On Recent Trends In Engineering, Science & Management (ICRTESM-2015)**, Jawaharlal Nehru University, JNU Convention Centre, New Delhi; March 15,2015, Paper ID:ICRTESM/JNU/2015/1144**

Publication in Proceeding of Conferences/ Symposium [National]

1. "Validity of single term energy formula for β-band"- Rajesh Kumar, Reetu Kaushik, S. Sharma and J. B. Gupta, *Proceedings of the DAE Symposium on Nuclear Physics (India),* Vol. 59 (2014) p 250-152. http://www.sympnp.org/proceedings/59/A101.pdf

2. "Correlation of average scaling coefficient with asymmetric parameter and average power index with quadrupole deformation parameter" - Vikas Katoch, Reetu Kaushik, S. Sharma and J. B. Gupta, *Proceedings of the DAE Symposium on Nuclear Physics (India),* Vol. 59 (2014) p 298-299. http://www.sympnp.org/proceedings/59/A125.pdf

3. "Systematic study of β-band and correlation with g- band using power law and soft rotor formula"- Vikas Katoch, Reetu Kaushik, S. Sharma and J. B. Gupta, *Proceedings of the DAE Symposium on Nuclear Physics (India),* Vol. 59 (2014) p 238-239. http://www.sympnp.org/proceedings/59/A95.pdf

4. "Systematic dependence of asymmetric parameter and evidence of Z=64 subshell effect in rare earth region" - Reetu Kaushik , S. Sharma and J. B. Gupta, *Proceedings of the DAE Symposium on Nuclear Physics (India),* Vol. 59 (2014) p. 234-235. http://www.sympnp.org/proceedings/59/A93.pdf

5. "Systematic dependence of asymmetric parameter in light and medium mass region"- Reetu Kaushik , S. Sharma and J. B. Gupta, *Proceedings of the DAE Symposium on Nuclear Physics (India),* Vol. 59 (2014) p 300-301. http://www.sympnp.org/proceedings/59/A126.pdf

Study of ^{152}Sm using interacting boson model-1

Satendra Sharma[1,*], Reetu Kaushik[2], Vikas Katoch[3] and J. B. Gupta[4]
[1]*Department of Physics, Yobe State University, KM 7, Gujba Road, P. M. B. 1144, Damaturu, Nigeria*
[2]*Research Scholar, Department of Physics, Mewar University, Gangrar, Rajasthan-312901, India*
[3]*RKG Institute of Technology (Uttar Pradesh Technical University), Ghaziabad, India*
[4]*Ramjas College, University of Delhi, Delhi-110007, India*
** email: ss110096@gmail.com*

Introduction

The energy ratio R_4 (=$E4_g/E2_g$) = 3.01 and R_β (=$E0_\beta/E2_g$) = 5.62 for ^{152}Sm (N=90) nucleus and these ratios are very close to the X(5) symmetry limiting values (R_4 = 2.9 and R_β = 5.65). Therefore, ^{152}Sm is the best example of X(5) symmetry of IBM-1 [1]. The large experimental data [2, 3, 4] is now available for ^{152}Sm from decay and reaction work. The interacting boson model-1 (IBM-1) [1] is used to study the energy spectra, B(E2) values/ ratios for inter-band and intra-band transitions. The theoretical results of present IBM calculation are compared with the predictions of DPPQ, BEM and RVM models [5-9] and the experimental data [2, 3, 4, 10, 11].

Result and Discussion

In ^{152}Sm the members of g-band and β_1-band are available up to 14^+, for β_2 up to 2^+ and γ_1 up to 5^+ [2]. In the present calculation the band-head of the g-, β- and γ–bands are very close to the experiment and the spacing of different members in the different bands is also like in the experiment [2-3]. For $K^\pi = 0^+_3$ band the calculated 0^+ state lies at 1.496 MeV compared to the 1.0829 MeV in experiment. The variation of E_I with spin (I) for different bands is presented in Fig. 1. The slopes of E_I vs. I for different bands in experiment [2-3] are similar to the theoretical slopes.

The variation of B(E2;Ig→Ig-2)

The variation of B(E2;Ig→Ig-2) vs. spin (Ig) is shown in Fig. 2. The experimental [3,4] B(E2) values increases rapidly on increasing Ig from 2^+ to 10^+ indicating the sharp change in the nuclear shape. In the previous IBM calculation [5], the B(E2) first increases when Ig increases from 2^+ to 4^+ and it decreases while Ig increased from 4^+ to 8^+ *unlike* the observed trend. But in the present IBM work, the B(E2) values follow the observed trend and values the more closer than other theoretical data. The BEM6 [6] data points are much below the observed data points. However, the BEM4 [6] values are close to present calculation. Only two data points are available for DPPQ [7], RVM1 and RVM2 [8, 9] to find any definite conclusion.

The theoretical results of vibrational model (VM), SU(5), O(6) and SU(3) limiting values, present calculation and IBM calculation of [5] along with the experimental data for B(E2) values[3,4] are shown in Fig. 2. It is clear that the observed data is quite below from the VM limiting values and is lying between SU(5) and SU(3) limiting values. The B(E2) values from present IBM calculation and BEM4 [6] are very close to the experimental data points and also present IBM calculation produces the observed slop of this ratio with I_g.

B(E2) ratios for β– band

In the β-decay of ^{152}Eu, 13 new transitions and 5 new levels were reported [10], which are included here for useful discussion.

In Table of Isotopes [11], the B(E2) ratio for ($2_\beta \rightarrow 0_g/2_g$) transition is 0.84 which is more than the SU(3) limiting value 0.7. This ratio may be large due to 0.2% M1 and 4% E0 mixing in the ($2_\beta \rightarrow 2_g$) 0.6886 MeV γ–ray. In a recent compilation work [3] this ratio is 0.17(1) compared to the theoretical value 0.12 & DPPQ value 0.076 [7].

The ($2_\beta \rightarrow 4_g$) 0.444 MeV γ–ray was overlapping with ($2^- \rightarrow 3_\gamma$) transition and gives B(E2; $2_\beta \rightarrow 2_g/4_g$) = 0.35 (the intensity of ($2^- \rightarrow 3\gamma$) γ–ray was 12 which gives this ratio 0.56) [11]. But in the recent compilation [3], this ratio is 0.30(3) compared to 0.030(1) in decay of ^{152}Eu [10].

In Table of Isotopes [11]; the ($4_\beta \rightarrow 4_g$) 0.6565 MeV γ–ray was not pure E2 but has 16% M1 and 5% E0 mixing, which gave the B(E2;$4_\beta \rightarrow 2_g/4_g$) = 0.11 and B(E2;$4_\beta \rightarrow 4_g/6_g$) = 0.76, but Peker [3] deduced these ratios equal to 0.21(2) and 3.6(22); Stewart et al. [10] deduced 0.11(2) and 0.08(2); and in the present IBM calculation these ratios are 9.3 and 231, respectively.

For ($6_\beta \rightarrow 4_g/6_g$), ($8_\beta \rightarrow 6_g/8_g$) and ($10_\beta \rightarrow 8_g/10_g$) transitions; the observed B(E2) ratios lie away from the respective Alaga values and theoretical values are close to the observed values. It is also evident that (β→β) transitions are stronger than (β→g) which is supported by present IBM calculation values (Results will be presented).

B(E2) ratios for γ–band

The experimental data was available for 21 ratios, for transition from γ–band. It is evident from the observed data that the (γ→β) transitions are stronger than (γ→g); and (γ→ γ) transitions are stronger are than (γ→β). Theory supports these aspects. Most of the B(E2) ratios lie on the transition from SU(5) to SU(3).

The theoretical B(E2) ratios for the transition from 5_γ, 6_γ, 7_γ and 9_γ states were not available from any previous work [6,7,8,9]. The present study is extended for these four states along with three other lower states i.e. 2_γ, 3_γ and 4_γ states for calculating the B(E2) ratios. The B(E2) ratios for the transition from 2_γ, 3_γ, 4_γ 5_γ, 6_γ, 7_γ and 9_γ states are compared with the present work and found that most of the theoretical values are close to the observed values (Results will be presented).

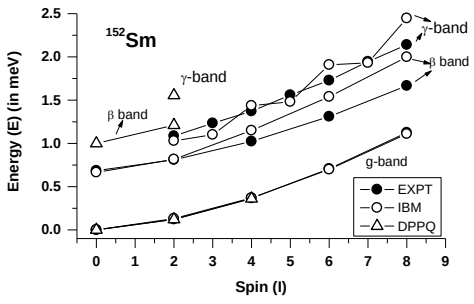

Fig 1: The variation of E_I with spin (I).

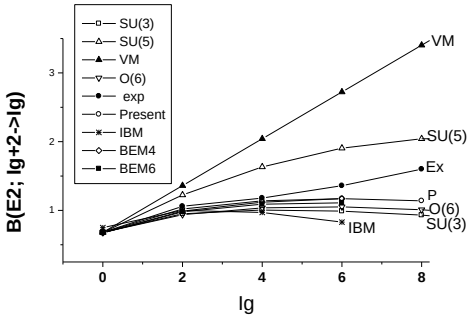

Fig 2: The variation of B(E2;Ig→Ig-2) with Ig for ground band. The experimental data of [3,4] are shown by solid circles (●), present IBM calculation by hollow circles (○), BEM4 [6] by hollow diamond (◊), BEM6 [6] by solid square (■), IBM [5] by star (*). The vibrational model (VM) is shown by (▲), SU(5) limiting values by (Δ), O(6) limiting values by (∇) and SU(3) limiting values by (□).

Acknowledgement

SS is grateful to Prof. Musa Alabe, Vice Chancellor, Yobe State University, Damaturu, Nigeria for encouragement and for providing the research facilities

References

[1] Casten R. F., *Nuclear Structure from a Simple Perspective*, (Oxford University Press, New York), 1990.
[2] Sakai M., Atomic Data & Nuclear Data Table 36, 399, 1984.
[3] Peker L. K., Nuclear Data Sheets 58, 93, 1989.
[4] Venkova Ts. and Andrejtscheff W., Atomic Data and Nuclear Data Table 26, 93, 1981.
[5] Chuu D. S., Han C. S., Hsieh S. T. and Yen M. M. King, Phys. Rev. C30, 1300, 1984.
[6] Tamura T., Weeks K. and Krishimoto T., Phys. Rev. C20, 307, 1979.
[7] Gupta J. B., Phys. Rev. C28, 1829, 1983.
[8] Bhardwaj S. K., Gupta K. K., Gupta J. B. and Gupta D. K, Phys. Rev. C27, 872, 1983.
[9] Bhardwaj S. K., Ph. D. thesis, Agra University, Agra, India, 1983.
[10] Stewart N. M., Eid E., El-Daghmah M. S. S. and Jabber J. K., Z. Phys. A335, 13,1990.
[11] Lederer C. K. and Shirley V. S., Table of Isotopes, 7th edn. (New York: Wiley, 1978).

Study of nuclear structure of ^{146}Sm from asymmetric rotor model

Satendra Sharma[1],* Emeka L. Agada[1], Rajesh Kumar[2], Vikas Katoch[3], Reetu Kaushik[4] and J. B. Gupta[5]

[1]*Department of Physics, Yobe State University, Damaturu, NIGERIA*
[2] *Department of Physics, Noida Institute of Engineering & Technology, Greater Noida-201306, INDIA*
[3] *Department of Physics, Raj Kumar Goel Institute of Technology, Ghaziabad, 201003, INDIA*
[4]*Research Scholar, Department of Physics, Mewar University, Gangrar, Rajasthan-312901, INDIA*
[5]*Ramjas College, University of Delhi, Delhi, INDIA*
* *email: ss110096@gmail.com*

Introduction

The structure of samarium isotopes is very interesting because the shape phase transition takes place from SU(5) to SU(3) limit of interaction boson model (IBM) [1]. This feature has attracted many researchers to study these isotopes experimentally and theoretically. The (^{11}B, 4n) reaction at 54 MeV on natural La target evaporated on gold was used [2] to study the lifetimes measurement of various energy levels of ^{146}Sm. The radioactive decay of ^{146}Eu [3] has given spin parity assignment in ^{146}Sm and angular distribution of 68 γ–rays. Peker [4] also compiled the experimental data for A = 146. The 0_2^+ state earlier observed [3] at 1.452MeV was not adopted in recent compilation [5] but new 0_2^+ and 0_3^+ states at 2.211 and 2.331 MeV were reported. Newly adopted [5] $5^+\gamma$, $8^+\gamma$ and $9^+\gamma$ states of $K^\pi = 2^+_1$ band at 2.8983, 3.0431 and 3.5674 MeV, respectively are included in the present work.

Several theoretical calculations, using IBM-1 [3, 6, 7], IBM-2 [8] and DPPQ [9] were carried out to explain the structure of ^{146}Sm. The compilations of experimental data [2- 5] enable us to present more elaborate analysis. Unfortunately, insufficient data is available for ^{146}Sm, therefore we have used data for other N=84 isotones for useful comparison for B(E2) values for inter and intra band transitions. The asymmetric rotor model [10] has been used for calculating the levels energy and transition probabilities.

The parameters used for calculation are A=146, Z=64, $E2^+g$ = 0.74724 KeV, γ= 26.44° and β= 0.0917°. The energy ratios are computed from experiment [5] and compared with the previous theoretical calculations [7-9] and present ARM calculation in Table 1. The calculated values are close to the experimental values indicating the vibrational nature of ^{146}Sm. The reduced transition ratios are given in Table 2 for g- and γ- bands. The present ARM results are compared with the observed [3-5, 9] and other theoretical calculations from DDPQ [9] and IBM [6- 8]. Most of the ratios are close to the observed values. Some of the γ-rays are having M1 admixture [5] (see Table 2). The energy values for ground state rotational and γ-vibrational bands are given in Table 3 and the experimental values [5] are compared with IBM-1 [3, 7], DPPQ [9] and ARM results. The B(E2) values for the transitions from g- and γ- band are also compared with other N=84 isotones for useful comparison (results will be presented).

Acknowledgement

SS and ELA are grateful to Prof. Yakubu Mukhtar, Vice Chancellor, Yobe State University, Damaturu, for providing the facilities for the research work. RK is wishing to express his gratitude to Dr. O. P. Agrawal, Chairman, and Dr. Ajay Kumar, Director, NIET, Gr. Noida for providing the research facilities.

References

[1] Casten R. F., Nuclear Structure from a Simple Perspective, (Oxford University Press, New York), 1990.
[2] S. Rozak, et al., Phys. Rev., C25, 300 (1982).
[3] T. I. Kracikova, et al., Phys. G: Nucl. Phys. 10, 571(1984).
[4] L. K. Peker, Nuclear Data Sheets, 41, 195(1984).
[5] L. K. Peker and J. K. Tuli, Nuclear Data Sheets, 82, 187(1997).
[6] O. Scholten, F. Iachello and A. Arima, Ann. Phys. (N. Y.), 115, 325-366 (1978).
[7] Satendra Sharma, International Journal of Research in Science, 2(2), 20-25 (2016).
[8] S. A. Eid and S. M. Diab, European Journal of Academic Essays 3(1), 37-41 (2016).
[9] J. B. Gupta, Phys. Rev. C28, 1829 (1983).
[10] A. S. Davydov and G. F. Filippov, Nucl. Phys. 8, 237 (1958).

Table 1. The energy ratios for g-and γ- bands.

Ratios	Expt. [5]	ARM	DPPQ [9]	IBM1 [7]	IBM2 [8]	SU(5)	O(6)	SU(3)
E4g+/E2g+	1.85	2.7	1.846	1.877	2.09	2	2.5	3.33
E2γ+/E2g+	2.206	2.2	2.282	2.046	2.21	2	2.5	3.33
E3γ+/E2g+	3.038	3.2		2.989	3.11	3	4.5	7
E4γ+/E2g+	3.264	2.7		3.381	3.70	4	7	12

Table 2. The B(E2; Ii → If/If') ratios.

Transition	Experimental Ratios			IBM1		IBM2	DPPQ	ARM
	[3]	[4]	[5]	[6]	[7]	[8]	[9]	
4g→2g/2g→0g	≥1.27(26)	≥1.30	1.82[9]	1.82	1.613	1.613	1.94	1.409
6g→4g/4g→2g	0.98(4)	<0.74			1.21	1.21		1.254
8g→6g/6g→4g		~0.16(5)						1.106
2γ→0g/2g	0.0012(4)	>0.01*	0.01**	0.01	0.014	0.014	0.018	0.025
3γ→2g/2γ	0.019(5)	0.049	0.018#		0.027	0.027	0.10	0.028
4γ→2g/4g	0.007	0.007	0.017$		0.005	0.005	0.1	0.079
9γ→8g/8_2		0.023	0.023&		0.15			0.000 1

*Multiple assignments. ** (2γ→2g) 900.797 KeV γ – ray has M1 admixture.
#1522.712 KeV (3γ→2g) and 621.85 KeV (3γ→2γ) γ-rays have the M1 admixture.
$1691.643 KeV (4γ→2g) and 1057.62 KeV (4γ→4g) γ-rays have the M1 admixture.
&524.3 KeV (9γ→8_2) γ – ray is M1 type transition.

Table 3. The energy levels of ground state rotational and γ- vibrational bands.

State	Expt. [5]	IBM1 [7]	IBM1 [3]	DPPQ [9]	ARM
2g	0.747115	0.7804	0.733	0.756	0.75
4g	1.38128	1.4648	1.353	1.375	2.06
6g	1.811682	2.0500	1.869	-	3.87
8g	2.7372	2.5331	2.287	-	6.20
2γ	1.647929	1.5969	1.610	1.725	1.65
3γ	2.26983	2.3333	2.417	-	2.40
4γ	2.438981	2.6387	2.256	-	2.76
5γ	2.898268	2.9296	-	-	4.64

Systematic dependence of asymmetric parameter and evidence of Z=64 subshell effect in rare earth region

Reetu Kaushik[1] , S. Sharma[*,2] and J. B. Gupta[3]
[1]*Research Scholar, Department of Physics, Mewar University, Gangrar, Rajasthan-312901, India*
[2]*Panchwati Institute of Engineering and Technology (Uttar Pradesh Technical University), National Highway- 58, Ghat Institutional Area, Meerut, PIN 250005, INDIA*
[3]*Ramjas College, University of Delhi, Delhi 110007, India*
[*]*email: ss110096@gmail.com*

The nuclear shape-phase transition at N = 88–90, and the role of Z = 64 sub-shell closure effect therein has been a subject of study on empirical basis and in the context of the N, Z, P and NpNn scheme [1,2,3,4]. It was pointed out by Gupta [1] that the filling of neutron orbitals at N = 86, 88 & 90 plays an important role in the shape-phase transition. The filling of the proton Nilsson orbitals of varying slopes leads to the variation of nuclear structure with varying Z, which leads to the Z = 64 subshell effect, which disappears at N=90. Gupta [1] observed that the effect of n-p interaction of the $\pi h11/2$ and $\nu h9/2$ orbitals, along with the contribution of the $\nu i13/2$ orbital leads to the shape-phase transition at N=88−90. The slopes of proton Nilsson orbitals explain the Z= 64 subshell effect.

The size of proton subshell gap between the $d_{5/2}$ and $h_{11/2}$ orbitals was reviewed by Gupta [2]. The increased gap at *Z*=64 was not inconsistent with experiment for occupation probabilities and the nuclear structure of *N*=82 isotones and $^{146\text{-}154}$Sm [2]. In IBM calculation there was no *a* priori need of the use of subshell closure [2]. In the empirical studies for this region the use of the *Z*=64 subshell does lead to elegant systematics in some cases. In this paper we have tested this for the asymmetry parameter (γ).

Asymmetric Rotor Model (ARM):

The Hamiltonian of ARM[5] is:

$$H = (\hbar^2/2)\,\Sigma\,(I_i^2/J_i) \qquad (1)$$

where, I_i is the projection of angular momentum on the intrinsic axes. The moment of inertia J_i are given by the hydrodynamic relation:

$$J_i = (4/3)\,J_0\,\mathrm{Sin}^2(\gamma - 2\pi/3) \qquad (2)$$

where, $J_0 = 4B\beta^2$. (3)

Simple analytical expressions for the energy of two levels for $I = 2$, defined as:

$$E^+_{2\,1,2} = \frac{9[1-(-1)^{\sigma_{1,2}}\sqrt{1-\frac{8}{9}X}}{X} \text{ (in units of } \hbar^2/J_0) \qquad (4)$$

where $\sigma_{1,2}$=0,1 and γ-function is written as $\varepsilon_{21,2}$.

Here, $\varepsilon^+_{2\,1} = \frac{9-\sqrt{81-72X}}{X}$ and $X=\mathrm{Sin}^2 3\gamma$.

Calculation of Asymmetric Parameter

The value of asymmetry parameter (γ) can be evaluated [6,7,8] using the experimental energies $E2_2^+$ and $E2_1^+$ of the two 2^+ states. The energy ratio $R\gamma=E_{2\gamma}/E_{2g}$. The asymmetry parameter is:

$$\gamma = (1/3)\,\sin^{-1}[(9/8)\{1-((R\gamma-1)/(R\gamma+1))^2\}].$$

It can be evaluated using: (a) The energy ratio $R_4=(E_{4g}/E_{2g})$ but only the nuclei with $2.8 \le R4 \le 3.33$ will be allowed [6,8] (see fig 1 of ref.6). (b) The B(E2) values also but these values are very small and available with uncertainties too. Therefore the values from energy ratio $R\gamma$ are more reliable.

Result and Discussions:

The variation of $E_{2\gamma}$ state (in MeV) versus neutron number (N) is shown in Fig. 1 for N=86-122. The data points are joined for same element so the N dependence of $E_{2\gamma}$ is visible. The value of $E_{2\gamma}$ is having maximum scattering (0.7 to 1.6 MeV) at N=104 for Yb to Pt isotopes corresponding to β hard core structure of these nuclei[9] The fig. 1 is reproduced from [9].

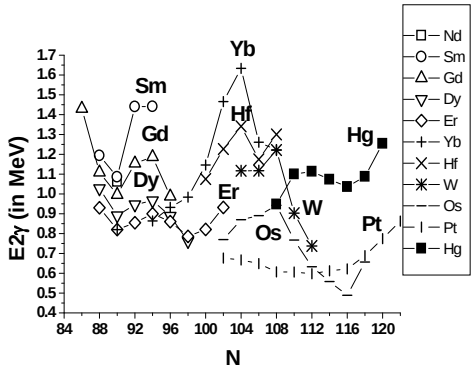

Fig. 1. The variation of energy of 2γ state (in MeV) versus neutron number (N).

The variation of $E_{2\gamma}$ versus proton number (Z) is shown in Fig. 2 for Z = 60 -80. The data points are joined for each isotones for N =86–116. The value of $E_{2\gamma}$ is suddenly increasing from 0.8 to 1.6 MeV for a fixed value of Z= 70 when N is changing from 90 to 104. The $E_{2\gamma}$ decreases sharply on increasing Z from 60 to 68 for each isotones i.e. N= 88-98 indication shape phase transition from Vibration to Rotation i.e. SU(5) to SU(3) limits of IBM. The slope for N= 88 and 90 are same and there is no indication for subshell effect in this fig.

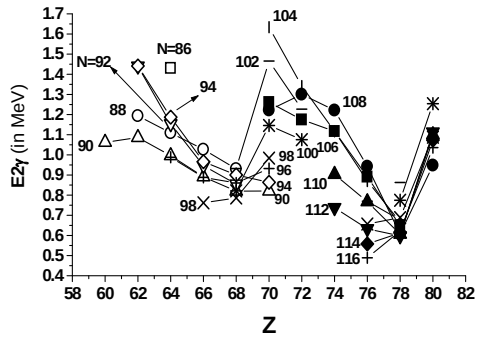

Fig. 2. The variation of energy of 2γ state (in MeV) versus proton number (Z) for Z = 60 -80.

The variation of asymmetric parameter (γ) versus proton number (Z) for N= 82 -96 isotones for Z= 58-72 region is shown in Fig.3. The gap is maximum i.e. 7.6 at Z= 64 when N changes from 88 to 90 indication the subshell effect at Z=64 for N<90. Since the γ is evaluated from E_{2g} and $E_{2\gamma}$. However the Z=64 subshell effect is not evident in $E_{2\gamma}$ (see fig. 2) and in $E_{0\beta}$ (see fig.4 ref. [9]). It is evident only in E_{2g} [4] and R_4 [4 and see fig. 12 of ref. 10].

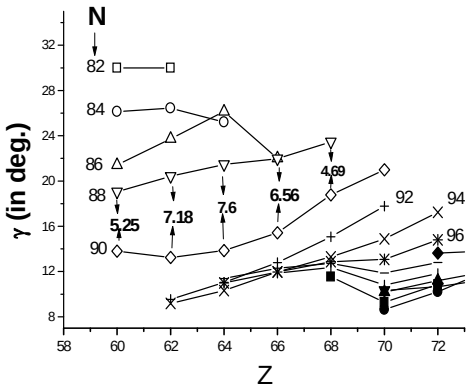

Fig. 3. The variation of asymmetric parameter (γ) versus proton number (Z) for N= 82 -96 isotones for Z= 58-72 region.

References:

[1] J. B. Gupta, Phys. Rev. **C87** (2013) 064318.
[2] J. B. Gupta, Phys. Rev. **C47** (1993) 1487.
[3] J. B. Gupta, Phys. Rev. **C89** (2014) 034321.
[4a] F. Iachello & A. Arima, The Interacting Boson Model (Cambridge University Press, Cambridge, 1987).
[4b]R. F. Casten, Nuclear structure from simple perspective, (2000) Oxford University Press, Oxford.
[5] A. S. Davydov & G. F. Filippov, Nucl. Phys. **8** (1958) 237
[6] J. B. Gupta & S. Sharma, Physica Scripta **39**(1989)50
[7] H. M. Mittal, S. Sharma & J. B. Gupta, Physica Scripta **43** (1991)558.
[8] S. Sharma, Ph. D. Thesis, University of Delhi (1989) unpublished.
[9] J. B. Gupta, A. K. Kavatheker, Pramana J. of Phys. 61(2003) 167.
[10] Rajesh Kumar, S. Sharma and J. B. Gupta, Armenian J of Physics **5** (2012) 62.

Systematic study of β-band and correlation with g- band using power law and soft rotor formula

Vikas Katoch[1,*], Reetu Kaushik[2], S. Sharma[3,#] and J. B. Gupta[4]
[1]*Research Scholar, Department of Physics, Singhania University, Jhunjhunu, Rajasthan-333515, India*
[2]*Research Scholar, Department of Physics, Mewar University, Gangrar, Rajasthan-312901, India*
[3]*Panchwati Institute of Engineering & Technology (U.P. Technical University), Meerut-250005, India*
[4]*Ramjas College, University of Delhi, Delhi-110007, India*
[#]ssharma_phy@yahoo.co.uk

Introduction

The nuclear structure of even Z even N medium mass transitional nuclei consist of ground state band, $K^{\pi}=0_1$ β-band, $K^{\pi}=2_1$ γ-band and other higher bands [1]. As we move away from closed shell, energy levels are low lying from spherical to deformed nuclei and energy deviated from ideal rotor behavior. The energy of these transitional nuclei in ground band can also be studied using Bohr Mottelson energy expression [1], Soft Rotor Formula (SRF) [2], Power Law (PL) [3] etc. Recently, Gupta et al. (2013) [4] modified SRF for non zero band head $K^{\pi}=2_1$ γ-band and reproduced the level energies. Here same formula applied for $K^{\pi}=0_1$ β-band and the level energies are reproduced and compared with experimental energies. The power law [3] is also used for recalculation of level energies and for useful comparison.

Method

The SRF of Gupta (1971) and Brentano et al. (2004) [2] for ground state band is:

$$E(I) = \frac{\hbar^2 I(I+1)}{2\theta(1+\sigma I)} \qquad (1)$$

where, σ and θ are softness parameter and moment of inertia (MOI). For β-band, the level energies are $E(0_\beta)$, $E(2_\beta)$, $E(4_\beta)$, $E(6_\beta)$, $E(8_\beta)$ and $E(10_\beta)$ in KeV for spin I=0, 2, 4, 6, 8 and 10. The difference of $[E(2_\beta) - E(0_\beta)]$ and $[E(4_\beta) - E(0_\beta)]$ are denoted as $\Delta E(20_\beta)$ and $\Delta E(40_\beta)$. The Equ. (1) for spin 2 and 4 gives:

$$\Delta E(20_\beta) = \frac{3}{\theta(1+2\sigma)} \qquad (2)$$

and $$\Delta E(40_\beta) = \frac{10}{\theta(1+4\sigma)} \quad . \qquad (3)$$

On dividing equation (3) by equation (2), the θ is cancelled and σ can be calculated. Using σ and θ for different spin the values of level energies is reproduced. Similarly, the PL energy expression $E_I=aI^b$ [3] is used for β-band. The values of 'a' and 'b' parameters are obtained by subtracting band head difference $E(0_\beta)$ and the energy difference of spin 2 and 4. Using these parameters, level energies are reproduced.

Result and Discussion

The values of root mean square deviation (RMSD) of the reproduced level energies are obtained using PL and SRF from experimental level energies [5]. It is observed that the RMSD values are small using power law in comparison to the SRF. Most of the nuclei having RMSD value lie below 40 KeV using power law except N=88 whereas using SRF it is lie below 100 KeV. The variation of RMSD versus N using SRF and PL is shown in Fig. 1(a, b). The MOI from SRF for β-band and ground band is studied with energy ratio of both the bands and shown in Fig. 2(a, b). It is observed from the diagrams that as the energy ratio rises from spherical behavior to deformed limit, the MOI increases except ^{150}Sm in β-band and ^{150}Nd out of the fit of smooth curve. The systematics of softness parameters of both the bands also has same correlation with energy ratios.

Conclusion

It is evident from variation of RMSD vs. R_4 curve that the level energies of β-band are well reproduced in PL and the values of RMSD ≤ 40 KeV except N=88 isotones (RMSD≈ 50 KeV). The variation of MOI (θ)

vs. R_4 for g- band and β- band show a strong correlation.

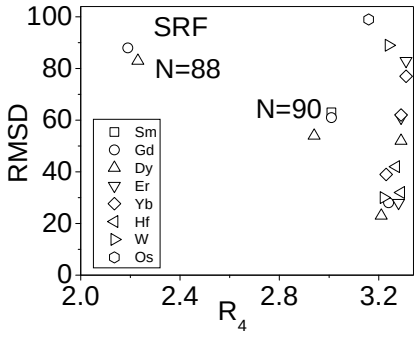

Fig. 1(a) The variation of RMSD vs R_4.

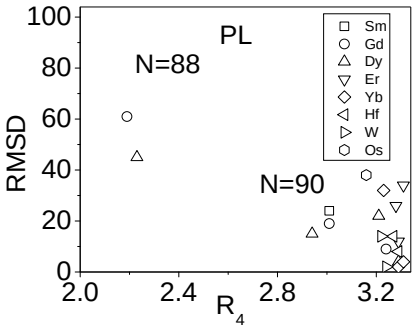

Fig. 1(b) The variation of RMSD vs R_4.

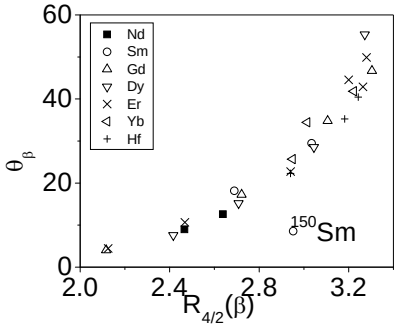

Fig. 2(a) The MOI vs. $R_{4/2}$ for β-band.

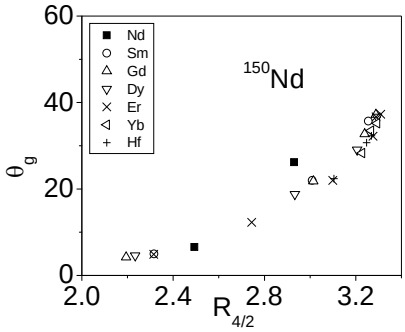

Fig. 2(b) The MOI vs. $R_{4/2}$ for ground band.

Acknowledgement:

One of us SS is thankful to the Shri Pankaj Goel Chairman, Panchwati Institute of Engineering & Technology, Meerut for supporting research facility in the Institute. VK is thankful to the Shri Dinesh Goel, Chairman, Raj Kumar Goel Institute of Technology, Ghaziabad for providing platform for research work. J. B. Gupta appreciates post-retirement association with Ramjas College.

* *Raj Kumar Goel Institute of Technology (Uttar Pradesh Technical University), Ghaziabad.*

References:

[1] A. Bohr & B. R. Mottelson, Nuclear Structure, Vol. II (Benjamin, N.Y) 1975.
[2] R. K. Gupta, Phys. Lett. **36B** (1971) 173 & P von Brentano et al., Phys. Rev. **C69**, (2004) 044314
[3] J. B. Gupta, A. K. Kavathekar and R. Sharma, Physica Scripta **51** (1995) 316.
[4] J. B. Gupta, Satendra Sharma and Vikas Katoch, Pramana J. of Phys. 81(2013) 75-86
[5] www.nndc.gov.bnl, July, 2014

Validity of single term energy formula for β-band

Rajesh Kumar[1*], Reetu Kaushik[2], S. Sharma[3] and J. B. Gupta[4]
[1]*Department of Physics, Noida Institute of Engineering & Technology (U. P. Technical University), Greater Noida-201306, India*
[2]*Research Scholar, Department of Physics, Mewar University, Gangrar, Rajasthan-312901, India*
[3]*Panchwati Institute of Engineering & Technology (U.P. Technical University), Meerut-250005, India*
[4]*Ramjas College, University of Delhi, Delhi 110007, India*
[*]*Email: rajeshkr573@gmail.com, rajeshkr0673@yahoo.co.in*

There are various empirical formulae to study the level structure of ground band of medium mass nuclei. The expression for rotational spectra is:

$$E(I) = (\hbar^2/2\theta)\, I(I+1). \quad (1)$$

Where θ and I are the moment of inertia and spin respectively [1]. The deviation from eq. 1 has been observed for almost all the nuclei because of centrifugal stretching etc. which can be taken into account only up to some extent [2, 3] ($3.1 \leq R_4 \leq 3.33$) by apply an expansion in power of I(I + 1), i.e.

$$E(I) = A\, I(I+1) + B[I(I+1)]^2 + C[I(I+1)]^3 + \cdots \quad (2)$$

where A, B and C have their usual meaning. For harmonic vibrator, the energy can be written as:

$$E(I) = a\, I. \quad (3)$$

Das et. al. [4] suggested the energy expression for anharmonic vibrator:

$$E(I) = aI + bI(I-2). \quad (4)$$

The energy spectrum of ground band in well deformed nuclei ($R_4 \approx 3.33$) exhibit rotational characteristics and for shape transitional nuclei large deviations have been observed. In the literature, one finds quite a few variants, which involve two, three or more terms in terms of spins. Gupta et al [5] observed that the values of fitting parameters often depended on the number of levels used for calculation. They [5] suggested a very different form of energy expression in the form of a single term energy formula called power law:

$$E(I) = a\, I^b \quad (5)$$

where the coefficient "a" and index "b" are the constants for the band. Also b is a non-integer. The values of a_I and b_I are given below:

$b_I = \log(R_I)/\log(I/2)$ and $a_I = E_I / I^b$.

This is the most-simple expression among all the other formulae. The validity of this formula was well proved for the medium mass nuclei. Recently, it was also tested for the light N < 82 region. This formula was equally successful in expressing the ground band energies in the A=150-200 region [5]. Mittal et. al [6] verified its validity for light mass Xe-Sm nuclei. Recently, Kumar et. al [7] and Kumar [8] presented correlation of kinetic moment inertia with power formula index in $100 \leq A \leq 150$ region. Gupta and Hamilton [9] also illustrated the use of this formula to determine the degree of deformation of shape transitional nuclei.

Considering its simplicity, we have taken a project to test the validity and utility of power law in various bands of even –even nuclei. Here, we discuss the advantages of this formula in predicting the nuclear structure of β-band in a few nuclei.

The validity of this expression (Equation 5) for β-band would be tested by a check of the constancy of "b" and "a" with the spin I. It is also tested by plotting log (E_I) against log (I).

In the present work, we search for the constancy of "b" and "a" coefficients with the spin (I) for β-band. In figure 1, we have plotted log(E_I) against log(I) for isotopes of different deformation (N = 88, 90) for β-band levels which indicates that the log(E_I) is linearly dependent on log(I). This is also a good measure to test constancy of level energies with spin (I). Here, almost linear dependence (Fig. 1) would be an indication of the constancy of index "b" and coefficient "a" with spin (I).

To test the above hypothesis for constancy of index "b" and "a" of single term energy formula (Equation 5) for β band, we look at the N = 88, 90 (^{152}Sm, ^{152}Gd and ^{154}Gd) isotones in Fig. 2 and Fig. 3 respectively. In ^{152}Sm and ^{154}Gd, the value of 'b' is

almost constant near 0.5 (see Fig. 2). Thus the almost constancy of index 'b' of this formula in β band, illustrates the test of nuclear shape deformation with spin for excited bands. The coefficient "a" is plotted versus spin (I) in Fig.3 for these three isotopes and the fig. indicating that "a" is linearly dependent on spin and decreases on increasing the spin. Also the slopes for ^{152}Sm and ^{154}Gd are almost same.

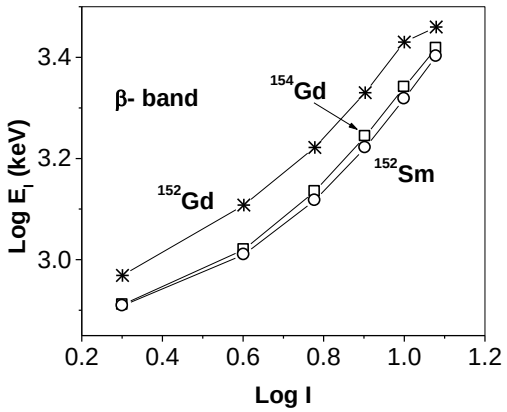

Fig. 1 The variation of Log E_I vs. Log I for β-band.

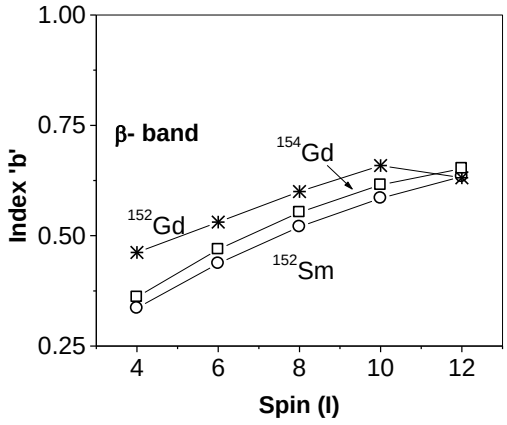

Fig. 2 The variation of index 'b' vs. Spin (I).

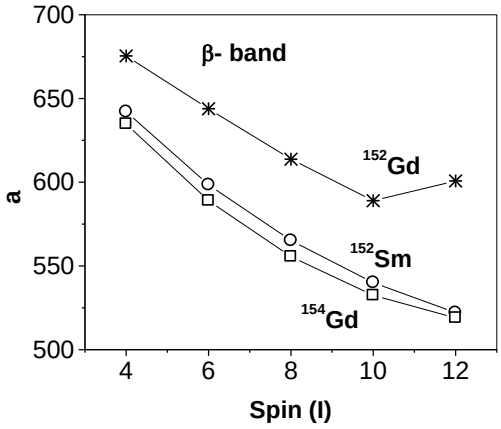

Fig. 3 The variation of coefficient 'a' vs. Spin (I).

Acknowledgements

J. B. Gupta appreciates post-retirement association with Ramjas College. RK and SS express their gratitude to Dr. O. P. Agrawal, Chairman, NIET, Greater Noida and Shri Pankaj Goel, Chairman, PIET, Meerut for providing the facilities for the research work.

References

[1] A. Bohr and B.R. Mottelson, Nuclear Structure, **Vol.-II** (New York, 1975) 145.
[2] S. Sharma & J.B. Gupta, Symp. Nucl. Phys. **28B** (1985) 205.
[3] S. Sharma, Ph. D. Thesis, University of Delhi (1989) unpublished.
[4] T.K. Das, R.M. Dreizler and A. Klein, Phys. Rev. **C2** (1970) 632.
[5] J.B. Gupta, A.K. Kavathekar and R. Sharma, Physica Scripta, **51** (1995) 316.
[6] H.M. Mittal, V. Devi and J.B. Gupta, Physica Scripta, **81** (2010) 015202.
[7] Rajesh Kumar, V. Katoch, S. Sharma and J.B. Gupta, Int. J. Mod. Phys. **E21** (2012) 1250082.
[8] Rajesh Kumar, Ph. D. Thesis, Uttar Pradesh Technical University (2013) unpublished.
[9] J.B. Gupta and J.H. Hamilton, Phys. Rev. **C83,** (2011) 064312.

Correlation of average scaling coefficient with asymmetric parameter and average power index with quadrupole deformation parameter

Vikas Katoch[1,*], Reetu Kaushik[2], S. Sharma[3,#] and J. B. Gupta[4]
[1]*Research Scholar, Department of Physics, Singhania University, Jhunjhunu, Rajasthan-333515, India*
[2]*Research Scholar, Department of Physics, Mewar University, Gangrar, Rajasthan-312901, India*
[3]*Panchwati Institute of Engineering & Technology (U.P. Technical University), Meerut-250005, India*
[4]*Ramjas College, University of Delhi, Delhi-110007, India*
[#]ssharma_phy@yahoo.co.uk

Introduction:

The nuclear structure of even-even nuclei in ground state band and other excited bands with non zero band head is collectively built [1]. The level energy in medium mass region deviates below the ideal rotor energy formula $E_I = AI(I+1)$. The ground band of medium mass nuclei are studied using various energy formulae e.g. Soft Rotor Formula [2], VMI etc. Gupta et al. [3] proposed the power law and studied the systematics of ground band. The level energy from Power Law is

$$E = aI^b \quad (1)$$

where, a and b are scaling coefficient and power index.

The power law parameters (average scaling coefficient and average power index) are obtained using spin up to I=12 in Eq. (1).

In RTR model the asymmetric parameter (γ) is obtained using $E(2_1)$ of ground band and $E(2_2)$ of γ-band for medium mass region. The asymmetric parameter:

$$\gamma = (1/3)\sin^{-1}[(9/8)\{1-((R\gamma-1)/(R\gamma+1))^2\}]. \quad (2)$$

where, $R_\gamma = E(2_2)/E(2_1)$. The quadrupole deformation parameter (β) is related with B(E2) values, energy (E) and atomic mass (A) of the nuclei as:

$$\beta = \left(\frac{4\pi}{3ZR_0^2}\right)\left[\frac{B(E2)\uparrow}{e^2}\right]^{1/2} \quad (3)$$

and

$$\beta = (466 \pm 41)E^{-1/2}A^{-1} \quad (4)$$

where, R_0 is $1.2A^{1/3}$fm, B(E2)↑ is in $e^2\,b^2$, Z is atomic number, E is the energy of spin I=2 of ground band and A is atomic mass. The β is taken from [4] and [5].

The correlation of average scaling coefficient, asymmetric parameter and average power index and deformation parameter versus N is studied quadrant -1.

Systematics dependence of a_{AV} and γ with N

In quadrant-I (60< Z< 66, 82< N< 104), as neutron number increases, the asymmetric parameter as well as scaling parameter decreases fast up to N=92 and after N>92, both parameters remains uniform for Nd, Sm, Gd and Dy nuclei in Fig. 1.(a and b).

In quadrant II (66< Z<82, 82< N< 104), the asymmetric parameter as well as scaling parameter decreases as neutron number rises towards N=104 Fig for Q-II,III,IV to be presented).. From N=102 to N=104 both parameters decrease slowly. In quadrant-III (60< Z<66, 104< N<126), as neutron number increases, the W and Os nuclei shows a dip at N=108 and for N>108 both parameters rises, whereas the Pt nuclei shows separate fast increasing trend. In quadrant –IV N<82, for N > 64, the scaling parameters as well as asymmetric parameters, both are increases as neutron number rises. Here Xe nuclei shows separate rising trend with both parameters (Figs. to be shown in poster).

Systematics dependence of b_{AV} and β with N

In quadrant-I, the deformation parameter β and power index parameter b_{AV} sharply rises as N increases from 86 to 92. For N>92, both parameters show uniform trend and saturates in fig. 2.1(a and b).

In quadrant-II, the Er and Yb nuclei show same trend for both parameters for N=88-104. The β rises for Hf and W nuclei when N increases from 88 to 98 and decreases towards N=100 and again rises on increasing N. The b_{AV} rises for Er-Os nuclei when N increases from 88 to 104. The Pt has different behavior. In quadrant-III, the Pt nuclei shows same trend with both parameters whereas after N>108, the W and Os nuclei shows same trend.

In quadrant-IV, the nuclei Ba, Ce, Nd and Sm shows same trend, whereas the Xe nuclei has a dip at Z=66 in power index parameter and a up in deformation parameter.

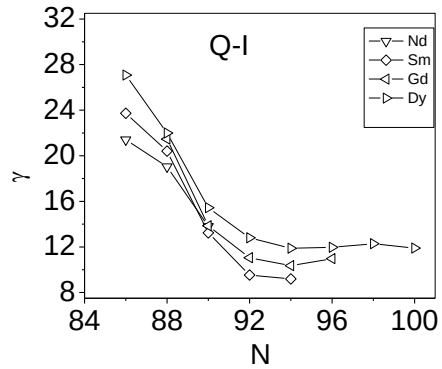

Fig.1 (a) The plot of γ vs. N in Q-I.

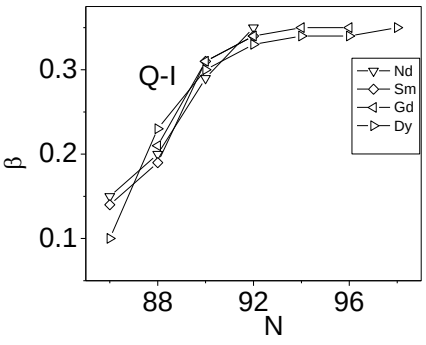

Fig. 2(a) The plot of β v N in Q-I.

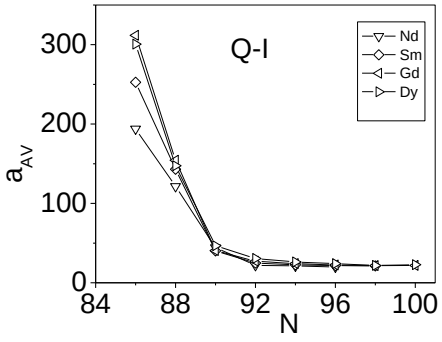

Fig. 1(b) The plot of a_{AV} vs. N in Q-I.

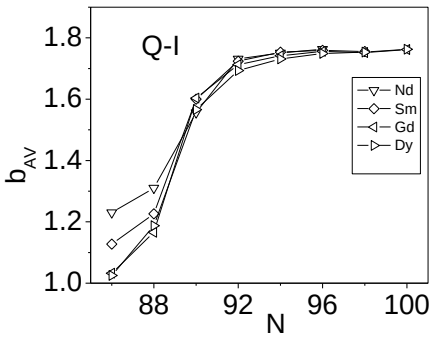

Fig. 2(b) The plot of b_{AV} vs. N in Q-I.

Conclusion: The average scaling coefficient with asymmetric parameter and average power index with N show strong correlation in all four quadrants.

References:

[1] A. Bohr & B. R. Mottelson, (1975) Nuclear Structure Vol. II (Benjamin, N.Y)
[2] R. K. Gupta, Phys. Lett. 36B (1971)173
[3] J. B. Gupta, A. K. Kavathekar and R Sharma, Physica Scripta 51 (1995) 316.
[4] Raman et al. Atomic and Nuclear Data Tables Vol. 78, issue 1 (2001) 1-128.
[5] www.nndc.bnl.gov, July 2013.

Systematic dependence of asymmetric parameter in light and medium mass region

Reetu Kaushik[1] and S. Sharma[*]

[1]*Research Scholar, Department of Physics, Mewar University, Gangrar, Rajasthan-312901, India*
Panchwati Institute of Engineering and Technology (Uttar Pradesh Technical University),
National Highway- 58, Ghat Institutional Area, Meerut, PIN 250005, INDIA
[*]*email: ss110096@gmail.com*

Introduction

The study of collective nuclear structure with N, Z, N_B and N_pN_n provide a detailed information of nuclear interactions involved. Several studies have been carried out to study the collectivity, deformation and systematic dependence of other nuclear properties on N_pN_n. de-Shalit & Goldhaber [1] pointed out the important role of valence nucleons. Talmi [2] noted the constancy of nuclear level structure in semi-magic isotones/isotopes. Hamamoto [3] observed that the p^+ & n^0 both are required for producing deformation. In IBM-1[4], the structure of nuclei depends on the total boson numbers N_B. The concept of F-spin multiplets was based on this and was well explained by Brentano et al. [5]. Casten [6] noted that the E_{2g}+ have smooth dependence on N_pN_n. Various studies [7] have been carried out to study the collectivity, deformation and systematic dependence of various nuclear observables on the product N_pN_n.

Gupta [8] observed that 1/α was linearly dependent on N_pN_n, where the coefficient α contributes for rotational part of energy in the SU(3) symmetry limit of IBM[4] as,

$$E([N](\lambda, \mu) KLM) = \alpha L(L+1) + \beta C(\lambda, \mu)$$

The B(E2; $2_1^+ \rightarrow 0_1^+$) values were also related with N_pN_n. Gupta et al. [9] noted a systematic dependence of γ–g B(E2) ratios on the N_pN_n in different parts of the major shell space Z=50–82, N<82 and N=82–126. Casten and Zamfir [6] presented a review on the evolution of nuclear structure based on N_pN_n product. The N_pN_n scheme was further modified to use P- factor [9].

In this paper, we study the role of valence nucleons and holes on the nuclear structure, through N_pN_n. Casten and Zamfir [7] covered the various regions, viz., A=100, 130, 150 (Z<64, Z>64) and A=190. We present our results for 50≤Z≤82 and 82≤N≤126 region on *quadrant wise basis*.

The values of asymmetry parameter (γ) have been calculated for 50≤Z≤82 and 82≤N≤126 region and the whole data is divided into four quadrants and it has been plotted with N_pN_n to study its systematics dependence.

Calculation of Asymmetric Parameter

The value of γ can be evaluated using the experimental energies $E2_2^+$ and $E2_1^+$ states [10]. The energy ratio $R\gamma = E_{2\gamma} / E_{2g}$ and γ is:

$$\gamma = (1/3) \sin^{-1}[(9/8)\{1-((R\gamma-1)/(R\gamma+1))^2\}].$$

It can be evaluated using: (a) The energy ratio $R_4=(E_{4g}/E_{2g})$ but only the nuclei with 2.8≤R4≤3.33 will be allowed [11, 12]. (b) The B(E2) values which are very small and available with uncertainties. Therefore the values from energy ratio Rγ are more reliable.

Result and discussions

The variation of γ versus Np.Nn product for quadrant-I for 50≤Z≤66 and 82≤N≤104 has been shown in Fig. 1. There is smooth dependence of γ with NpNn. The γ decreases from a maximum value of 30° for N_pN_n =0 (i.e. SU(5) limit of IBM) to a minimum values of about 9°(i.e. SU(3) limit of IBM). The γ saturates for $N_pN_n \geq$ 30. This shows non-dependence of γ with N_pN_n

because for a fixed value of N_pN_n the γ is having varying values.

The variation of γ versus N_pN_n for quadrant-II for 66≤Z≤82 and 82≤N≤104 has been shown in Fig. 2. There is smooth dependence of γ with N_pN_n except Yb for N_pN_n >50 and few Pt isotopes.

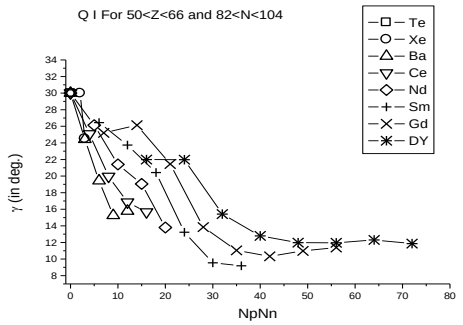

Fig.1 The variation of asymmetric parameter (γ) versus N_pN_n.

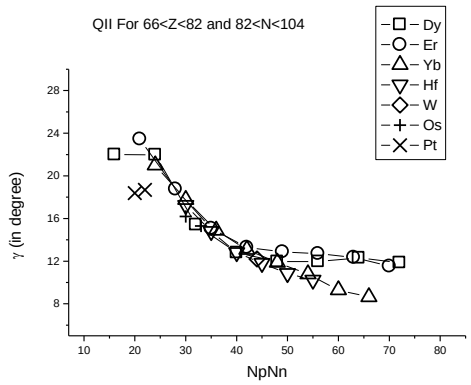

Fig. 2 The variation of asymmetric parameter (γ) versus N_pN_n product for quadrant-II.

The variation of γ versus N_pN_n for quadrant-III for 66≤Z≤82 and 104≤N≤126 has been shown in Fig. 3. There is smooth dependence of γ with N_pN_n except Hg isotopes.

The graphs of γ against N_pN_n vividly displays the formation of isotonic multiplets in quadrant-I, strong dependence on N_pN_n in quadrant-II and weak constancy with Z in quadrant-III is illustrated and support the findings of Gupta [13].

Acknowledgements

We are grateful to Professor J. B. Gupta for his valuable guidance. SS express his gratitude Shri Pankaj Goel, Chairman, PIET, Meerut for providing the facilities for the research work

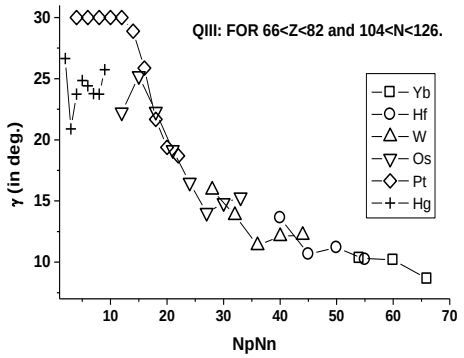

Fig. 3 The variation of asymmetric parameter (γ) versus N_pN_n product for quadrant-III.

References

[1] A. deShalit and M. Goldhaber, Phys. Rev. **92,** 1211(1953).
[2] I. Talmi, Rev. Mod. Phys. **34,** 704 (1953).
[3] I. Hamamoto, Nucl. Phys. **73,** 225 (1965).
[4] R.F. Casten, *Nuclear Structure from a Simple Perspective* (IInd Edition, Oxford University Press, 2001).
[5] P. von Brentano et. al., J. Phys**.** *G*11, L85 (1985*)*.
[6] R. F. Casten, Nucl. Phys. **A443,** 1 (1985).
[7] R. F. Casten and N.V. Zamfir, J. Phys. G Nucl. Part. Phys. **22,** 1521(1996).
[8] J. B. Gupta, Phys. Rev. C33, 1505 (1986).
[9] J. B. Gupta, J.H. Hamilton and A.V. Ramayya, Phys. Rev. **C42,** 1373 (1990).
[10] Recent data for energies have been taken from http://www.nndc.bnl.gov
[11] S. Sharma, Ph. D. Thesis, University of Delhi (1989) unpublished.
[12] J. B. Gupta and S. Sharma, Physics Scripta, **39**(1989)50.
[13]] J. B. Gupta, Eur. Phys. J. A. **48**(2012)177.

THE SYSTEMATIC DEPENDENCE OF (E2;4G→2G)/B(E2;2G→0G) RATIO ON N AND Z FOR ND-HG NUCLEI

Satendra Sharma[1], Reetu Kaushik[2]

[1]*Department of Physics, Yobe State University, KM 7, Gujba Road, P. M. B. 1144, Damaturu, Yobe State, (Nigeria)*

[2]*Research Scholar, Department of Physics, Mewar University, Gangrar, Rajasthan, (India)*

ABSTRACT

The systematic dependence of experimental B(E2; 4g→2g)/ B(E2;2g→0g) branching ratio with N and Z is carried out for Nd- Hg even –even nuclei. The SU(5) and SU(3) limits of interacting boson model are also discussed. The N and Z dependence of B(E2) branching ratio has been observed. The Z=64 subshell effect is also seen for N≤ 90 region.

Keywords: B(E2; 4g→2g)/ B(E2;2g→0g) branching ratio, nuclear structure, Nd –Hg nuclei, SU(5), SU(3), Z=64 subshell effect

I. INTRODUCTION

The concept of collectivity in nuclei is one of the most fundamental findings in history of nuclear physics. Various nuclear models have been applied to describe this collective behaviour of atomic nuclei. The geometrical models depicting the nucleus as a liquid drop with a given nuclear shape and algebraic models, take into account the pairs of proton and/or neutron only. Despite the often very dissimilar theoretical approaches, most of the collective models have some common basic features, such as predictions of energies rotational, vibrational and other higher multi-phonon bands or B(E2) ratios for inter and intra band transitions, which have been observed in a wealth of non- magic atomic nuclei.

The energy ratio R_4 is a key observables which can be used to assess the collectivity of nuclei and it is equal to 2 for an ideal spherical harmonic vibrator or SU(5) limit and 10/3 in an axially symmetric deformed rotor or SU(3) limit of interacting boson model (IBM)[1]. The transition rates also provide another good measure of nuclear collectivity [2], which is less sensitive to anharmonicities than energies of various bands. The $B(E2;4_g\rightarrow2_g)/B(E2;2_g\rightarrow0_g)$ branching ratio is a particularly good example, which is equal to 2 in the spherical limit or SU(5) and 1.4 in the deformed limit or SU(3)[1]. Significant deviations from these two limiting values can be found; if one moves away from the closed shell.

In the present work, we have compiled the observed data of $B(E2;4_g\rightarrow2_g)/B(E2;2_g\rightarrow0_g)$ branching ratio from the website of Brookhaven National Laboratory[3] for Nd – Hg nuclei. The variation of this B(E2) ratio with N and Z has been studied. The SU(3) and SU(5) limits are also included for useful comparison. The result & discussions and conclusion are given in § II and III respectively.

II.RESULT AND DISCUSSIONS

2.1 The variation of experimental B(E2;4g→2g)/ B(E2; 2g→0g) ratio verses neutron number (N)

To avoid the overlapping of experimental data of the nuclei and to have a clear picture for a definite conclusion about the dependence of B(E2;4g→2g)/B(E2;2g→0g) ratio on N, the whole data is divided into two parts and shown in two figures i.e. Fig. 1 for Nd- Er nuclei and in Fig. 2 for Yb- Hg nuclei. The vibrational model or SU(5) limit at 2 and rotational model or SU(3) limit at 1.4 are shown in the Fig 1 and Fig. 2. The data points are joined for same value of Z, so that the effect of N will be visible.

For Nd, this ratio increases sharply from 0.73 to 1.61(maximum value at N=88) as N increases from 84 to 88 and if N is further increased from 88 to 92 it decreases slowly from 1.61 to 1.31(see Fig. 1). The same feature is observed for Sm, where this ratio increases from 1.65 to 1.9 on increasing N from 86 to 88 and beyond N=88 it drops sharply and approaches to Alaga value of 1.4 for N=92. In case of Gd, the BE(2) ratio decreases from 1.82 to 1.46 as N increases from 88 to 94. Also in Er, this ratio decreases from 1.78 to 1.5 as N increases from 88 to 100 and minimum value of 1.18 at N=96. Therefore, for N=88 (Sm, Gd and Er) isotones, this ratio ≈1.8 is very close to the VM limit of 2.0 indication vibrational nature. However for Dy (N=88, 92, 94, 96) this ratio is close to Alaga value indication deformed rotor nature and for N=90; Dy indicating transitional nature because this ratio (=1.63) is lying in between SU(5) and SU(3) limiting value (see Fig. 1).

For Yb and Hf nuclei, BE(2) ratio is ranging between 1.4 to 1.6 for different values of N and close to SU(3) limit (see Fig. 2). In case of W, the ratio increases sharply from 1.1(3) to 1.74(15) on increasing N from 94 to 100 and decreases very slowly on increasing N from 108 to 112 (almost remains around Alaga value).

For N=96 the data point of Os is close to the other N=96 isotones (Yb, Hf, W) data points. When N increases from 108 to 112, the ratio for Os increases from 1.4(4) to 1.68(11) and when N is increased from 112 to 116 the B(E2) ratio decreases from 1.68(11) to 1.22(4) indicating prolate to oblate shape-phase-transition as observed by Kumar and Baranger [4].

For N=98, the B(E2) [=1.87(24)] for Pt is close to VM value and for N=102 the ratios is minimum [=0.92(22)]. The B(E2) ratio for Pt decreases from 1.65 to 1.56 when N increases 106 from 114 and again increases from 1.56 to 1.73 as N increases from 114 to 116(attains maximum value =1.73(11) at 116). If N is increased from 116 to 120 this ratio drops linearly with the same slope as observed for Os (N=112 to 116).This indicates the similar nature of Pt and Os nuclei for this region.

For two nuclei; ^{182}Hg and ^{184}Hg; the B(E2) ratio is 4.6(3) and 2.8(8) respectively; which are anomalously more than VM limiting value and not included in the Fig.2. The B(E2) ratio is smallest in case of ^{198}Hg; which is non magic nucleus; has only two vacancy of p+ for Z =82. This ratio is also very small in case of $^{144}Nd_{84}$ [=0.73(9)] (see Fig.1); which is also a non- magic nucleus; which has only two valence n^0 outside N=82. It supports the findings of Cakirli et.al. [5], that the B(E2;4g→2g)/B(E2;2g→0g) ratio is anomalously small in non magic nuclei, as it cannot be explained with collective approaches.

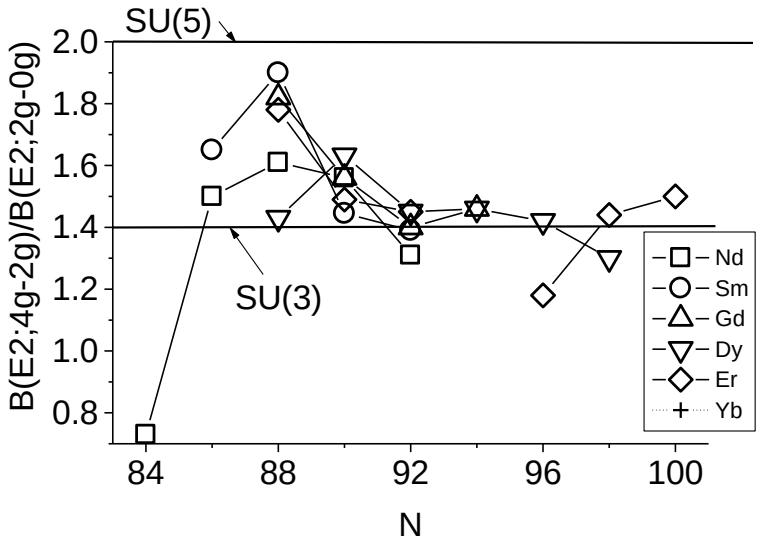

Fig.1: The variation of experimental B(E2;4g→2g)/B(E2;2g→0g) ratio vs. neutron number (N) for Nd-Er nuclei. The vibrational limit SU(5) at 2.0 and rotational limit SU(3) at 1.4 are shown by dotted lines for comparison.

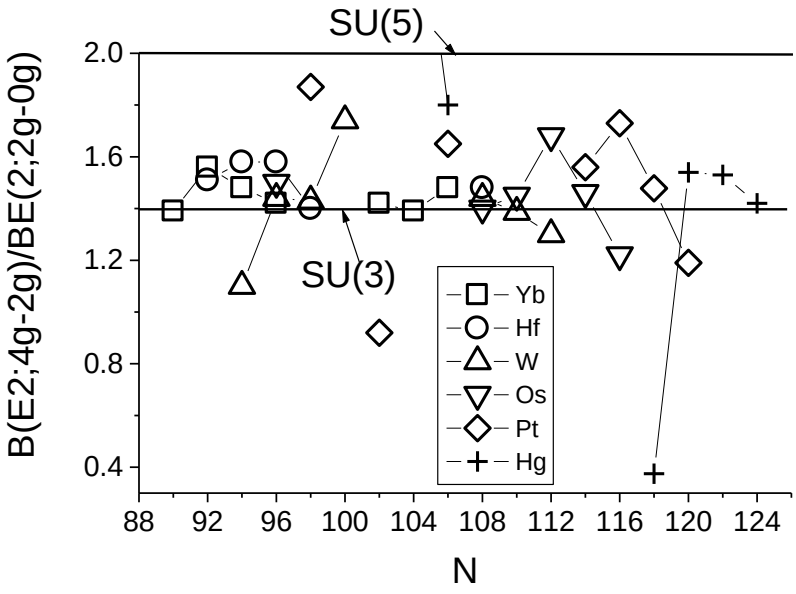

Fig.2: The variation of experimental B(E2;4g→2g)/B(E2;2g→0g) ratio vs. neutron number (N) for Yb-Hg nuclei. The vibrational limit SU(5) at 2.0 and rotational limit SU(3) at 1.4 are shown by dotted lines for comparison.

2.2 The variation of experimental B(E2;4g→2g)/ B(E2; 2g→0g) ratio verses proton number (Z).

The variation of observed B(E2;4g→2g)/ B(E2; 2g→0g) ratio with proton number (Z) is shown in Fig. 3, 4 and 5 for N=84 to 92, N=94 to 102 and N= 104 to 124 isotones respectively and the experimental points are joined

for same value of N to observe the effect of Z. The vibrational limit (VM) or SU(5) at 2 and rotational limit or SU(3) at 1.4 are also shown by dotted lines for useful comparison in each figure.

It is evident from Fig. 3, that the BE(2) ratio for N=88 isotones increases on increasing Z from 60 to 62 (attains the maximum values for Sm_{88}) and decreases for Gd and Dy (attains minimum value close to SU(3) limit for Dy_{88}) and again for Er it increases. For N=88, the B(E2) ratio is close to SU(5) limiting value for Sm, Gd and Er while Dy reflects SU(3) nature and Nd in between these two limits. Also, the Sm_{88} is least deformed and Dy_{88} is most deformed. For N=86 isotones the B(E2) data is available only for two nuclei and it is increasing on increasing N from 60 to 60 as in the case of N=88.

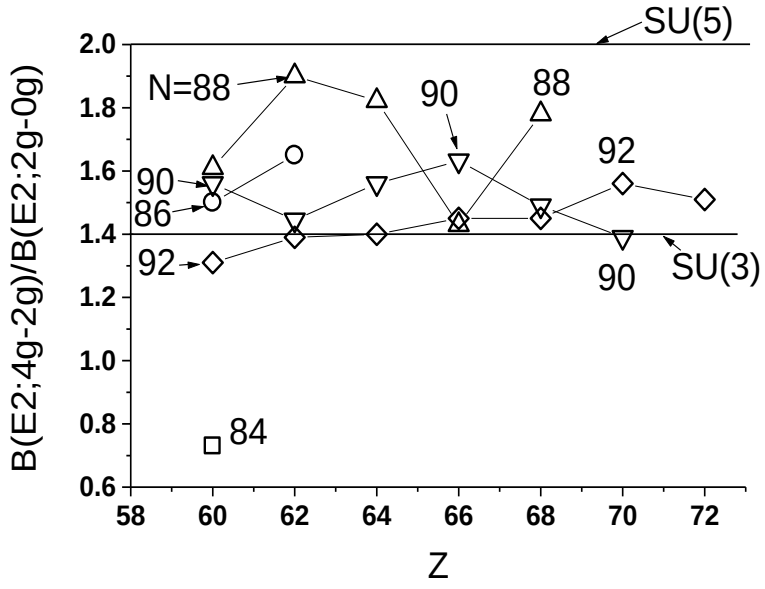

Fig.3: The variation of experimental B(E2;4g→2g)/ B(E2; 2g→0g) ratio vs. proton number (Z). The vibrational limit SU(5) at 2.0 and rotational limit SU(3) at 1.4 are shown by dotted lines for comparison. The experimental points are joined for same value of N to observe the effect of Z on this B(E2) ratio for each isotones for N=84-92.

For N=90 isotones the behaviour of B(E2) is just opposite to N=86 and 88; the B(E2) ratio initially decreases as N increases from 60 to 62 and increases as N increases from 62 to 66 just opposite to N=88. It is evident from the figure that the gap is maximum between the two curves for N=88 and 90 around Z= 64 indication the subshell effect at Z=64 for N<90. It is supporting the findings of Casten [6] and Casten and Zamfir [7].

In general, for N=90 isotones, the B(E2) ratio is somewhat independent of Z indicating constant structures because the values of this ratio are ranging between 1.45 to 1.6 and it support the findings of Gupta [8]. For N=90 isotones, this B(E2) ratio initially decreases on increasing Z from 60 to 62 (attains minimum values which is close to SU(3) limiting value for Sm_{90} unlike Sm_{88} for which this ratio is close to SU(5) limiting value) and increases slowly on increasing Z from 62 to 66; and attains maximum value(=1.6) for Dy_{90}; and beyond Z=66 the BE(2) decreases linearly on increasing Z from 66 to 70 (and approaches 1.4 value for Hf_{90}). It is clear from Fig. 3 that Sm_{90} and Hf_{90} are most deformed in comparison to other N=90 isotones.

For N=92 isotones, this ratio goes on increasing very slowly from 1.31 to 1.56 on increasing Z from 60 to 74 and is close to SU(3) limiting value of 1.4. However for N=94, this ratio is almost constant because its values are 1.46±0.05, 1.46±0.07, 1.48±0.07, 1.58±0.10 and 1.1±0.3 for Gd, Dy, Yb, Hf and W isotopes respectively indication Z independency. For N=94, 96 and 98 isotones (see Fig. 4) the ratio is close to SU(3)

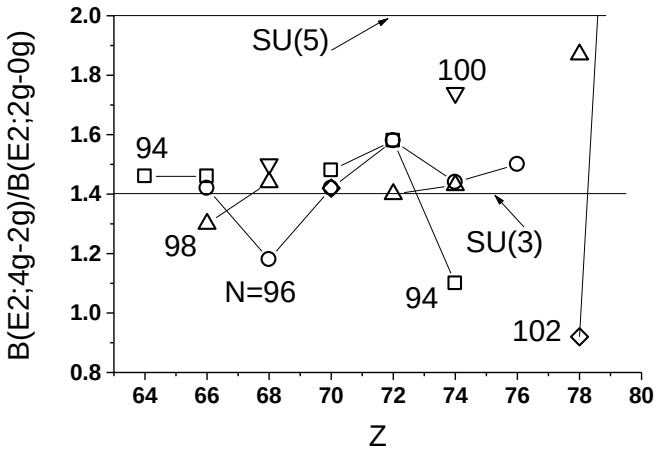

Fig.4: Same as Fig.3 for N=94 to 102.

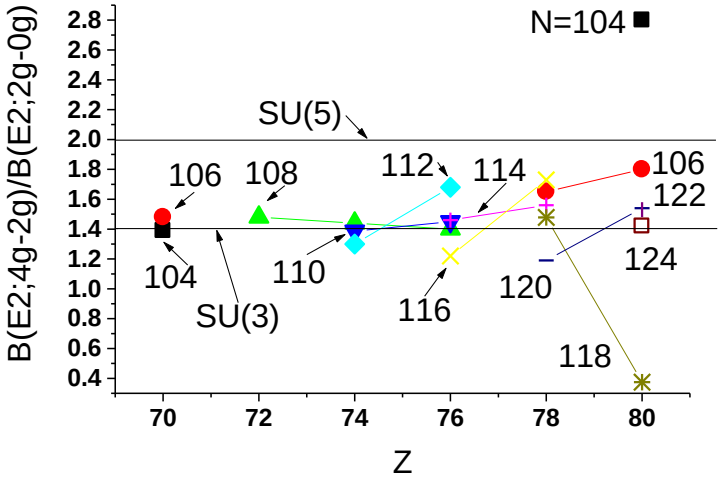

Fig.5: Same as Fig.3 for N=104 to 124.

limiting value indicating deformed nature. For other isotones the B(E2) ratio is lying between SU(5) and SU(3) or O(6) limiting values (see Fig.5) as predicted by the asymmetry rotor model [9].

III. CONCLUSION

The variation of B(E2; 4g→2g)/ B(E2;2g→0g) ratio with N and Z is shown for Nd – Hg nuclei. It is found that the there is shape phase transition for N=88 and 90 isotones (Nd, Sm, Gd, Er) from an ideal spherical harmonic vibrator or SU(5) to an axially symmetric deformed rotor or SU(3). Also B(E2) ratio is anomalously small for two nuclei i.e., $^{198}_{80}Hg_{118}$ (=0.375±0.018) and $^{144}_{60}Nd_{84}$ (=0.73±0.090) with only two vacancy of p+ for Z =82

and two valence n^0 outside N=82, respectively; which supports the findings of Cakirli et.al. [5]. The present study supports; the subshell effect around Z=64, for N≤ 90 as observed by Casten [6] and Casten and Zamfir [7]; and the constant nuclear structure of N=90 isotones as pointed out by Gupta [8].

IV.ACKNOWLEDGEMENTS

One of us (SS) expresses his gratitude to the Prof. Alabi Musa, Vice Chancellor, Yobe State University, Damaturu, Yobe State, Nigeria for encouragement and for providing the facilities for the research work. We are grateful to Professor J. B. Gupta, Ramjas College, University of Delhi for his valuable guidance.

REFERENCES

[1] R. F. Casten, *Nuclear Structure from a Simple Perspective,* Oxford University Press, New York, 1990. F. Iachello and A. Arima, *The Interacting Boson Model,* Cambridge University Press, Cambridge, 1987.

[2] A. Bohr and B. R. Mottelson, *Nuclear Structure, Vol. II, Benjamin, New York, 1975.*

[3] http://www.nndc.bnl.gov

[4] K. Kumar & M. Baranger, **"**Nuclear deformations in the pairing-plus-quadrupole model (V).: Energy levels and electromagnetic moments of the W, Os and Pt nuclei", *Nucl. Phy. A 122 (1968) 273-324.*

[5] R. B. Cakirli, R. F. Casten, J. Jolie, and N. Warr, "Highly anomalous yrast B(E2) values and vibrational collectivity", *Phys. Rev. C 70 (2004) p. 047302.*

[6] R. F. Casten, "NpNn Systematics in Heavy Nuclei", *Nucl. Phys. A443, 1 (1985).*

[7] R. F. Casten and N. V. Zamfir, "The evolution of nuclear structure: the NpNn scheme and related correlations", *J. Phys. G Nucl. Part. Phys.* 22, 1521(1996).

[8] J. B. Gupta, "A microscopic explanation of the isotonic multiplet at N = 90 and of the F-spin multiplet in Dy-Hf", *Eur. Phys. J. A. 48(2012)177.*

[9] Satendra Sharma and Reetu Kaushik, "Test of Asymmetry Rotor Model for the B(E2;4g→2g)/B(E2;2g→0g) Branching Ratio in Medium Mass Region", *International Journal of Computer & Mathematical Sciences, Vol. 4, Special Issue (2015) p. 160-167.*

Biographical Notes

Dr. Satendra Sharma is working as Professor and Head, Department of Physics, Yobe State University, Damaturu, Yobe State, Nigeria.

Mrs. Reetu Kaushik is a research Scholar in the Department of Physics, Mewar University, Gangrar, Rajasthan, India. She has published 01 research papers in International Journal, 6 papers in the Proceedings of Department of Atomic Energy Symposium on Nuclear Physics and 1 paper in International Conference.

International Journal of Computer & Mathematical Sciences
IJCMS
ISSN 2347 – 8527
Volume 4, Special Issue
March 2015

Test of Asymmetry Rotor Model for the B(E2; 4g→2g)/ B(E2;2g→0g) Branching Ratio in Medium Mass Region

Satendra Sharma* **and Reetu Kaushik**[1]
Department of Physics, Yobe State University, KM 7, Gujba Road, P. M. B. 1144, Damaturu, Yobe State, Nigeria
[1]Research Scholar, Department of Physics, Mewar University, Gangrar, Rajasthan-312901, India

Abstract
The predictions of asymmetric rotor model (ARM) of Davydov and Filippov for B(E2; 4g→2g)/ B(E2;2g→0g) branching ratio are compared with the experimental data in medium mass region. The SU(5) and SU(3) limits of interacting boson model are also shown for useful comparison. It is noted that the ARM is partially successful in explaining this branching ratio.

Key Words: Asymmetric rotor model, B(E2; 4g→2g)/ B(E2;2g→0g) branching ratio, nuclear structure, medium mass region.

1. Introduction

The concept of collectivity in atomic nuclei is one of the most fundamental findings in history of nuclear structure physics. The macroscopic, microscopic and geometrical nuclear models have been applied to describe this collective behaviour of nuclei. The geometrical models depicting the atomic nucleus as a liquid drop with a given nuclear shape and algebraic models, take into account the pairs of proton and/or neutron only. Despite the often very dissimilar theoretical approaches, most of the collective models have some common basic features, such as predictions of energies of g- band, β- band, γ- band and other higher multi-phonon bands or B(E2) values and B(E2) ratios for inter and intra band transitions, which have been observed in a wealth of nuclei away from closed shells.

The energy ratio R_4 ($=E_{4g}/ E_{2g}$) is a key observables which can be used to assess the collectivity of nuclei and it is equal to 2.0 for an ideal spherical harmonic vibrator i.e., SU(5) limit and 3.33 in an axially symmetric deformed rotor, i.e. SU(3) limit of interacting boson model (IBM)[1]. The inter/ intra band transition rates also provide another good measure of nuclear collectivity[2], which is less sensitive to anharmonicities than energies of various bands. The $B(E2;4_g\rightarrow2_g)/B(E2;2_g\rightarrow0_g)$ is a particularly good example, as it is 2.0 in the spherical limit or SU(5) and 1.4 in the deformed limit or SU(3)[1]. Significant deviations from these two limiting values can be found; if one considers very small numbers of valence neutrons (Nn) and/or protons (Np), which are used in the IBM; also in asymmetric rotor model (ARM) of Davydov and Filippov [3] where asymmetric parameter (γ) changes from 0^0 to 30^0 which corresponds to above mentioned two limits of IBM i.e. SU(3) and SU(5) respectively.

International Journal of Computer & Mathematical Sciences
IJCMS
ISSN 2347 – 8527
Volume 4, Special Issue
March 2015

In the present work we have compiled the experimental data of $B(E2;4_g \rightarrow 2_g)/B(E2;2_g \rightarrow 0_g)$ branching ratio from the website of Brookhaven National Laboratory[4] for medium mass region (Nd - Hg). The observed data is compared with the ARM predictions for asymmetric parameter (γ) equals to 0^0 to 30^0. The SU(3) and SU(5) limits are also included to get new information about the structure. The details of asymmetric rotor model, result & discussions and conclusion are given in § 2, 3 and 4, respectively.

2. ASYMMETRIC ROTOR MODEL

Davydov and Filippov [3] investigated the energy levels corresponding to rotation of nucleus which does not change its internal state. They established that the violation of axial symmetry of even –even nuclei affect the rotation spectrum of axial nucleus with appearance of some new rotational states having total angular momentum of 2, 3, 4,⋯. If the deviation from axial symmetry is small, then these levels lie very high and are not excited. The energy of rotation of a non-spherical even-even nucleus is given, in the adiabatic approach, by Schrödinger eq.:

$$(H - E)\Psi = 0 \quad (1)$$

where E is measured in units of $\frac{\hbar^2}{4B\beta^2}$, and the operator H is given by the formula:

$$H = \frac{1}{2}\sum_{\lambda=1}^{3} J_\lambda^2 \sin^{-2}(\gamma - \frac{2\pi\lambda}{3}) \quad (2)$$

where J_λ are the projection of the total angular momentum along the axes of a coordinate system fixed in the nucleus. The wave function corresponding to the state with total moment J, can be represented as:

$$\psi_{JM} = \sum_{K\geq 0} |JK\rangle\, A_K \quad (3)$$

$$\text{where } |jk\rangle = [\frac{(2J+1)}{16\pi^2}(1+\delta_{KO})]^{\frac{1}{2}}\{D^J_{MK} + (-1)^J D^J_{M,-K}\} \quad (4)$$

The function D^J_{MK} in eq. (4) is the function of the Euler angles that determine the orientation of the principal axis of the nucleus with respect to the laboratory space. It can be shown that the wave functions (3) from the basis of totally symmetric representation of the group D_2, the elements of which are the rotation through 180^o around each of three principal axes of the nucleus [see ref. [3] and [4]). The wave function of the rotational 2^+ states of the non-axial nucleus can be rewritten as [3]:

$$\Psi_{21m} = \sqrt{\frac{5}{8\pi^2}}\,[A_1 D^2_{mo} + \frac{B_1(D^2_{m2} + D^2_{m,-2})}{\sqrt{2}}] \quad (5)$$

$$\Psi_{22m} = \sqrt{\frac{5}{8\pi^2}}\,[A_2 D^2_{mo} + \frac{B_2(D^2_{m2} + D^2_{m,-2})}{\sqrt{2}}], \quad (6)$$

where, the value of A_K coefficients in the wave function of eq. (5, 6) can be obtained by using the value of γ:

$$A_1 N_1 = [\sin\gamma \sin 3\gamma + 3\cos\gamma \cos 3\gamma + (9 - 8\sin^2 3\gamma)^{\frac{1}{2}}]$$

$$B_1 N_1 = 3\sin\gamma \cos 3\gamma - \cos\gamma \sin 3\gamma,$$

$$N_1^2 = 2\sqrt{(9 - 8\sin^2 3\gamma)} \times [(9 - 8\sin^2 3\gamma) + \sin\gamma \sin 3\gamma + 3\cos\gamma \cos 3\gamma],$$

$$A_2N_2 = \sqrt{(9-8sin^2 3\gamma)} - \sin\gamma \sin 3\gamma - 3\cos\gamma \cos 3\gamma,$$
$$B_2N_2 = 3\sin\gamma \cos 3\gamma - \cos\gamma \sin 3\gamma, \quad (7)$$
$$N_2^2 = 2\sqrt{(9-8sin^2 3\gamma)} \times [\sqrt{(9-8sin^2 3\gamma)} - \sin\gamma \sin 3\gamma - 3\cos\gamma \cos 3\gamma]$$

Similarly for 3^+ state the wave function can be written as:

$$\Psi_{3m} = \sqrt{\frac{7}{16\pi^2}}\left(D^3_{m2} - D^3_{m,-2}\right), \quad (8)$$

The spin 4^+ wave function are given by Davydov and Rostovsky [4]:

$$\Psi_{41} = \sqrt{\frac{9}{8\pi^2}} D^4_{mo},$$
$$\Psi_{42} = \sqrt{\frac{9}{16\pi^2}}\left(D^4_{m2} + D^4_{m,-2}\right) \quad (9)$$
$$\Psi_{43} = \sqrt{\frac{9}{16\pi^2}}\left(D^4_{m4} + D^4_{m,-4}\right), \text{ etc.}$$

Putting the eq.(3) in eq.(1) and making use the value of matrix element of the operator of the rotational energy eq.(2) acting on the wave function eq.(4)

$$\langle JK|H|JK\rangle = \frac{\alpha+\beta}{4}[J(J+1) - K^2] + \frac{\delta K^2}{2}$$
$$\langle JK+2|H|JK\rangle = \frac{\alpha-\beta}{4}[(1+\delta_{KO})(J-K) \times (J-K-1)(J+K+1)(J+K+2)]^{\frac{1}{2}}, \quad (10)$$
$$\alpha = sin^{-2}(\gamma - \tfrac{2\pi}{3}), \qquad \beta = sin^{-2}(\gamma + \tfrac{2\pi}{3}),$$
$$\delta = sin^{-2}\gamma, \qquad \delta_{ko} = \begin{cases} 0, for\ K \neq 0, \\ 1, for\ k = 0, \end{cases} \quad (11)$$

One obtains for each value of J a system of algebraic equations for the coefficients A_K in the wave function (3). For J = 4, the Schrodinger eq.(1) is reduced to a system of equation as [4]:

$$\begin{bmatrix} 5(\alpha+\beta) - E & 3/2 \cdot \sqrt{5}(\alpha-\beta) & 0 \\ 3/2 \cdot \sqrt{5}(\alpha-\beta) & 4(\alpha+\beta) + 2\delta - E & \frac{\sqrt{7}}{2} \cdot (\alpha-\beta) \\ 0 & \frac{\sqrt{7}}{2} \cdot (\alpha-\beta) & (\alpha+\beta) + 8\delta - E \end{bmatrix} \begin{vmatrix} A_0 \\ A_2 \\ A_4 \end{vmatrix} = \begin{vmatrix} 0 \\ 0 \\ 0 \end{vmatrix} \quad (12)$$

The energy of the corresponding rotational states can be determined from the condition that the system (12) has a solution. The three values of E can be obtained by solving the cubic equation:

$$x^3 = \frac{45x^2}{2sin^2 3\gamma} - \left(39\ell^2 + 117\ell\frac{\cos 3\gamma}{sin^2 3\gamma} - \frac{81}{sin^4 3\gamma} - \frac{78}{sin^2 3\gamma}\right)x - 70\ell^3 \cos 3\gamma + 5\left(42 - \frac{9}{2sin^2 3\gamma}\right)\ell^2 + 5\ell\left(81\frac{\cos 3\gamma}{sin^4 3\gamma} + 42\right) - \frac{270}{sin^4 3\gamma} + \frac{70}{sin^2 3\gamma} = 0 \quad (13)$$

where $x = \frac{E}{\hbar^2 B\beta^2}$ and $\ell = \frac{4T\beta}{\hbar^2 B\beta^2}$ (14)

For a rough estimate of ℓ, the value of T= 40MeV, $\frac{\hbar^2}{B\beta^2}$ = 400 keV and β = 0.2 gives the value of ℓ= 80. Similarly, the energy E for 2^+ states can be determined from the:

$$\begin{vmatrix} \frac{3}{2}(a+b) - 6T\beta\cos\gamma - E & 6T\beta\sin\gamma + (a-b)\sqrt{3}/2 \\ 6T\beta\sin\gamma + (a-b)\sqrt{3}/2 & 6T\beta\cos\gamma + \frac{(a+b)}{2} + 2c - E \end{vmatrix} = 0 \quad (15)$$

where $a = \hbar^2[4B\beta^2 sin^2(\gamma - \frac{2\pi}{3})]^{-1}$, $b = \hbar^2[4B\beta^2 sin^2\left(\gamma + \frac{2\pi}{3}\right)]^{-1}$ and

$c = \hbar^2[4B\beta^2 sin^2\gamma]^{-1}$ (16)

Substituting the values of a, b, c and expending the determinant (15) we obtained the second degree equation:

$$x^2 - \frac{9x}{2sin^2 3\gamma} - \frac{9\ell^2}{4} - \frac{27\cos 3\gamma}{4sin^2 3\gamma}\ell + \frac{9}{2sin^2 3\gamma} = 0 \quad (17)$$

where x and ℓ are defined in Eq. (14). The two roots of Eq. (17) can be written as (in unit of $\hbar^2/4B\beta^2$),

$$E_{21} = \frac{9(1-\sqrt{1-8/9\,sin^2 3\gamma})}{sin^2 3\gamma} \quad (18)$$

$$E_{22} = \frac{9(1+\sqrt{1-8/9\,sin^2 3\gamma})}{sin^2 3\gamma} \quad (19)$$

The energy level of I=3 state is given by:

$$E(3) = \sum_{\lambda=1}^{3} 2/sin^2\left(\gamma - \frac{2\pi\lambda}{3}\right) = \frac{18}{sin^2 3\gamma} \quad (20)$$

and energies of I=5 states are given by:

$$E_\tau(5) = \left[45 \pm 9\sqrt{9 - 8\,sin^2 3\gamma}\right]/sin^2 3\gamma \quad (21)$$

In Eq. (21) $\tau = 1$ for the minus sign on the square root and $\tau = 2$ for the plus sign gives the energy of 5_{1+} and 5_{2+} states corresponding to $K^{\pi} = 2^{+}$ and $K^{\pi} = 4^{+}$ bands, respectively. The value of asymmetry parameter can be obtained using the Eqs. (18) and (19) and the asymmetric parameter (γ) becomes:

$$\gamma = \frac{1}{3}\sin^{-1}\left[1 - \left(\frac{1-R_\gamma}{1+R_\gamma}\right)^2\right]^{1/2} \quad \text{, where } R_\gamma = \frac{E_{22}}{E_{21}} \tag{22}$$

2.1 Reduced Transition Probabilities

The reduced transition probability B(E2; $I_i \rightarrow I_f'$) between two numbers of the same rotational band with quantum number K is expressed as:

$$B(E2; I_K \rightarrow I_K') = \frac{5}{16\pi} e^2 Q_0^2 |\langle I_2 K_0 | I' K \rangle|^2 \tag{23}$$

where we have used

$$\sum_{m1\ m2\ m3} |\langle I_1 I_2 M_1 M_2 | IM \rangle|^2 = (2I+1) \tag{24}$$

For Coulomb excitation, the B(E2), reduced transition probability in the case of symmetric rotor (even-even nuclei) is expressed;

$$B(E2; I_K \rightarrow I_K') = \frac{5}{16\pi} e^2 Q_0^2 |\langle I_{200} | I' + 2, 0 \rangle|^2$$

$$B(E2; I_K \rightarrow I_K') = \frac{5}{16\pi} e^2 Q_0^2 \frac{(I+1)(I+2)}{(2I+1)(2I+3)} \tag{25}$$

The non-spherical nuclei have rotational levels which are due to very fast electric quadrupole transition probability B(E2; I→I′). According to equation (25), B(E2; $I_i \rightarrow I_f'$) increases as the value of intrinsic quadrupole moment Q_0 increases. If the transition takes place between the ground state (I=0) and the first excited state (I=2) of nuclei, then

$$B(E2) = \frac{5}{16\pi} e^2 Q_0^2 \tag{26}$$

For transition between rotational level of spin I=2 and I=0, the BE(2) value can be expressed (in unit of $e^2Q_0^2/16\pi$):

$$b(E2; 2_1 \rightarrow 0_1) = B(E2; 2_1 \rightarrow 0_1)/\ e^2Q_0^2/16\pi = (1/2)\{1+ [(3-2\sin^2(3\gamma)/\ (9-8\sin^2(3\gamma)^{1/2}]\} \tag{27}$$

where the intrinsic quadrupole moment of an axial nucleus with nuclear core deformation β is:

International Journal of Computer & Mathematical Sciences
IJCMS
ISSN 2347 – 8527
Volume 4, Special Issue
March 2015

$Q_0 = 3ZR^2\beta/(5\pi)^{1/2}$. (28)

Also the B(E2) value for other transitions can be written as[3]:

$B(E2;4_i \rightarrow 2_f) = 5/126\,[\cos\gamma\,(6A_{0i}\,A_f + \sqrt{35}A_{2i}\,B_f) + \sin(\sqrt{15}A_{2i}A_f + A_{0i}B_f + \sqrt{35}A_{4i}B_f)]^2$ (29)

where A_f and B_f are the coefficients that determine the wave functions of spin 2_1^+ and A_λ coefficients determine the wavefunction of spin 4_{1+}. Using the values of coefficients determined the wavefunctions, one can calculate the probabilities of electric quadrupole transitions between various rotational states of the nucleus. The ARM $B(E2;4_g \rightarrow 2_g)/B(E2;2_g \rightarrow 0_g)$ branching ratio is deduced from eqs. (27, 29) using asymmetric parameter (γ) from equation (22).

3. Result and Discussions

3.1 Calculation of Asymmetric Parameter (γ)

The values of asymmetry parameter (γ) can be evaluated using eq. (22) by puting the the experimental energies of $E2_2^+$ ($=E_{22}$) and $E2_1^+$ ($=E_{21}$) states [5]. It can be evaluated using:

(a) The energy ratio $R_4=(E_{4g}/E_{2g})$ but only the nuclei with $2.8 \leq R4 \leq 3.33$ will be allowed [6,7].

(b) The B(E2) values which are very small and available with uncertainties.

Therefore the values from energy ratio $R\gamma$ are more reliable. The calculated values of asymmetry parameter (γ) for all nuclei of medium mass region are used to calculate the $B(E2;4_g \rightarrow 2_g)/B(E2;2_g \rightarrow 0_g)$ branching ratio.

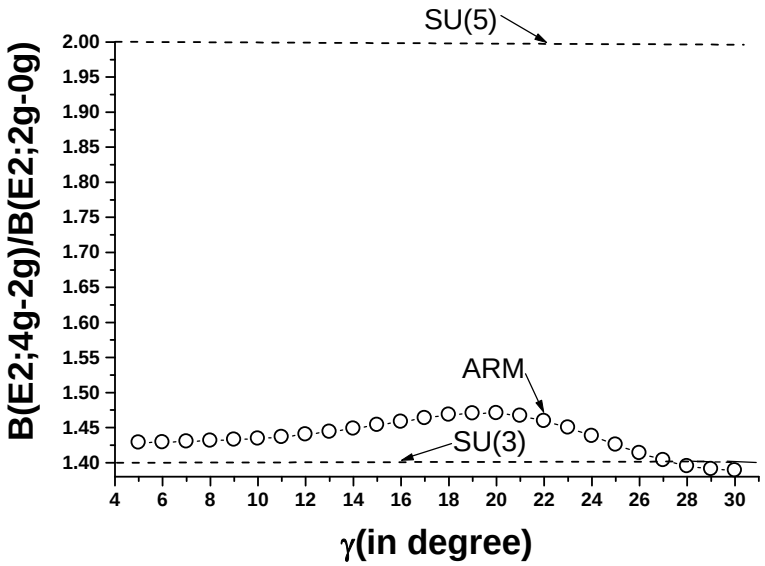

Fig.1 The Variation of B(E2;4g→2g)/ B(E2; 2g→0g) ratio from ARM (shown by hollow circles) vs. asymmetry parameter (γ) in degree. The vibrational limit SU(5) at 2.0 and rotational limit SU(3) at 1.4 are shown by dotted lines for comparison.

3.1 Variation of ARM $B(E2;4_g \rightarrow 2_g)/B(E2;2_g \rightarrow 0_g)$ ratio versus Asymmetry Parameter (γ)

International Journal of Computer & Mathematical Sciences
IJCMS
ISSN 2347 – 8527
Volume 4, Special Issue
March 2015

The variation of B(E2;4g→2g)/ B(E2; 2g→0g) ratio from ARM vs. γ is shown in Fig.1. The ARM data points are shown by hollow circles and the vibrational or SU(5) limit at 2.0 and rotational or SU(3) limit at 1.4 are shown by dotted lines for useful comparison. It is clear from the figure that the ARM predictions are very close to the SU(3) limiting value and also it is increases very slowly on increasing γ from 0^0 to 20^0 forming a peak at 20^0 and decreases slowly beyond 20^0 approaches 1.4 which is SU(3) limiting value at $\gamma \approx 27^0$. The ARM ratio is away from vibration model limit of 2.0 this shows that it cannot explain the vibrational nature of the nuclei

3.1 Variation of Experimental and ARM B(E2;$4_g \rightarrow 2_g$)/B(E2;$2_g \rightarrow 0_g$) ratio versus Asymmetry Parameter (γ)

The variation of B(E2) ratio from experiment and ARM with γ is shown in Fig.2. The ARM data points are shown by solid triangles and SU(5) limit at 2.0 and SU(3) limit at 1.4 are shown by dotted lines. Two nuclei are having B(E2) ratio anomalously more than 2.0 and not shown in the Fig.2, e.g. ^{182}Hg and ^{184}Hg for them the B(E2;$4_g \rightarrow 2_g$)/B(E2;$2_g \rightarrow 0_g$) ratios are 4.6(3) and 2.8(8) respectively. There are some other nuclei in medium mass region those are having this ratio anomalously lesser than 1.4 i.e. SU(3) limiting value e.g., ^{150}Nd, ^{164}Dy, ^{164}Er, 168W, ^{182}W, ^{184}W, ^{192}Os, ^{180}Pt and ^{198}Hg having values 1.31(10), 1.30(7), 1.18(13), 1.1(3), 1.386(20), 1.30(9), 1.22(4), 0.92(22) and 0.375(18) respectively. It is noted that in medium mass region (Nd-Hg), this B(E2) ratio is smallest in case of ^{198}Hg [=0.375(18)] which is non magic nucleus with only two vacancy of protons for Z=82. This ratio is also very small in case of $^{144}Nd_{84}$ [=0.73(9)]; which is also a non-magic nucleus; which has only two valence neutrons outside N=82. It supports the findings of Cakirli et.al. [8] that the value of this B(E2) ratio is anomalously small in non magic nuclei, as it cannot be explained with collective approaches. The values of B(E2;$4_g \rightarrow 2_g$)/B(E2;$2_g \rightarrow 0_g$) ratios for N=88 isotones (Nd, Sm, Gd, Er) are lying between SU(3) and SU(5) limits indicating the shape phase transition for these nuclei. However the nature of the Dy_{88} is different and its value is close to SU(3) limit. Other data points are lying between SU(5) and SU(3) limits. While the ARM predictions are very close to the SU(3) limit.

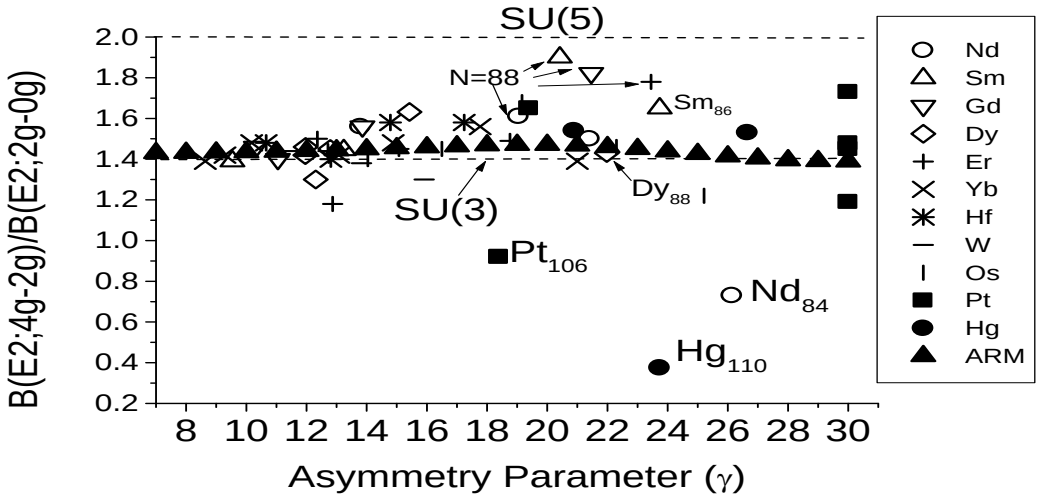

Fig.2 The Variation of experimental B(E2;4g→2g)/ B(E2; 2g→0g) ratio vs. asymmetry parameter (γ) in degree. The vibrational limit SU(5) at 2.0 and rotational limit SU(3) at 1.4 are shown by dotted lines for comparison. The ratio from ARM is shown by solid triangles.

4. Conclusions

The predictions of asymmetric rotor model (ARM) of Davydov and Filippov for B(E2; 4g→2g)/ B(E2;2g→0g) branching ratio are compared with the experimental data in medium mass region. It is found that the observed data point of this ratio for N=88 isotones (Nd, Sm, Gd, Er) are indicating the shape phase transition from an ideal spherical harmonic vibrator or SU(5) to an axially symmetric deformed rotor or SU(3). It is also noted that this B(E2) ratio is anomalously small in case of two non- magic nuclei i.e., $^{198}_{80}Hg_{118}$ [=0.375(18)] and $^{144}_{60}Nd_{84}$ [=0.73(9)] with only two vacancy of protons for Z =82 and two valence neutrons outside N=82, respectively; which supports the findings of Cakirli et.al. [8]. The data points for other nuclei are lying between SU(5) and SU(3) limits. The calculated B(E2) ratios of ARM are very close to the SU(3) limit of IBM indicating that it can explain the structure of only well deformed nuclei. Therefore the ARM is partially successful in explaining this branching ratio.

Acknowledgements

One of us (SS) expresses his gratitude to the Prof. Alabi Musa, Vice Chancellor, Yobe State University, Damaturu, Yobe State, Nigeria for encouragement and for providing the facilities for the research work. We are grateful to Professor J. B. Gupta, Ramjas College, University of Delhi for his valuable guidance.

References

[1] F. Iachello and A. Arima, The Interacting Boson Model (Cambridge University Press, Cambridge, 1987).
[2] A. Bohr and B. R. Mottelson, Nuclear Structure, Vol. II, Benjamin, New York, 1975.
[3] A. S. Davydov and G. F. Filippov, Rotational states in even atomic nuclei, Nucl. Phys. 8, (1958) p. 237.
[4] A. S. Davydov and V. S. Rostovsky, Relative transition probabilities between rotational levels of non-axial nuclei, Nucl. Phys., Vol. 12 (1959) p. 58.
[5] Recent data for energies have been taken from http://www.nndc.bnl.gov
[6] S. Sharma, Ph. D. Thesis, Study of Nuclear Structure of some medium mass nuclei, University of Delhi (1989) unpublished.
[7] J. B. Gupta and S. Sharma, Interband B (E2) ratios in the rigid triaxial model, a review, Physics Scripta, 39(1989) p.50.
[8] R. B. Cakirli, R. F. Casten, J. Jolie, and N. Warr, Highly anomalous yrast B(E2) values and vibrational collectivity, Phys. Rev. C 70 (2004) p. 047302.

Systematic dependence of B(E2)↑ on asymmetry parameter γ_0

Rajesh Kumar[1*], Reetu Kaushik[2], S. Sharma[3]
[1]*Department of Physics, Noida Institute of Engineering & Technology, (Mahamaya Technical University), Greater Noida-201306, India*
[2]*Research Student, Dept. of Physics, Mewar University, Gangrar, Chittorgarh, Rajasthan- 312901, India*
[3]*Panchwati Institute of Engineering & Technology(Mahamaya Technical University), Meerut-250005, India*
[*]*Email: rajeshkr573@gmail.com, rajeshkr0673@yahoo.co.in*

Introduction

The reduced electric quadrupole transition probability, $B(E2;0_1^+\rightarrow 2_1^+)$ of even–even nuclides have been compiled by Raman et. al [1] and its variation versus A have been shown for $0\leq A\leq 260$ region. The observed values have been compared with various theoretical models [1]. The $B(E2;0_1^+\rightarrow 2_1^+)$ is a good indicator of the collectivity in even-even nuclei. The intrinsic quadrupole moment, Q_0, can be deduced from the $B(E2;0_1^+\rightarrow 2_1^+)$ value, i.e.

$$B(E2;0_1^+\rightarrow 2_1^+) = (5/16\pi)\, e^2Q_0^2.$$

In Rigid Triaxial Rotor (RTR) model [2] the $b(E2;2_1^+\rightarrow 0_1^+)$ values in unit of $(e^2Q_0^2/16\pi)$ are related to asymmetry parameter γ_0:

$$b(E2;2_1^+\rightarrow 0_1^+) = \tfrac{1}{2}\{1+[(3-2\mathrm{Sin}^2 3\gamma_0)/(\sqrt{(9-8\mathrm{Sin}^2 3\gamma_0)}]\}.$$

The RTR model is a simple way to describe nuclear structure of a nucleus. This model was widely used to explain energy levels, B(E2) values and B(E2) ratios for inter and intra-band transitions. Earlier, Bohr & Mottelson [3] observed that nuclei are no longer to be considered deformed in the original sense at $\gamma_0=24^0$ and the nucleus is expected to take any shape, including triaxial. Earlier, a review on inter-band B(E2) ratio in the RTR model for rare earth and light mass region have been presented by Gupta & Sharma [4] and Mittal-Sharma-Gupta [5] to test the internal consistence of the RTR model predictions.

In the present work, we search for a systematic dependence of $B(E2;0_1\rightarrow 2_1)$ values on asymmetry parameter (γ_0) in rare-earth region. The whole data is divided into four quadrants as suggested by Gupta et. al [6].

Result and Discussions

Determination of γ_0

There are various methods [2, 4, 5] to calculate γ_0. The determination of γ_0 from the energy ratio R_γ ($=E_{2\gamma}/E_{2g}$) is more relevant as discussed by Gupta & Sharma [4]. We have calculated γ_0 from R_γ using the equation:

$$\gamma_0 = \frac{1}{3}\sin^{-1}\left[\frac{9}{8}\left\{1-\left(\frac{R_\gamma-1}{R_\gamma+1}\right)^2\right\}\right]^{1/2}.$$

The energy values of $E_{2\gamma}$ and E_{2g} are taken from the website of National Nuclear Data Centre, Brookhaven National Laboratory, USA [7].

The variation of $B(E2; 0_1^+\rightarrow 2_1^+)$ vs. γ_0

The dependence of energy of first 2^+ states of even-even nuclei on neutron number tells about the nuclear core deformation. We have extended this search of systematic in the reduced electric quadrupole transition rate B(E2) values for Z=50-82, N=82-126. To understand the variation of B(E2) with γ_0, the whole data is divided into four quadrants as discussed in ref. [5,8,9]. The variation of B(E2) values against γ_0 are shown in figs. 1 to 3. For Quadrant-I (Q-I), the plot of B(E2) values vs. γ_0 is shown in fig. 1 for Ba-Dy. The plot of B(E2) values versus γ_0 yields a smooth falling curve of B(E2) with increasing γ_0 reflecting the smooth decrease of nuclear deformation. The data points are not lying on the straight line. For Quadrant-II (Q-II), the plot of B(E2) values vs. γ_0 is shown in fig. 2. Most of the data points are lying on the straight line and indication that the B(E2) values are linearly dependent on γ_0. The variation of B(E2) vs. γ_0 for Q-III is same as for Q-I (see Fig. 3).

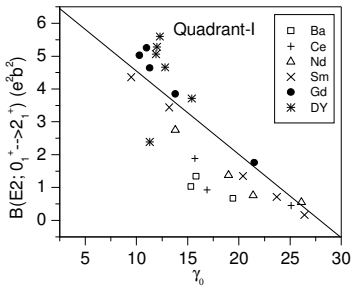

Fig. 1 Plot of B(E2) vs. γ_0 in Q-I.

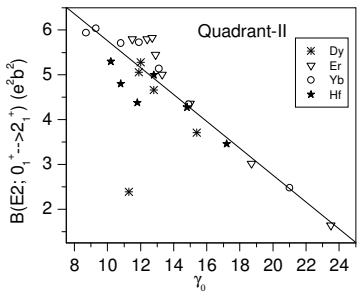

Fig. 2 Plot of B(E2) vs. γ_0 in Q-II

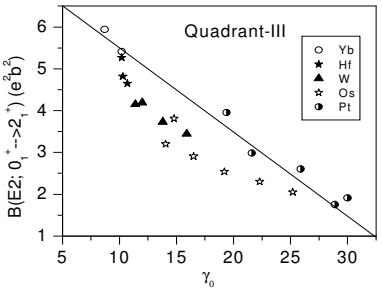

Fig. 3 Plot of B(E2) vs. γ_0 in Q-III

The authors RK and SS are expressing their gratitude to Dr O. P. Agrawal, Chairman, NIET, Greater Noida and Shri Pankaj Goel, Chairman, PIET, Meerut for providing the facilities for the research work. We are also grateful to Professor J. B. Gupta, Ramjas College, University of Delhi, for fruitful discussion.

References

[1] S. Raman, C. W. Nestor, Jr. & P. Tikkanen, Atomic Data and Nuclear Data Tables **78,** 1–128 (2001)

[2] A.S. Davydov and G.F. Filippov, Nucl. Phys. 8 (1958) 237.

[3] A. Bohr and B.R. Mottelson, Nuclear Structure, vol.-II (New York 1975) 145.

[4] J.B. Gupta and S. Sharma, Physica Scripta, 39 (1989) 50.

[5] H.M. Mittal, S. Sharma and J.B. Gupta, Physica Scripta, 43 (1991) 558.

[6] J.B. Gupta, J. H. Hamilton & A.V. Ramayya, Int. J. Mod. Phys. 5(1999) 1155.

[7] http://www.nndc.bnl.gov. Recent data have been taken in the month of July 2013.

[8] S. Sharma and Rajesh Kumar, Adv. Studies Theor. Phys. Vol. 4 (2010) 109.

[9] Rajesh Kumar, Ph. D. Thesis, Gautam Buddh Technical University (unpublished) 2013.

Acknowledgement